January 27, 1983

# COMPLETE CALORIMETRIC DETECTOR

## for the DO Area

R.C. Ball, C.T. Coffin, H.R. Gustafson, L.W. Jones, I.D. Leedom, M.J. Longo, B.P. Roe, and J.L. Stone

University of Michigan

R.J. Abrams, C. Halliwell, and D.W. McLeod

University of Illinois, Chicago

J.M. Lo Secco

California Institute of Technology

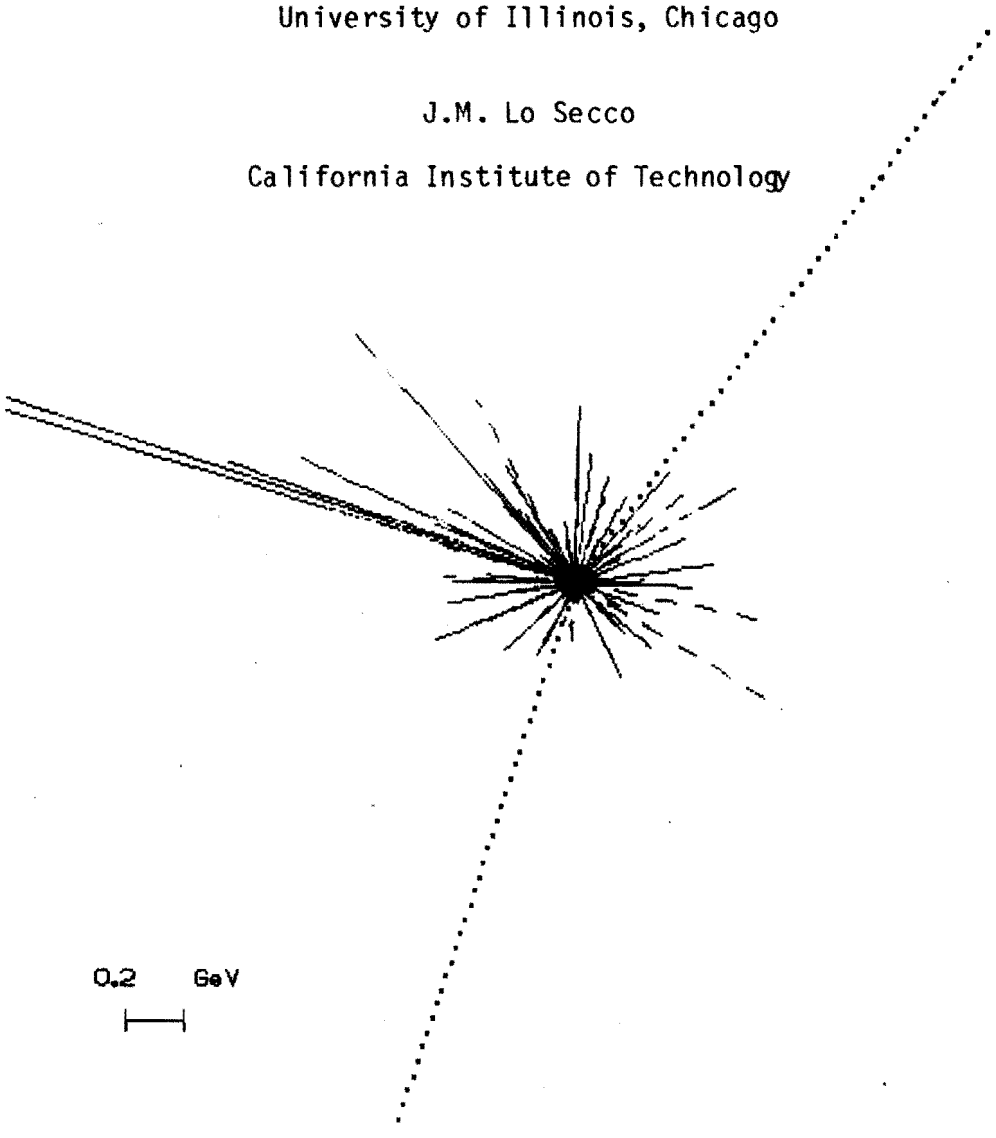

## SUMMARY

We propose a calorimetric detector (CCD) for DO which would have complete coverage in both hemispheres to within approx. 1 mr of the beams. The detector is carefully designed to avoid cracks or dead regions so that missing transverse momentum can be measured to approx. 1 GeV/c for each event. Other features of the detector are fine segmentation and good energy resolution. A complete muon detector wall would surround the detector.

The most interesting physics to come from the Fermilab Collider will very probably be something totally unanticipated. It is therefore important that any detector at DO should stress physics that cannot be duplicated by the CDF detector. We have therefore sought to develop a design which will complement the CDF. The proposed design uses no magnetic field and achieves almost $4\pi$ coverage with calorimetry with some sacrifice in luminosity.

The ability to measure missing $P_T$ with good accuracy is a powerful new technique which is not duplicated by any existing or approved detector. In effect, this places another strong constraint on events containing neutrinos or other invisible particles in the final state. Some of the physics questions which this detector can uniquely address are:

(1) A measurement of the $W^{\pm}$ mass through the decay $W \rightarrow e + \nu$ to approx. 2% accuracy. This is possible because the missing $P_T$ gives a measurement of two components of the neutrino momentum and leads to an extremely clean W signal. Because of the background suppression it will be possible to observe the $e^{\pm}$ angular distribution down to small angles.

(2) By measuring the Z mass using $Z \rightarrow 2e$ decays in the same apparatus, we can measure $M_Z/M_W$ to approx. 0.5% accuracy because detector systematics

cancel out in the ratio. With a determination of the Weinberg angle from other experiments, this gives $\rho \equiv M_W^2/(M_Z^2 \cos^2\theta_W)$, a very important barometer of new physics beyond the standard model. Note that $M_W$ can not be measured at $e^+e^-$ colliders with $\sqrt{s}$ below 170 GeV.

(3) The ratio $(Z^\circ \to 2\nu)/(Z^\circ \to 2e)$ can be measured to ~10% accuracy. This is a direct measure of the number of neutrino species. This is one of the most fundamental measurements yet to be made in high energy physics, because it is an indicator of the total number of fermion generations.

(4) Searches for new particles which decay into neutrinos or other "invisible" particles. This list includes gluinos, scalar quarks, leptoquarks, and ditechnileptons. The detector would be generally sensitive to unexpected new physics which might show up as events with large missing $P_T$. This is a very important new capability.

In addition this detector can address most of the standard questions in hadron-hadron interactions. The proposed detector has been designed to complement the CDF detector in that we have calorimetry down to approx. 1 mr while CDF has calorimetry only down to 35 mr. We note that approx. half the particles and 90% of the energy from a $\sqrt{s}$ = 2 TeV $\bar{p}p$ interaction are expected to be within 35 mr of either beam. Our detector would cover essentially the entire range of pseudorapidity. It will allow a detailed study of the angular distribution of the energy flow, which is important in understanding the general features of hadron-hadron interactions.

Besides the above physics for which the proposed detector would have unique capabilities, it would also be competitive with other detectors in most other kinds of physics. This includes studies of jets, direct photon production, and, with the addition of a minivertex detector, searches for heavy flavors.

INDEX

# I. PHYSICS BACKGROUND

In this section we give a general discussion of the physics which we can address with the proposed detector. Specifics will be discussed in Sect. III, Physics with the Proposed Detector.

## 1. Testing the Standard Model

In the standard model the weak interactions are mediated by intermediate bosons with masses in the 100 GeV range. There is one charged boson $W^{\pm}$ mediating the charged-current weak interactions and one neutral boson $Z^{\circ}$ which mediates the neutral-current interactions.

The standard electroweak model makes very specific predictions for the masses of the W and Z bosons. The current best estimates with radiative corrections are[1]

$$M_Z \cong \frac{38.5 \text{ GeV}}{\sin \theta_W \cos \theta_W} = 93.8 \pm 2.5 \text{ GeV} \quad (1)$$

$$M_W \cong \frac{38.5}{\sin \theta_W} = 83.0 \pm 3.0 \quad (2)$$

with the width of the W and Z both expected to be approx. 3.0 GeV. Radiative corrections raise both the W and Z masses by about 3 to 4 GeV above the lowest order prediction. There may be additional corrections to the masses beyond those included in the standard model's radiative corrections.[2,3] With these corrections, $M_Z$ can be written

$$M_Z = \frac{38.5 \text{ GeV}}{\sin \theta_W \cos \theta_W} (1 + \Delta)^{-1/2} \quad (3)$$

where $\Delta$ is a measure of possible corrections not included in the standard model. It can be determined if $\cos^2 \theta_W$ is known to sufficient accuracy and the ratio $M_W/M_Z$ can be measured. We define

$$\rho = \frac{M_W^2}{M_Z^2 \cos^2 \theta_W} = 1 + \Delta \quad (4)$$

For example, a measurement of $M_W/M_Z$ to 0.5% will give $\Delta$ to $\pm 0.01$. The top quark gives a contribution to $\Delta$ of approx. $0.002\ (M_t/M_W)^2$. Other potential contributions to $\Delta$ are higher dimensional Higgs representations, dynamical symmetry-breaking effects, additional fermion generations, etc.[4]

In spite of the success of the standard model, a number of alternative models which are consistent with present data have been proposed. In many alternative models there are two or more Z's. Barger has recently reviewed the non-standard models.[5] In many models there are two Z bosons which straddle the standard mass. Other models predict two Z's whose masses both lie somewhat above the standard mass. The width of the nonstandard Z's can be much broader than the standard model prediction. A variety of decay modes is also possible. More than one W might also exist.

There are also a variety of composite models in which the W and Z as well as the quarks and leptons are not fundamental but are composites of more fundamental objects. A brief review of some of the general properties of such models has been given by Abbott, Farhi, and Tye.[6] The masses of composite W's and Z's are expected to be in the range 100-170 GeV. The branching ratio of the Z into electron or muon pairs is 0.03 for 3 families as in the standard model. There may be several W's or Z's or excited states of the bosons. There may be a continuum of weak quanta.

It is clear that measurements of the W and Z masses are an important check on the standard model. If the standard model predictions are approximately correct, precision mass measurements will give estimates of the radiative corrections and so give information on higher-order weak interactions. A measurement of the mass of the $Z^\circ$ is straightforward through the decay $Z \rightarrow 2e$. The leptonic decays of the W include a neutrino so the mass determination is more difficult. A determination of the W mass from the $P_T$ distribution of high energy electrons has been discussed,[7] but this assumes an

integrated luminosity ~$10^{39}$ $cm^{-2}$ and what appears to be too low a value for the average $P_T$ of the W's at Fermilab Collider energies. It also requires extraordinarily good knowledge of the energy response of the detector and an understanding of the $e^{\pm}$ backgrounds from other sources such as heavy quark decays. This method of determining the W mass is based on the Jacobian peak in the $e^{\pm}$ transverse momentum distribution near $P_T=M_W/2$. Unfortunately the Jacobian peak gets smeared by the $P_T$ distribution of the W, caused by gluon emission. As we discuss below, these effects are difficult to predict reliably.

Because of the intense interest in a determination of the W mass, a considerable theoretical effort has gone into estimating the $P_T$ distribution of W's at Collider energies. In principle this smearing is calculable in QCD, but a consensus about the result has not been reached. According to Altarelli et al.[8a] and others[8b] it is a general and unambiguous prediction of QCD that at a fixed $\tau \equiv M^2/s$ the average $P_T$ increases linearly with $\sqrt{s}$ or the average $P_T^2$ increases linearly with s for Drell-Yan production,

$$\langle P_T \rangle = \text{constant} + \alpha_s(Q^2) \quad f(\tau, \alpha_s(Q^2)) \sqrt{s} \qquad (5)$$

or

$$\langle P_T^2 \rangle = \text{constant} + \alpha_s(Q^2) \; F(\tau, \alpha_s(Q^2)) \; s \qquad (6)$$

where the constant term represents the intrinsic transverse momentum of the quarks in the colliding hadrons and the linear rising term in s or $\sqrt{s}$ is the QCD part.

A recent review of Drell-Yan production from an experimental point of view has been given by B. Cox[9], and E. Berger[10] has recently reviewed the theoretical situation. The experimental data, which exist so far only for $\sqrt{s} < 62$ GeV, agree well with either Eq. 5 or 6 at fixed $\tau$. This growth of $\langle P_T^2 \rangle$ with s has been considered as strong evidence for an underlying quantum

field theory of the strong interactions. For $p + p \rightarrow \mu^+\mu^- + X$ at $\sqrt{\tau} = M/\sqrt{s} = 0.22$, it is found[10]

$$\langle P_T^2 \rangle = 0.52 + 0.0014\ s \qquad (7)$$

or

$$\langle P_T \rangle = 0.45 + 0.025\ \sqrt{s} \qquad (8)$$

Berger[10] has used these empirical fits to estimate $\langle P_T \rangle$ for $W^{\pm}$ and $Z^\circ$ production at the CERN $\bar{p}p$ collider ($M/\sqrt{s} \cong 0.17$). From Eq. 8, he concludes $\langle P_T \rangle \cong 14$ GeV. Eq. 7 gives $\langle P_T^2 \rangle^{1/2} \cong 20$ GeV. Berger cautions that this prediction can only be considered a guide. The extrapolation uses pN data, not $\bar{p}p$ data, and QCD calculations (with some corroboration from experimental data) indicate that the slope should be larger for $\bar{p}p$. On the other hand, the slope is expected to decrease with decreasing $\tau$, and logarithmic terms in Eq. 5 and 6 may affect the extrapolation. Berger's prediction is that for $W^{\pm}$ and $Z^\circ$ production at the CERN $\bar{p}p$ collider, $\langle P_T \rangle$ will be in the range 10 to 20 GeV/c.

At $\sqrt{s} = 2000$ the average $P_T$ for $W^{\pm}$ and $Z^\circ$ production should be somewhat higher. At the Fermilab Collider $\sqrt{\tau} \cong 0.04$ for W and Z production, and no data exist for this small a value of $M/\sqrt{s}$. Berger estimates[10] that $\langle P_T \rangle = 20$ to 30 GeV/c for W and Z production at $\sqrt{s} = 2000$ GeV.

Most discussions of the Jacobian peak method for determining $M_W$ assume a $\langle P_T \rangle$ for the W's which is $\lesssim 10$ GeV/c. If the average $P_T$ is substantially larger than this, the Jacobian peak becomes smeared out, and the mass resolution quickly worsens. This is illustrated in Figure I-1.

Other theoretical treatments, for example, that of Halzen, Martin and Scott,[11a] do not show the rise in $\langle P_T \rangle$ with increasing $\sqrt{s}$ predicted by Altarelli and others.[8] Until experimental information becomes available, we shall adopt the point of view that the average $P_T$ for W and Z production at the Fermilab Collider is somewhere between 10 and 35 GeV/c. Fortunately, as discussed below, we have devised a method for determining the W mass which

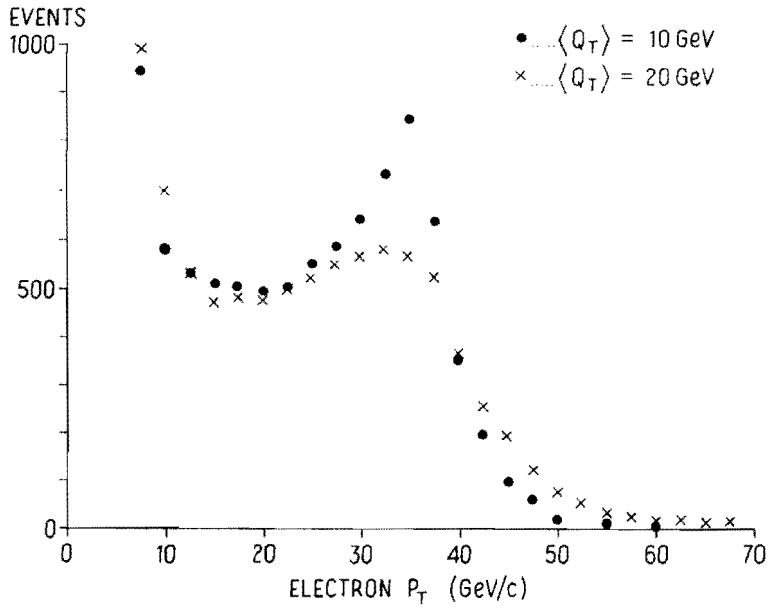


Figure I-1: Distribution of electron transverse momentum from W → (all) for two values of $\langle Q_T \rangle$, the average transverse momentum of the W's. The distribution is integrated over all electron angles. Only electrons from events with W production are included. Backgrounds from heavy flavor production, not associated with W production, are not.

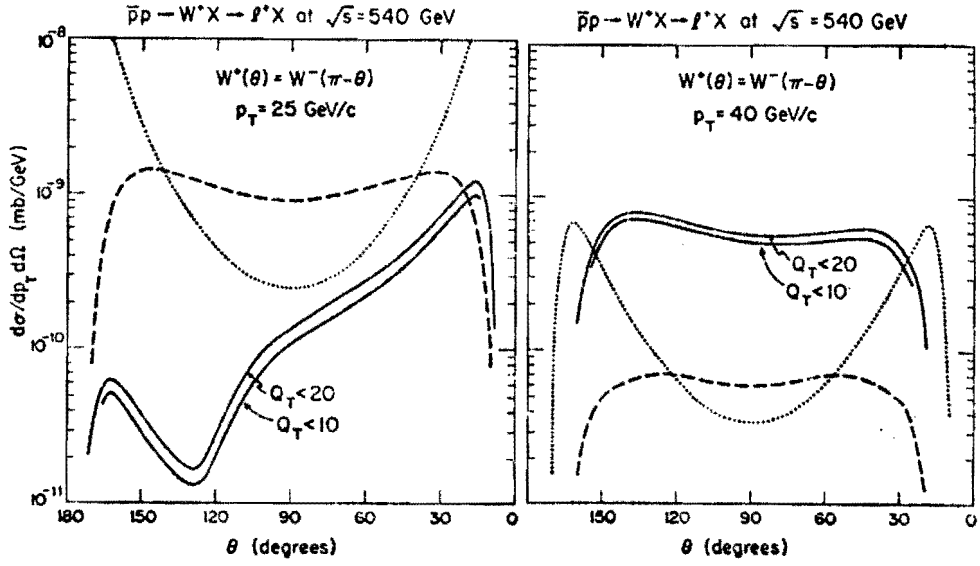


Figure I-2: The solid curves are predicted angular distributions for $e^+$ from $W \to e^+ + \nu$ decays at $\sqrt{s}$ = 540 GeV for two possible cuts on the transverse momentum of the W, $Q_T < 20$ and $Q_T < 10$ and for two values of $P_T$, the transverse momentum of the electron. The sum of the dashed and dotted curves represent one estimate of the background of electrons from semileptonic decays of heavy quarks. The $e^-$ distributions are identical, but mirrored about 90°. [From Ref. 11b].

uses the missing $P_T$ as a measure of the neutrino momentum and which works well independently of the $P_T$ spectrum of the W's.

Another important prediction of the standard model is the angular distribution of charged leptons from $W \to e + \nu$. The predicted distributions at $\sqrt{s}$ = 540 GeV are shown as the solid lines in Fig. I-2 for two values of $P_T$, the transverse momentum of the charged lepton, and two possible cuts on $Q_T$, the transverse momentum of the W. The dashed and dotted curves show one estimate of the background of charged leptons from the semileptonic decay of heavy flavors. At relatively small $P_T$, $\lesssim$ 25 GeV/c, the background from heavy flavors is large. This emphasizes the need for being able to place additional constraints on the events to reduce the background from heavy flavors. In Sect. III we discuss additional constraints such as large missing $P_T$, the absence of additional charged leptons, and the presence of a jet opposite the direction of the W (as reconstructed from the lepton and missing $P_T$). With these constraints the heavy flavor background will be very small. With the proposed detector, the charge of the electron will not be known, so the angular distribution will effectively be folded about 90°. The asymmetry will not be measured.

The transverse momentum distribution of the W's is of considerable interest in itself. With a detector capable of measuring missing $P_T$ with reasonable accuracy it is possible to measure the transverse momentum distribution of the W's directly by equating the missing $P_T$ to the $P_T$ of the neutrino.

The mass of the Z° can be measured fairly easily from the decay $Z \to 2e$. Here the main limitation will be systematics in the energy scale calibration of the detector. Fortunately the most interesting single number is $\rho \equiv M_W^2/(M_Z^2 \cos^2\theta_W)$. The detector systematics will cancel for the most part,

and the limit on the accuracy of $\rho$ will clearly come from the measurements of $M_W$. As Kane and Perl[12] stress, the measurement of $\rho$ is an extremely important probe of physics beyond the standard model. If $\rho \neq 1$ we learn either that there is SU(2) breaking at a higher mass scale, or that Higgs particles occur in other than doublet representations. A shift in the mass of the $Z^\circ$ from the expected value would be of great interest as a probe for new physics. If there are additional electrically neutral gauge bosons, they will shift $M_Z$ but not $M_W$. Grand unified models with symmetry breaking at intermediate scales would have a similar effect. Other possible mechanisms would shift both $M_W$ and $M_Z$.

Perhaps the most important unsolved problem in particle physics is that of the fermion generations. At this time there are three generations known, the lightest members of which are the $\nu_e$, $\nu_\mu$, and $\nu_\tau$. The massive members of any hypothetical fourth generation may well lie beyond the range of present accelerators. However, if the next generation replicates the lower ones and contains a low mass neutral lepton (i.e., a neutrino), it will be possible to ascertain this through the decay $Z \to 2\ \nu_X$. A measurement of the total number of neutrino species would also be of major importance in cosmology. A count of the number of neutrino species is possible by measuring the ratio $(Z^\circ \to 2\nu)/(Z^\circ \to 2e)$ which is approx. 2.0 times the number of neutrino species.[1,13] For a world with three species of neutrinos, this ratio is 6.0 and $(Z^\circ \to 2\nu)/(Z^\circ \to \text{all})$ is approx. 0.18. Such a measurement is only possible with a detector carefully designed to detect very rare events with large missing $P_T$. We believe this is possible with the proposed detector as discussed in Sect. III. Another approach to this question is to measure the absolute width of the $Z^\circ$ mass peak as observed through $Z^\circ \to 2e$ decays. To do this at a hadron collider the mass resolution of the detector must be known a priori to a very high degree of accuracy. The theoretical total width of the $Z^\circ$ is believed to

be calculable to sufficient accuracy once the mass of the t quark is known.[1] Experimentally, even a 10% error in estimating the mass resolution of the detector at the Z° mass would lead to an error of ±1.7 neutrino species. The absolute energy calibration of the detector cannot drift by more than 0.3% over a period of a year or so while the data are being taken to achieve even this accuracy.

This technique for determining the number of neutrino species seems somewhat more practical at an $e^+e^-$ storage ring because of the ability to scan across the Z° peak, but this requires a very good understanding of the detector, the storage ring resolution, and radiative effects.[14] If toponium or any other threshold is near the Z° peak, the measurement of $N_\nu$ by this technique may be impossible. Because of the uncertainties in measuring $N_\nu$ from a direct measurement of the width of the Z° peak, an alternative method has been proposed[14]. This is to run with an energy about 20 GeV above the Z° peak and use the reaction $e^+ + e^- \to \gamma + Z°$. The tag is the monochromatic $\gamma$ with energy approx. 20 GeV. The number of neutrino species is approx. half the ratio of $(e^+e^- \to \gamma$ + nothing else$)/(e^+e^- \to \gamma + \mu^+ + \mu^-)$. Gittleman et al.[14a] estimate that for $\Delta N_\nu = 0.3$, a run with integrated luminosity $6.0 \times 10^{37}$ $cm^{-2}$ would be required if there is no significant background to the $\gamma$ events due to beam-gas or beam-wall events. At SLC with an average luminosity of $3 \times 10^{30}$ $cm^{-2}$ $sec^{-1}$ and $2 \times 10^7$ sec per year, this would require a year of running at an energy well above the Z° peak.

## 2. Beyond the Standard Model

Several important tests of effects not included in the standard model have already been discussed above. These include a measurement of $\rho$ as well as the masses of the W and Z. A measurement of the number of neutrino species would also be a window on new physics.

In addition, intermediate bosons with masses above the W and Z would be directly observable if their masses are not too large. A $Z^{o\prime}$ with a substantial branching ratio to 2e would probably be observable if its mass is < 300 GeV. With the technique described below for measuring its mass, a W' with a branching ratio to e + $\nu$ comparable to the W could be observed if its mass is < 300 GeV.

There has recently been a considerable interest in supersymmetric models.[12,16] Such models associate a boson with every fermion and vice-versa. Thus each quark has as its counterpart a scalar quark or squark and the gluons have spin 1/2 counterparts called gluinos. One reason for the great interest in supersymmetry is that it may offer a solution to the hierarchy problem in grand unified theories. It also tends to have fewer divergence problems than other theories and reduces the number of arbitrary parameters in the Lagrangian. The mass scales in supersymmetric models are model dependent or unknown. There is some preference for masses ~ $M_Z$ for the scalar quarks and leptons; the mass of the gluino may be considerably lower.

From an experimental point of view, searches for supersymmetric particles are difficult because these particles are generally shortlived and their decay products include a photino $\tilde{\gamma}$ or Goldstino $\tilde{G}$; these are neutral, weakly interacting particles which for practical purposes are "invisible" in collider experiments. This emphasizes again the need for a detector which can detect rare events with relatively large missing $P_T$ or energy.

The most promising candidate for supersymmetric particle searches is the gluino $\tilde{g}$ which is likely to have the lowest mass of the strongly produced particles and is produced with relatively large cross sections.[12] Production can be in pairs, $\bar{p} + p \rightarrow \tilde{g} + \tilde{g} + X$, or in association with a scalar quark $\tilde{\phi}$, $p + \bar{p} \rightarrow \tilde{g} + \tilde{\phi} + X$. The likely decay modes are $\tilde{g} \rightarrow g + \tilde{G}$, $\tilde{g} \rightarrow g + \tilde{\gamma}$, or $\tilde{g} \rightarrow$

$q + \bar{q} + \tilde{\gamma}$. The scalar quarks decay into $q + \tilde{g}$, $q + \tilde{G}$, $q + \tilde{\gamma}$, etc. Thus the state will contain two or more invisible particles, but be otherwise rather indistinctive. The present lower limit on the gluino mass is approx. 5 GeV from beam dump experiments with 400 GeV protons.[15] The charged scalar leptons such as $\tilde{e}$ could be sought at $e^+e^-$ colliders with a missing $P_T$ or energy signature. The best prospects for detecting supersymmetric particles in the relatively near future seem to be at $\bar{p}p$ colliders if an appropriate detector is built.

Another major theoretical effort at the present time is in the area of technicolor.[12,17] Such theories can provide the mechanisms needed to generate the masses of fermions and gauge bosons. These theories lead to many new states with mass scales typically $\gtrsim$ 100 GeV; exactly which ones arise is model dependent. We discuss here only some representative states which are of particular interest to the proposed detector.

Promising candidates for a search at $\bar{p}p$ colliders are the leptoquark states predicted in technicolor. These are colored objects which are expected to have masses ~ 150 GeV and are pair produced in hadron collisions. They will decay into a quark and a lepton. In the scenario discussed by Dimopoulos, Raby, and Kane[17d] all of the technileptoquarks have a strong preference for decay into a top quark and a neutrino. Thus the final states will contain a pair of t-quark jets plus a spectacularly large missing $P_T$ (~ 100 GeV/c) from the neutrinos.

Another fascinating set of objects which appear in many technicolor theories are the ditechnileptons.[17c] These are colorless pseudo-Goldstone bosons. They can be quite light in a large class of models[17c] with possible masses between a few and 100 GeV. They are colorless and therefore weakly

coupled to gluons; however because of their low masses they may be produced with moderately large cross sections via Drell-Yan production in $\bar{p}p$ collisions through an intermediate $\gamma$ or $Z^\circ$. The decays are expected to be into three quark jets and a lepton. Thus very spectacular final states containing six quark jets plus 2 neutrinos will occur as shown in Fig. I-3.

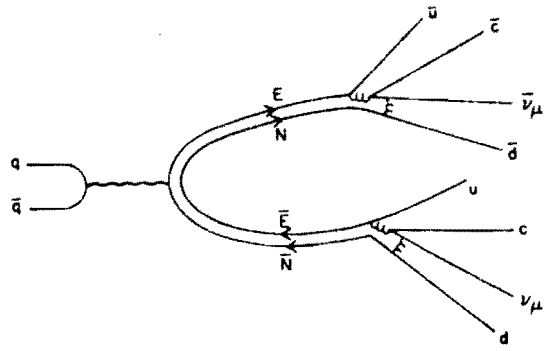


Figure I-3: Production and decay of ditechnilepton pairs. (From Ref. 17c).

Leptoquarks also appear in models in which the $W^{\pm}$, $Z^\circ$, quarks, and leptons are composite.[6] The composite leptoquarks carry a lepton number as well as a baryon number. Thus, for example, the production of electroquark pairs would be signalled by the appearance of final states with various combinations of high $P_T$ charged leptons and large missing $P_T$. These will include the combinations, $qqe^+e^-$, $qqe\nu$, and $qq\nu\nu$. Production cross sections for composite leptoquarks with a mass of 150 GeV are expected to be ~ 200 pb at $\sqrt{s}$ = 2000 GeV. Leptogluon states should also occur. These would have a similar signature; production cross sections should be about an order of magnitude larger.[18]

# II. DESCRIPTION OF THE DETECTOR

## 1. General

To measure missing transverse momentum accurately, the detector must completely surround the interaction point and get down to the smallest possible angles relative to the beams. Dead areas or holes must be avoided. Energy/momentum resolution must be good, particularly for particles with large transverse momenta. These requirements have been met in the proposed design which uses calorimetry to cover the entire angular range down to about 1 mr from either beam. An overall view of the proposed detector is shown in Figure II-1. The central detector consists of a central calorimeter organized into four quadrants with two end plug calorimeters, Fig. II-2 and II-3. The latter cover the angular range $30 < \theta < 350$ mr. The angular range $1 < \theta < 30$ mr in either hemisphere is covered by a forward and very forward calorimeter. Each of the calorimeters is preceded by tracking chambers. The first layers of each of the calorimeters consist of lead plates to detect photons and electrons, followed by steel. Outside the calorimeters is a muon detector wall.

The detector has no magnetic field. This greatly lowers the cost, and simplifies the tracking. For most physics the lack of a magnetic field has no significant disadvantages. The design is thus complementary to the CDF design, much as the UA2 design complements UA1.

The detector is designed to have the best possible energy resolution through the use of scintillation counter calorimetry. Very finely grained wire chambers with pulse-height readout are used to obtain very fine spatial resolution. In the complete detector we envision approx. 2800 photomultiplier tubes and over 20000 channels of pulse height information from the wire chambers. The scintillation counter calorimeter cells are organized in a way

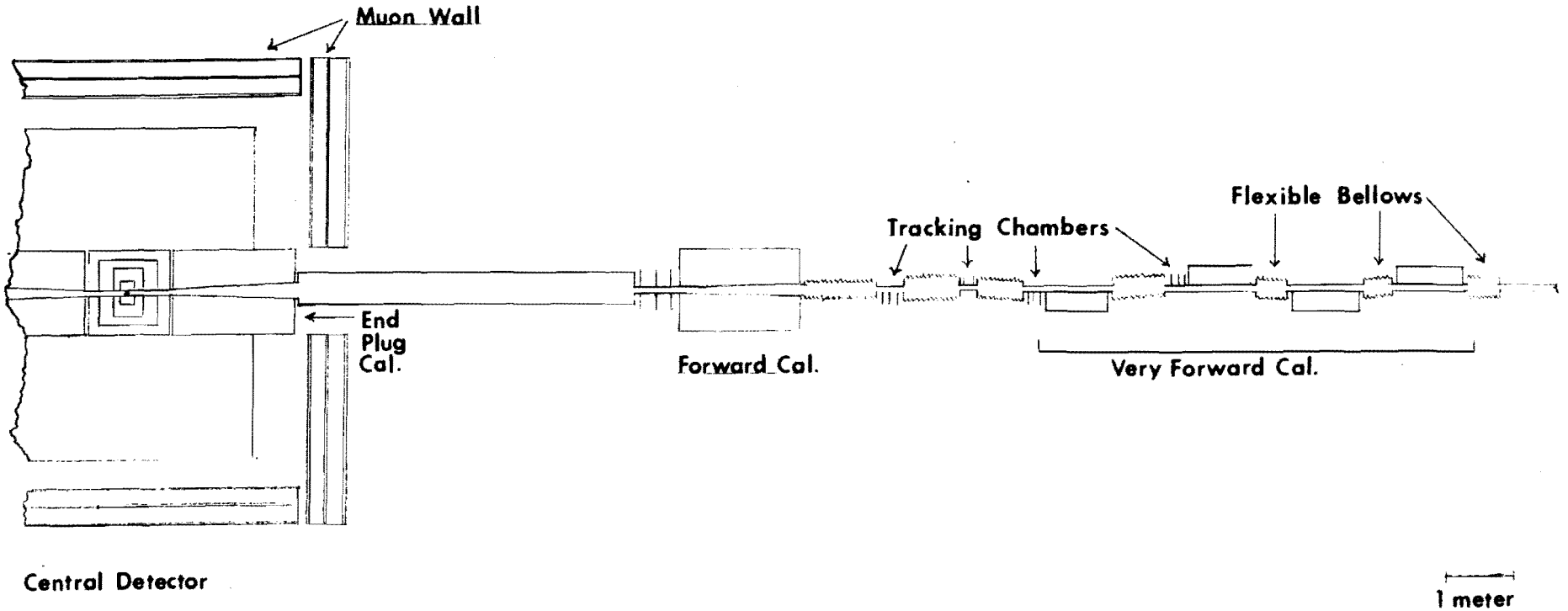


CCD Overall View (one hemisphere)

Figure II-1: Overall plan view of approx. one hemisphere of the proposed detector. Some details have been left out for clarity.

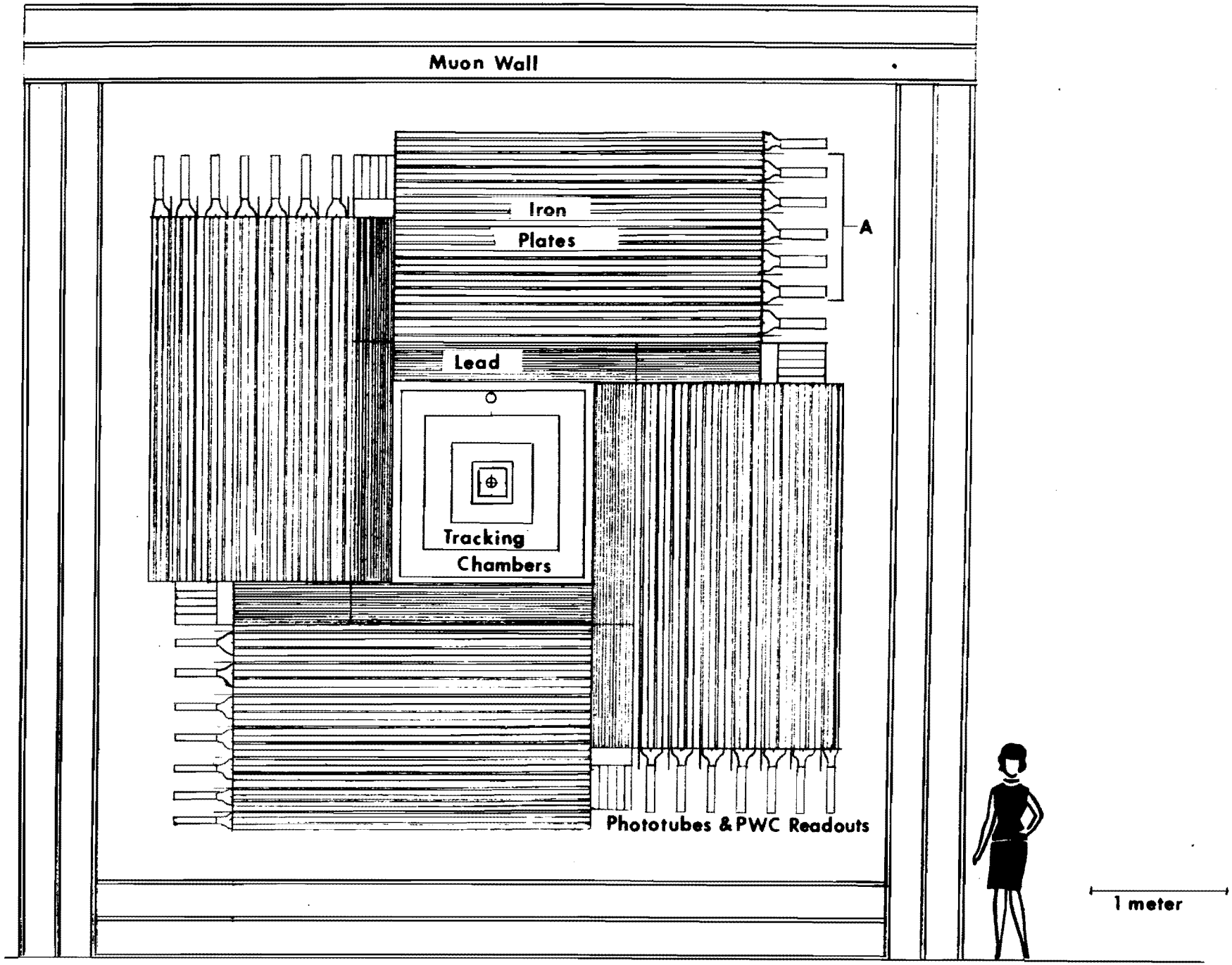


Figure II-2: A section of the central detector through the interaction point, as seen looking into the beam.

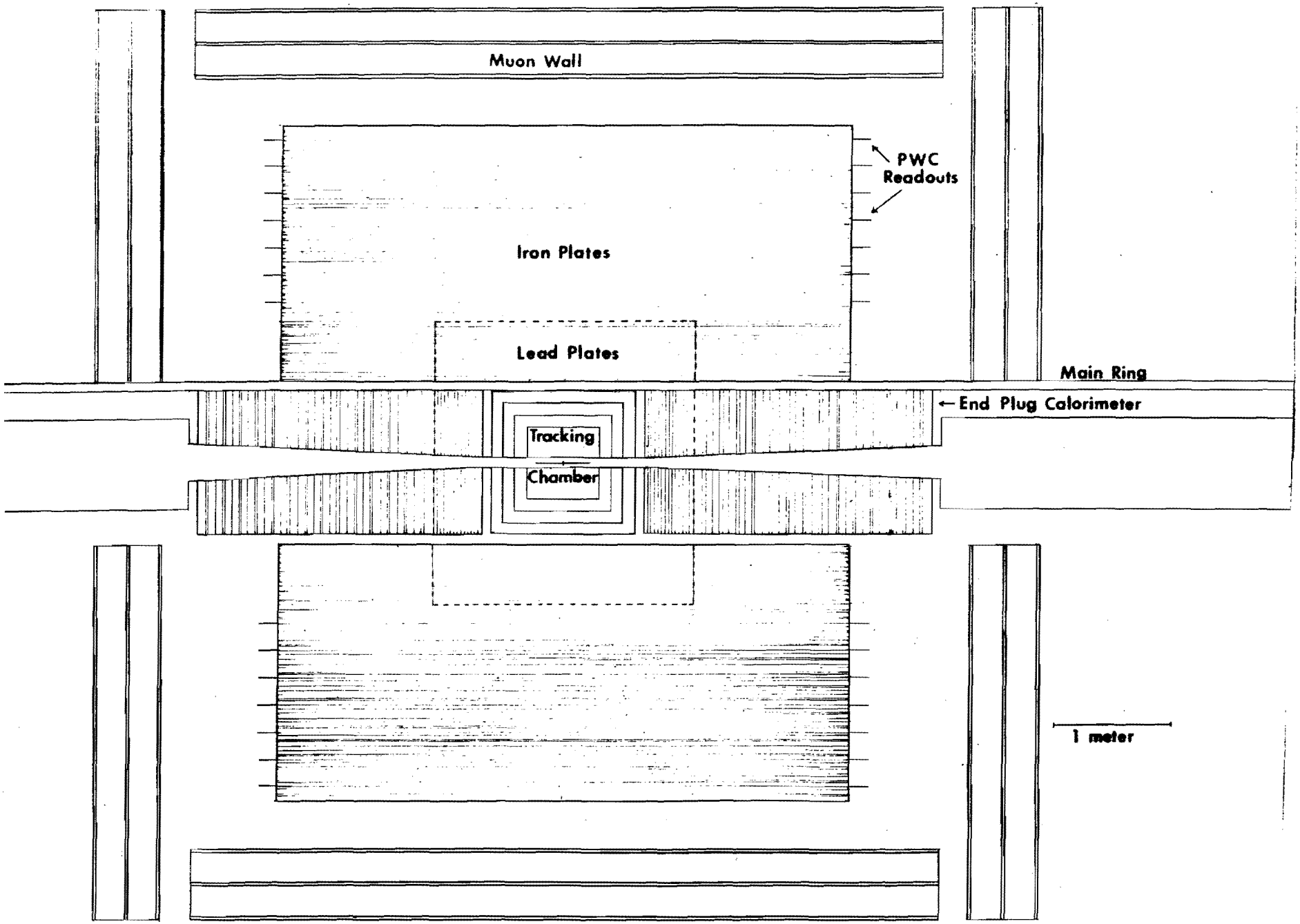


Figure II-3: A vertical section through the central detector parallel to the beam line. The dashed line indicates the extent of the lead in the electromagnetic section.

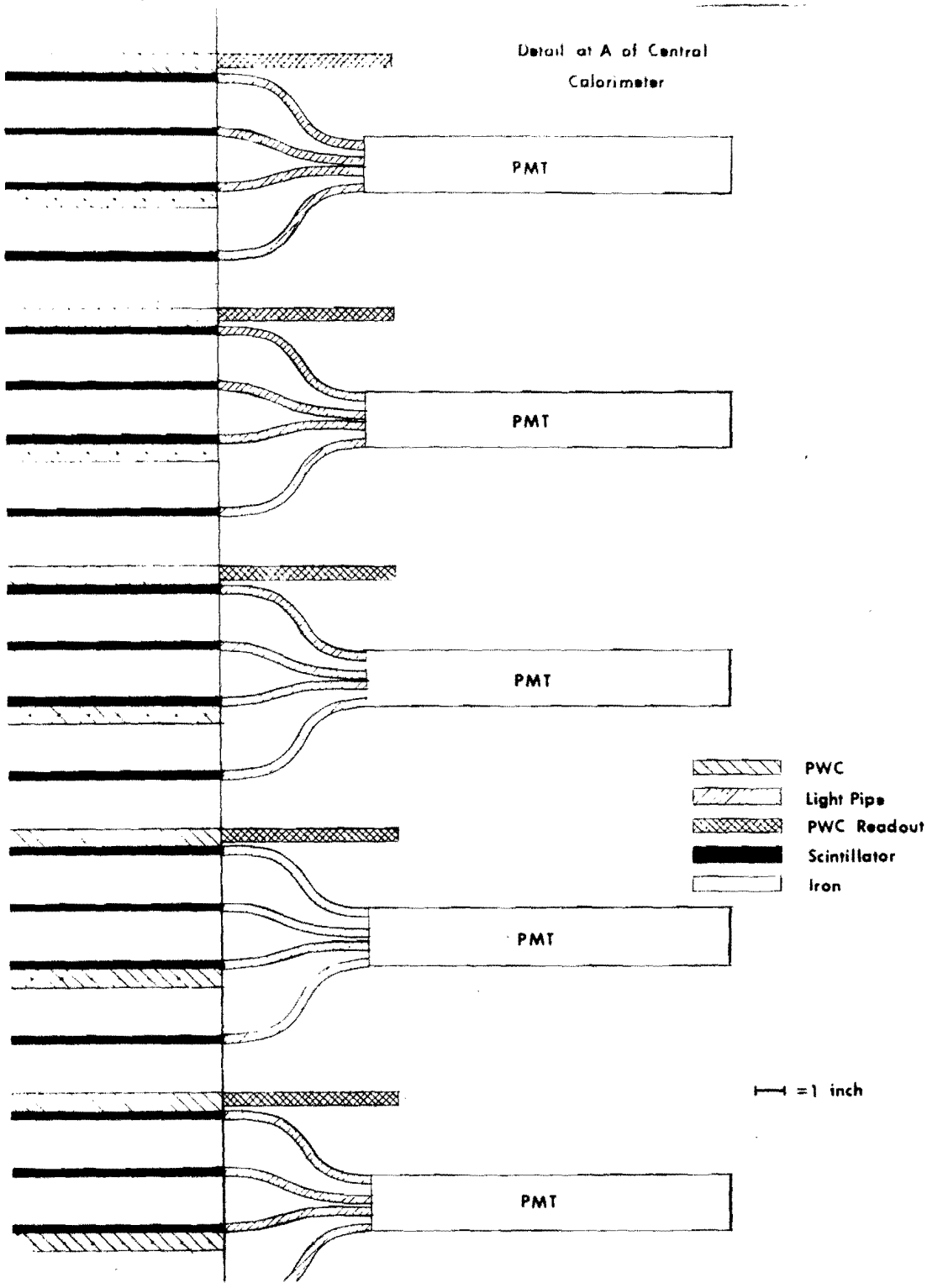


Figure II-4: A detailed view at A in Fig. II-2 of one end of a central calorimeter quadrant showing the arrangement of phototubes and light pipes. The PWC readouts for the short wires are also shown. The electronics for the cathode pad readout is not shown.

that facilitates triggering the detector on events with large transverse energy or large missing $P_T$.

## 2. Design Rationale

In studying detector designs which would be best suited to pursue the physics objectives we discussed in Sect. I, we have considered a number of alternative designs. We discuss here some of the criteria and the basis for our decisions.

(a) Magnetic field

There are at least four possible magnetic field options: solenoid (e.g.-CDF), transverse field (e.g.-UA1), forward/backward spectrometers (e.g.-CERN split field magnet, DO proposals by Rosen and by the ep collaboration), and no magnet at all. The CDF design is well conceived, but it would be a mistake to replicate it at the second detector. The UA1 design appears to have little advantage over CDF and the physics capabilities of the two detectors are comparable. By avoiding a central magnet we achieve a more compact detector which not only is less expensive but also reduces the decay path for $\pi$'s and K's. Since we must reject events with identified muons in our missing $P_T$ analysis, it is desirable to reduce muons from meson decays to the lowest practicable level. A central magnet also makes it much more difficult to avoid gaps or insensitive areas in the coverage, also an important design objective for studying missing $P_T$.

A forward spectrometer offers relatively less gain over calorimetry because the particle energies are higher and the available space limits the possible $\int Bdl$. The fractional energy resolution of a calorimeter is proportional to $1/\sqrt{E}$ while that of a magnetic spectrometer goes as E, so that calorimetry gains as $E^{3/2}$ over magnetic spectrometry. In the forward direction many of the particles have energies > 100 GeV and here calorimetry

seems optimal; calorimetry also allows the energy of neutral particles to be determined. The other virtue of a forward magnet is the bending of secondaries out of the beam pipe; we believe that our coverage to small angles (approx. 1 mr) greatly reduces this motivation.

Finally the absence of a magnet greatly simplifies the analysis. It also makes it possible to have a simple fast trigger that operates directly on raw angle-energy information from calorimeter phototubes without any track reconstruction. We note that the UA2 data reported so far has made no use of their magnetic spectrometer data.

We have therefore decided to design a detector based on calorimetry and tracking with no magnets.

(b) Forward detectors

In order to study particles at very small angles, it is not only necessary to track them but also to determine their energies. This requires moving a calorimeter to within about 2 cm of the circulating beam axis. Three options are possible: detectors in the vacuum chamber, "Roman pots", and the scheme we have adopted with flexible sections of vacuum pipe which can be translated laterally.

Locating the detectors within the beam vacuum is difficult for several reasons. The maintenance of the required high vacuum ($10^{-8}$ to $10^{-10}$ Torr) necessitates bakeout of components; this would damage or destroy detector elements such as scintillators. The installation, readout, and provisions for motion of calorimeters inside the beam vacuum would require very elaborate engineering. Radiation damage or malfunction of the detector would necessitate access to the machine vacuum with long down times.

Roman pots,[1] as used at the ISR and UA1 are a practical solution to this problem with small detectors. However, we require a meter or so of

calorimetry with coverage of a full $2\pi$ in azimuth. The required "pots", while possible in principle, would be an enormous engineering job.

Our solution is to surround a 3" vacuum pipe with calorimetry and translate the calorimeter laterally closer to the beam, once stable stored beams are established. This is made possible by connecting this section of vacuum pipe to the rest of the machine with flexible bellows. This scheme requires at least one pair of calorimeters per hemisphere, each with opposite displacement. Details will be discussed below.

(c) Spray from the forward calorimeters

A hadron or photon interacting near the inner edge of one of the forward calorimeters will generate a cascade which is only partially contained in the calorimeter. This creates two problems, an underestimate of the energy and a spray of particles which may strike detectors farther downstream. Both problems can be alleviated by reducing the number of sequential elements, i.e. - the number of surfaces that can contribute. The design in Fig. II-1 shows a forward and very forward calorimeter in each hemisphere. The intermediate calorimeter is necessitated by the limitation on transverse dimensions imposed by the main ring vacuum pipe which is 65 cm above the Doubler.

In the proposed design of the forward detectors, problems due to spray are minimized by spacing the tracking chambers as far downstream of the calorimeter elements as possible. We have studied the problem of background in the tracking chambers due to spray from upstream calorimeters using data from M5 tests and a Monte Carlo program. This is discussed in detail in Appendix A. The general conclusion is that spray will not be a problem with the proposed geometry.

In the design of Fig. II-1, the problem of underestimates of energy due to partial containment of cascades generated near the inner surfaces is

minimized by splitting the very forward calorimeters into four elements. Spray from the upstream calorimeters is caught by those farther downstream.

Possible design modifications and future embellishments of the proposed detector are discussed in Sect. VI.

### 3. The Central Detector

#### (a) General description

Detailed views of the central detector and end plug calorimeters are shown in Figures II-2 through II-4. If we imagine a muon leaving the interaction point it will first pass through approx. five planes of tracking chambers, then lead plates interspersed with scintillation counters and proportional chambers, followed by iron plates also interspersed with scintillators and proportional chambers, and finally through the muon wall which contains two 25 cm layers of iron sandwiched between 3 planes of proportional chambers. On its way out a typical muon would pass through 5 tracking chambers, 43 layers of scintillator, 21 PWC planes with separate readout of the anode wires and cathode pads, plus 3 PWC planes in the muon walls. On the average a muon would go through approx. 135 gm/cm$^2$ of lead, 1000 gm/cm$^2$ of iron in the calorimeters and 500 gm/cm$^2$ of iron in the muon walls, or a total of about 12 interaction lengths. This is important to reduce hadron punch-through to a negligible probability.

The central calorimeter is made up of four identical quadrants. These are arranged so that there are no dead areas or gaps. The design is such that the relation between energy deposition and light output will be approx. constant over the entire detector; any variation will be a smooth function of angle and position and can be readily measured in a test beam.

The main features of the central calorimeter are summarized in Table II-1. The 5504 scintillation counters are all identical, as are the iron and

TABLE II-1 CCD CENTRAL DETECTOR

ELECTROMAGNETIC SECTION

| | |
|---|---|
| Total lead plates, 15 per quadrant | 60 total |
| Size of each lead plate | 6'x10'x1/4" |
| Total thickness of Lead | 3.75" (9.5 cm) |
| Total weight of lead | 19 tons |
| Size of scintillation counters | 6" x9'x3/16" |
| Scintillator planes, 15 per quadrant | 60 total |
| Number of counters, 480 per quadrant | 1920 |
| Number of PM tubes, 160 per quadrant | 640 |
| Proportional chamber planes, 7 per quadrant | 28 total |
| Number of wires per plane | 192 short (9') 104 long (16') |
| Total number of wires | 3072 short (9') 1248 long (16') |
| Cathode pad towers, total | 1320 |

HADRONIC SECTION

| | |
|---|---|
| Total iron plates 28 per quadrant | 112 total |
| Size of each iron Plate | 9'x16'x1.5 |
| Total thickness of iron | 42" (107 cm) |
| Total weight of iron | 480 tons |
| Size of scintillation counters | 6" x9'x3/16" |
| Scintillator planes, 28 per quadrant | 112 total |
| Number of scintillation counters, 896 per quadrant | 3584 total |
| Number of PM tubes, 224 per quadrant | 896 total |
| Proportional chamber planes, 14 per quadrant | 56 total |
| Number of wires per plane | 192 short (9') 104 long (16') |
| Total number of wires | 5376 short (9') 2912 (16') |
| Cathode pad towers, total | 1496 |

TOTAL

| | |
|---|---|
| Total thickness (electromagnetic + hadronic) | 84 5/8" (215 cm) |
| Approximate total absorber weight | 520 tons |
| Total number of wires (1" spacing) | 8448 short (9') + 4160 long (16') 12608 TOTAL |
| Cathode pad towers | 2816 |
| Total number of PM tubes | 1536 |

lead plates. The iron plates are stock hot-rolled iron forced to be flat by compressing the entire stack. Small shims between each of the scintillators act as spacers and bear the compressional load. The scintillators will be laser cut so that the edges need not be polished. No significant machining of the iron or lead is required. These features will make the detector relatively inexpensive and greatly facilitate its construction.

(b) Scintillation counters

All of the scintillators are oriented perpendicular to the beam line so that all the photomultiplier tubes are on the sides of the central detector which run parallel to the beams. The light from four successive scintillators is brought directly to a phototube by short light pipes (Fig. II-4). There is no wavelength shifter and the phototubes are well outside of the calorimeter; thus "hot spots" from these sources should not be a problem. Each scintillator lies along a line of approx. constant $\theta$; this greatly facilitates triggering on $E_T$ or missing $P_T$ as discussed below.

The organization and dimensions of the scintillators somewhat resemble those in the UA1 detector, and we hope to draw from the UA1 group's experience. Because of the good light collection from the scintillator in the calorimeter, low cost acrylic-based scintillator can be used; yellow filters will probably be employed to reduce the attenuation of the light in the scintillator. A pulsed laser or argon lamp system with optical fibers to each scintillator, similar to the UA1 or UA2 systems, is envisioned for maintaining a constant gain in the phototubes.

(c) Proportional chambers

Each quadrant of the central calorimeter contains 21 proportional chamber planes, 7 in the electromagnetic section of the calorimeter and 14 in the hadronic section. The anode wires in alternate planes run parallel or

perpendicular to the beams with the wires spaced by 2.54 cm. The organization of the wires is shown schematically in Fig. II-5. Each of the short wires has its own analog readout channel. The long wires (parallel to the beam which we take to be the z-axis) have a readout on both ends to give the coordinate of the hit by current division as well as the $\phi$ coordinate from the wire position. Thus from the long wires there are two redundant pulse-height measurements of each hit which yield the z (or $\theta$) coordinate, the $\phi$ coordinate and the local energy deposition. The short wires give the x or y coordinate and the local energy deposition. This gives very fine-grained "views" of the energy flow through the calorimeter as projected on planes perpendicular and parallel to the beam. When the PWC information is combined with the more accurate energy measurements from the scintillators, we shall have an extraordinarily detailed and accurate picture of the energy flow in each event.

In addition to the anode wires, we also expect to have cathode pads which are organized in "towers" with a similar pulse height readout. A possible scheme is shown in Fig. II-6. Note that because the interaction region is approx. 0.5 m long, the tower concept is not as useful for simplifying the tracking of the energy flow as seen looking at a plane parallel to the beam (i.e., Fig. II-6b). Approximately four successive pads in depth are ganged together to give 2 samplings in depth in the electromagnetic section and 4 in the hadronic section. This subdivision leads to approx. 2800 towers with independent pulse-height readout. This gives finer-grained towers than any existing detector.

(d) PWC readout electronics

We contemplate reading out approx. 20000 channels of pulse height information from the PWC wires and pads. This can be done accurately and

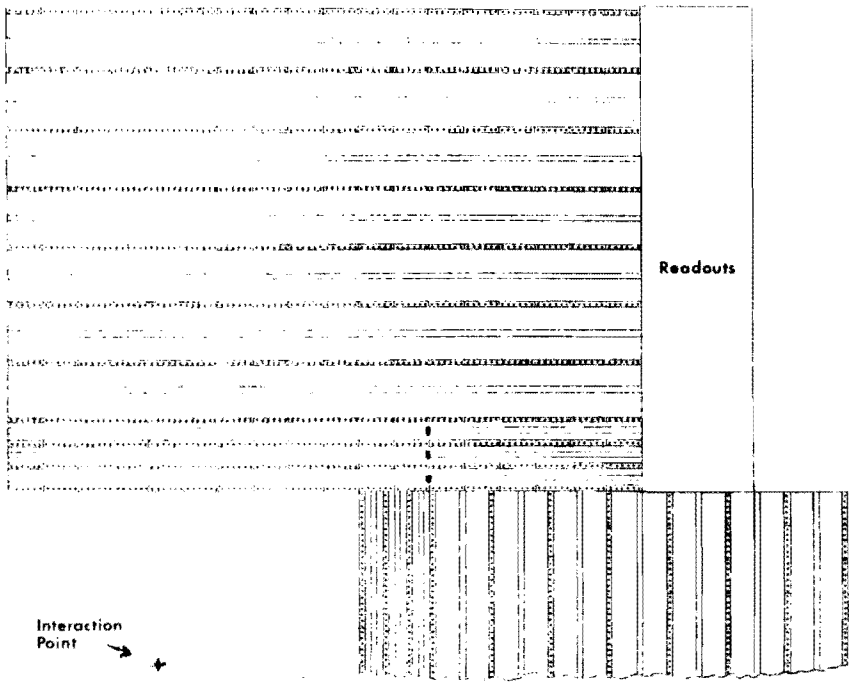


Figure II-5(a): The PWC wires for approx. one quadrant of the detector as seen looking into the beam. Each wire will have a pulse-height readout on both ends. The dashed line indicates the extent of the lead plates.

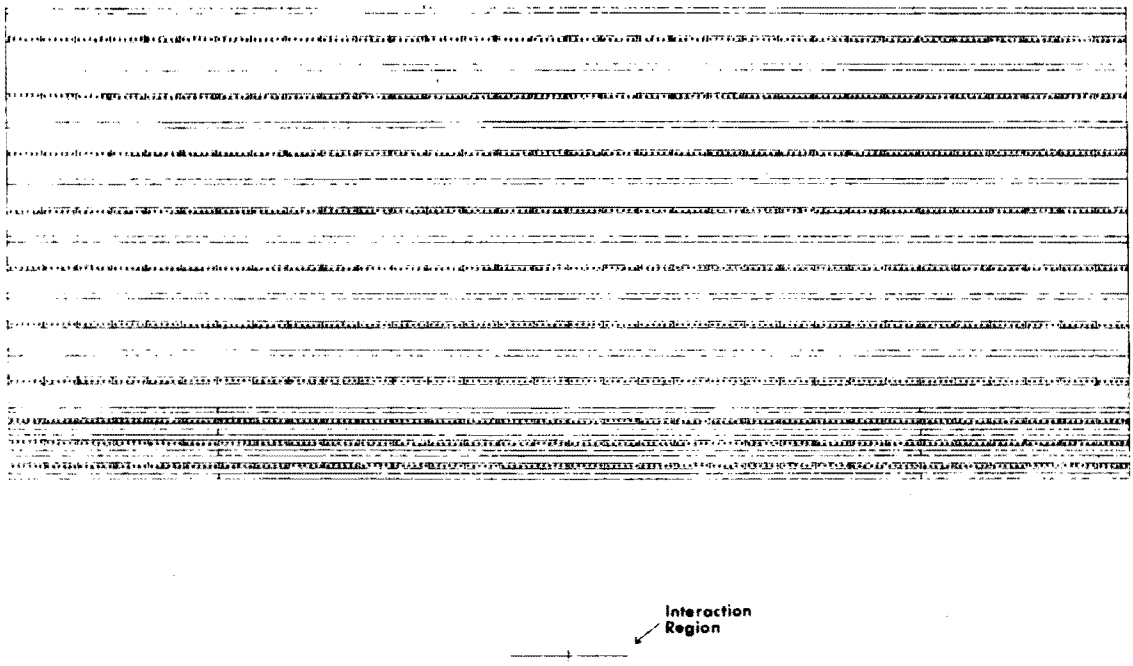


Figure II-5(b): The PWC wires for one quadrant of the central detector as seen in a section containing the beam. Each wire will have an independent pulse-height readout.

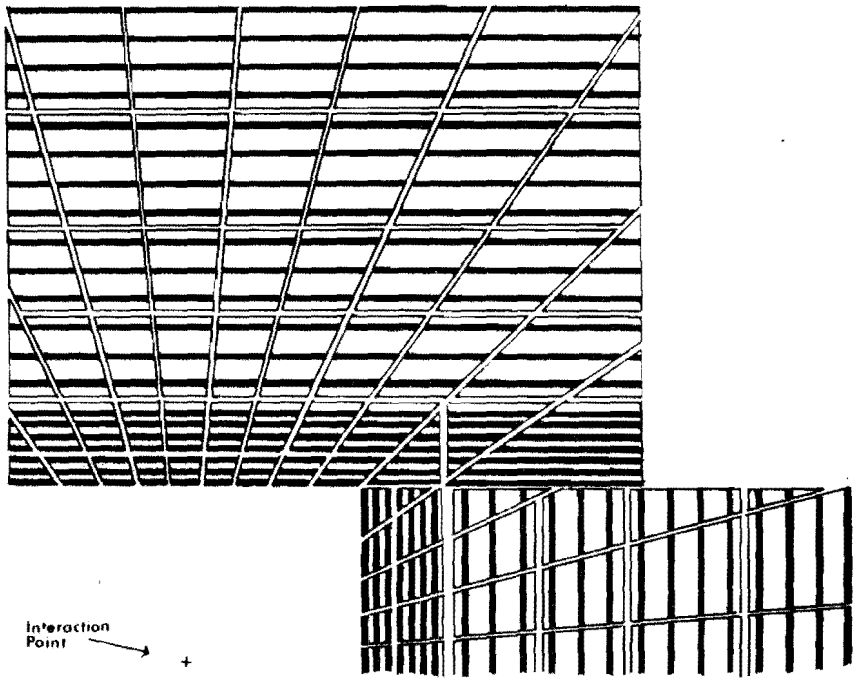


Figure II-6(a): Organization of the cathode pad towers in approx. one quadrant of the central detector as seen looking into the beam (schematic). Each trapezoidal block containing 3 or 4 successive pads will be read out separately.

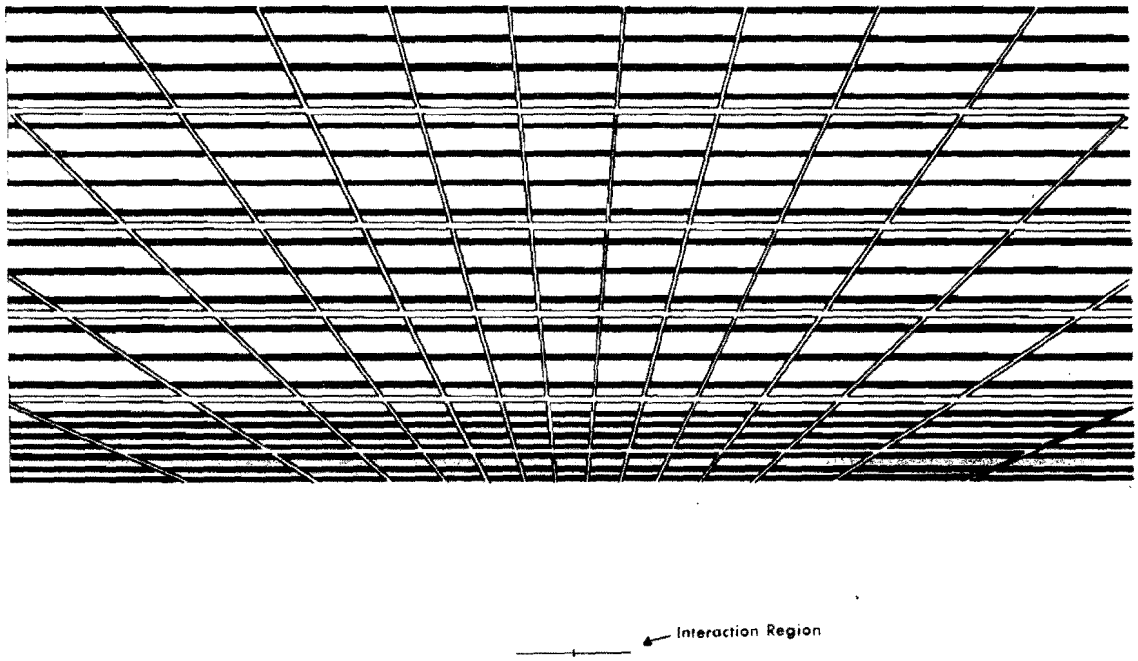


Figure II-6(b): Organization of the cathode pad towers for one quadrant of the central detector as seen in a section containing the beam line (schematic). Pads will be read out in groups of 3 or 4 in depth to give 2 samplings in the electromagnetic section and 4 in the hadronic. This subdivision gives a total of 2816 towers with independent readout.

inexpensively with a system that was developed by the University of Michigan group for E613.[2] We summarize here the main features of the system.

Accuracy: 12 bits (4096 counts)

Dynamic range: 0.1 to 100 min. ion. particles/wire

Channel-to channel uniformity: 5%

Resolving time: $\approx$ 0.8 $\mu$s

Readout time: $<$ 6 ms depending on complexity of event

Cost per channel: $7

The cost per channel is based on our E613 experience and includes construction (by an outside vendor), cabling, and power supplies. In E613, 6000 channels were in service. Reliability was excellent. For the 20000 channels planned in the proposed detector we anticipate somewhat lower costs. This gives a total cost of $<$ $140,000 for the PWC readouts.

### 4. End Cap Calorimeters

The organization of the end cap calorimeters is generally similar to that of the central calorimeters, except that only cathode pads, not the PWC wires, are read out. The calorimeter scintillators are divided into three segments radially and eight sectors in the direction of increasing $\phi$. The light from the scintillators is collected with wavebars which run parallel to the beam. All of the wavebars are along the outside periphery in the gap between the end cap calorimeter and the central calorimeter (necessitated by the main ring vacuum pipe as seen in Fig. II-3). The calorimeters have three layers in depth, one for the electromagnetic section and two for the hadronic.

An expanded view of part of one of the end cap calorimeters is shown in Figure II-7. Both the scintillators and cathode pads are organized in towers. Great care has been taken to avoid cracks or dead spots. The design is such

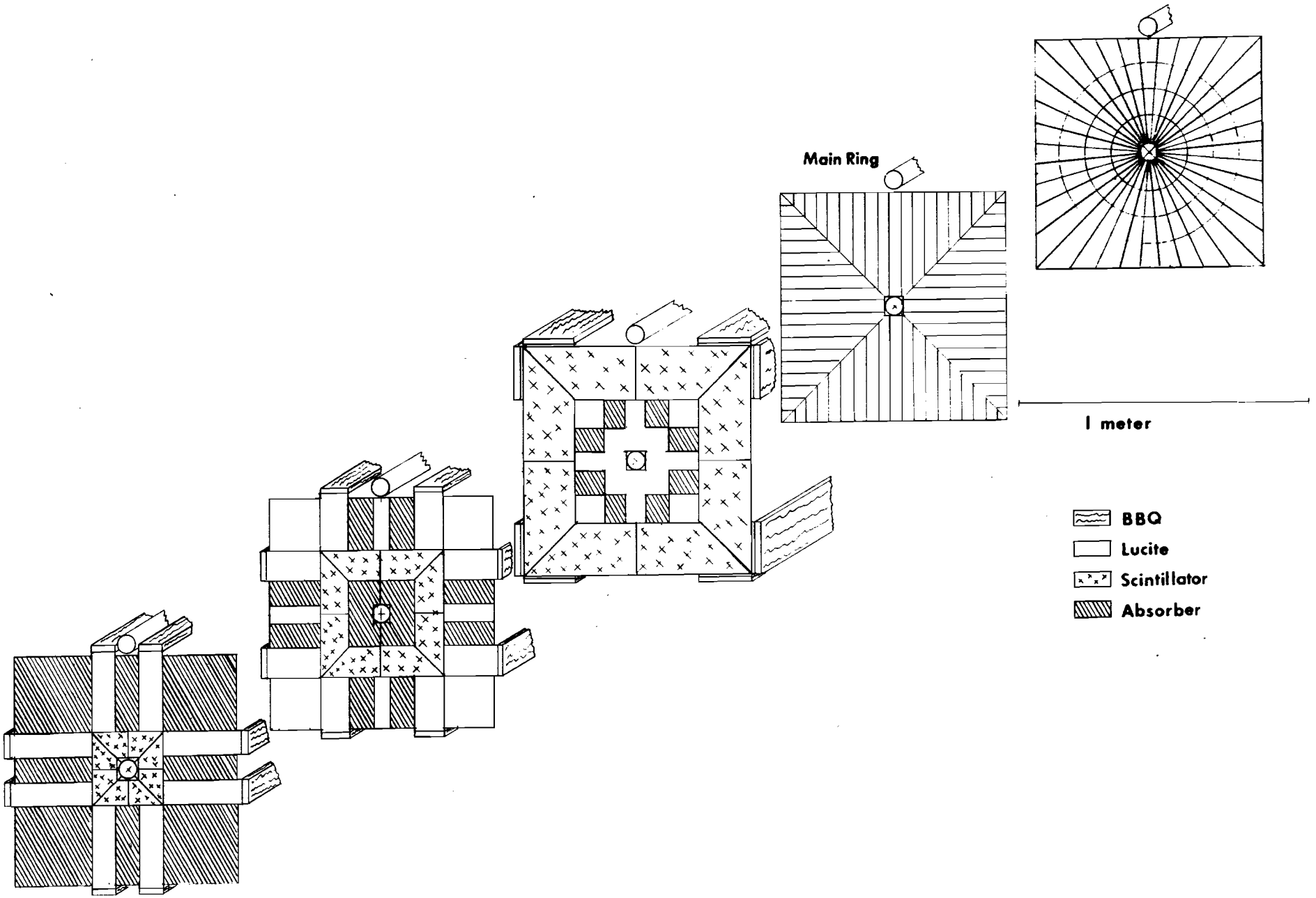


Figure II-7: Exploded view showing the absorber, scintillator, light pipes, and PWC pads for several layers of an end cap calorimeter. The forward and very forward calorimeters would be similar. Only the cathode pads in the PWC's are read out.

that a particle passing through at any position goes throught the same amount of lead, iron, and plastic. Each of the end caps contains 72 photomultiplier tubes and 2016 cathode pads. The pads are ganged in depth to give a total of 864 separate PWC readout channels. The same readout electronics will be used as in the central calorimeter PWC's.

### 5. Forward and Very Forward Calorimeters

The forward calorimeters will be approx. 8.5 m on either side of the interaction point. They cover the approx. angular range $3 < \theta < 30$ mr. Their design is very similar to the end cap calorimeters and need not be discussed in detail.

The very forward calorimeters cover the approx. angular range $1 < \theta < 3$ mr. This is accomplished by moving these calorimeters and their tracking chambers closer to the circulating beams, once the beams are stable. This requires that the calorimeters be split into two "halves" left and right of the beam. The successive sections are connected with a standard flexible bellows to allow the required horizontal motion. The calorimeters are also split into two sections longitudinally so that particles lost from the upstream ones are caught in the farther ones. This insures that almost all of the energy is contained even for particles striking the inner edge of one of the first two sections. This design is simpler than "Roman pots" and allows coverage of the complete range in $\phi$. It does not require any detectors in the vacuum.

The design of these calorimeters is very similar to the end cap and forward calorimeters. An overall view of one section is shown in Figure II-8.

We have made estimates of the background in the farthest tracking chambers due to particles produced in the calorimeters farther upstream. This

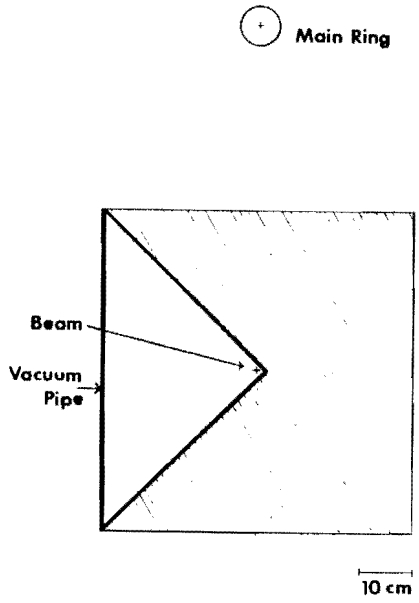


Figure II-8: A front view of one of the very forward calorimeters. These can be moved closer to the beams once they are stable.

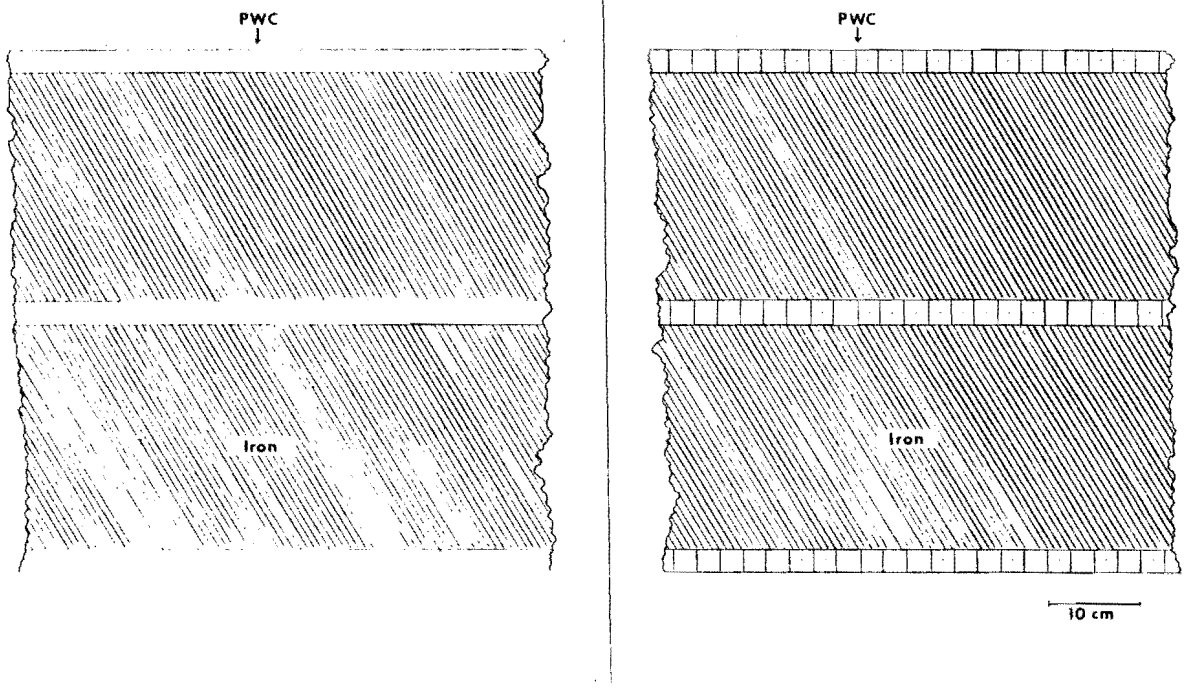


Figure II-9: A detailed view of part of one muon wall as seen in a section parallel to the beam (left) and looking into the beam (right).

is discussed in detail in Appendix A. The general conclusion is that background in the tracking chambers due to spray from the calorimeters will on the average produce $\lesssim$ 0.2 background tracks per event.

### 6. Muon Walls

The muon walls contain two layers of iron, each 10" thick with three planes of wire chambers, as shown in Figure II-9. The wires are spaced approx. 2.54 cm. The same analog readout discussed for the central calorimeter wire chambers will be used. Both ends of each wire will be read out to give the position of the hit along the wire by charge divison. The total weight of the muon wall is approx. 1100 tons.

The muon walls will be used to identify events containing a muon. They completely surround the central detector. It is also assumed that muon detectors will follow the forward calorimeters. These have been omitted in the drawings for simplicity.

### 7. Tracking Chambers

Tracking charged particles with the proposed detector is extremely simple because of the absence of a magnetic field. We assume tracking chambers of a more or less conventional design, but we have not settled on a specific scheme. We tend to favor multiwire chambers with wire spacing ~ 2 mm over drift chambers. An accuracy of ± 1 mm is quite sufficient for our purposes. Time resolution is better, and the electronics and data analysis are much simpler with the multiwire chamber design.

A lead or tungsten converter ~3 rad. lengths thick might be used just ahead of the last plane of tracking chambers to help identify electrons as is done in UA2.

A final decision on a tracking chamber design will be made after a careful study of designs being used at other detectors around the world.

## 8. Triggering the Detector

We anticipate that the most generally useful triggering scheme will be based on total transverse energy $\sum E_T$ and missing transverse momentum $-\sum \vec{P}_T$, where we define

$$\sum E_T = \sum E_{Ti}$$

and

$$|\sum \vec{P}_T|^2 = (\sum P_{xi})^2 + (\sum P_{yi})^2$$

with the sums over hadrons, $\gamma$'s, and electrons. Both of these quantities are typically much larger for events containing "new physics" than for the great majority of events which come from soft hadron-hadron interactions. The missing transverse momentum, in particular, will be large for events with a high $P_T$ neutrino or other invisible particle. This occurs for example in $W^{\pm} \to e^{\pm} + \nu$, $Z \to 2\nu$, and decays of hypothetical particles such as gluinos and leptoquarks.

The arrangement of scintillators and phototubes in the proposed central detector is ideal for implementing such triggers, both because of the fine granularity (>1500 phototubes) and the fact that each scintillator lies along a line of approx. constant $\theta$. A linear sum of the phototubes weighted by $\sin\theta$ gives a very good measure of $E_T$. The "$\sin\theta$" weighting can also include any first-order correction for a $\theta$ dependence of the calorimeter energy response. A schematic diagram of a $\sum E_T$ trigger is shown in Fig. II-10. An adjustable threshold is provided so that small pulses can be disregarded in forming the trigger if desired.

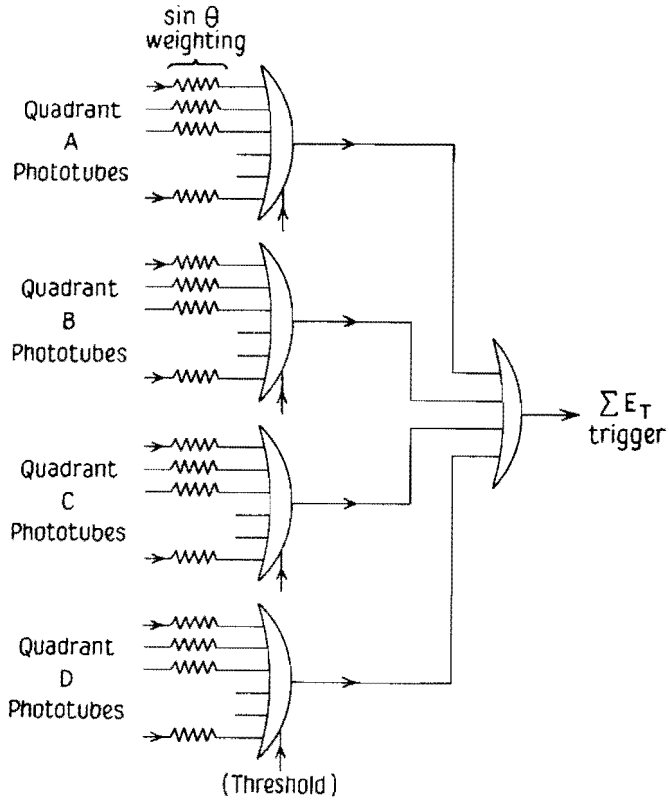


Figure II-10: Schematic of the transverse energy trigger. The trigger is based on a linear summation of pulse heights from each phototube in the central calorimeter with a weight proportional to sin Θ.

A missing transverse momentum trigger can be implemented as the logical "OR" of analog differences such as

$$\underset{\text{Quad A}}{\Sigma E_i \sin \Theta_i} - \underset{\text{Quad B}}{\Sigma E_i \sin \Theta_i}$$

This is not quite as sharp as the $E_T$ trigger but should be sufficiently accurate to conservatively identify events of interest when used in conjunction with a requirement on $\Sigma E_T$.

Other trigger requirements that could be easily imposed are high multiplicity in the central detector or small missing energy. These seem to be less useful constraints, but may turn out to be important.

# III. PHYSICS WITH THE PROPOSED DETECTOR

We have made extensive Monte Carlo studies which simulate the characteristics of the proposed detector and physics at $\sqrt{s}$ = 2000 GeV. These have been used to optimize the detector design and to test how well it can do the physics discussed in Sect. I. We discuss here a number of examples which serve to illustrate the capabilities of the detector. This list is by no means complete. As always, there is the distinct possibility that the most important physics done by the detector is completely unanticipated. We cannot do Monte Carlo studies of unexpected phenomena; however, a detector with the broadest capabilities is the most likely to discover new phenomena. In addition to being able to do an impressive amount of foreseeable physics, the proposed detector may also have the best chance of seeing something unexpected.

## 1. General Description of the Monte Carlo

In the discussion below we assume a run with a total integrated luminosity of $10^{36}$ cm$^{-2}$. This is based on an average luminosity of $1.8 \times 10^{29}$ and a total run of approx. 5 months, as discussed in Sect. IV.

Most of the Monte Carlo studies have been done with ISAJET.[1] This seems to be the most complete and realistic program available for simulating high energy hadron interactions. Separate sections of the program can be used to generate "minimum bias" events (MINBIAS), jet events and heavy quarks (TWOJET), and W and Z production and decay (DRELLYAN). In addition, special subroutines have recently been added to generate gluinos and scalar quarks (SUPERSYM).[2] The latter can also be used to simulate leptoquark production which should be very similar to the production of pairs of scalar quarks with the same mass.

ISAJET includes reasonable estimates of heavy flavor production. Quarks are dressed into realistic hadron jets. These hadrons are given realistic branching ratios for decays into their possible decay modes. Beam jets are generated (except for minimum bias events). Checks have been made to show that the results agree reasonably well with early results from the CERN collider.[1]

In the Monte Carlo studies with ISAJET we have generally used the Baier et al. parton distributions[3] with $\Lambda_{QCD}$ = 0.5 GeV. This value of $\Lambda_{QCD}$ was assumed because the Baier et al. structure functions were derived using this value. If a lower value of $\Lambda_{QCD}$ is used, the structure functions should also be revised.[4] Except as noted otherwise total production cross sections for each process are those calculated by ISAJET with $\Lambda_{QCD}$ = 0.5.

Events generated by ISAJET are fed into another program that simulates the proposed detector and places cuts or constraints on the events. These cuts, where appropriate, are chosen to isolate the desired signal from the backgrounds. In general, for physics which involves missing $P_T$ we assume that events which contain a muon or electron with momentum >1.5 GeV/c would be cut. This greatly reduces backgrounds from the semileptonic decay of heavy flavors where the charged leptons are accompanied by unseen neutrinos.

In the detector simulation we assume that the calorimeters have a fractional energy resolution of $0.65/\sqrt{E}$ for hadrons and $0.20/\sqrt{E}$ for $\gamma$'s and electrons. This hadron energy resolution is consistent with that found for similar hadron calorimeters. For example, G. Bellettini et al.[5] report an energy resolution of $0.65/\sqrt{E}$ with 5 cm iron plates using wavebar readout. Abramowicz et al.[6] find $\sigma/E \cong 0.7/\sqrt{E}$ with 5 cm plates. With 3.8 cm iron plates and excellent light collection in the central calorimeter, we might expect to do somewhat better. The energy resolution assumed for $\gamma$'s and electrons is probably pessimistic, but this is not a limiting factor in any of

the physics discussed below.

The detector Monte Carlo includes the estimated angular resolution of the detector. The probability of a hadron passing through the calorimeter without interacting is also included. This effect could only be significant for $K_L^\circ$ because charged hadrons punching through the detector would be considered as "muons" and vetoed and because of the relatively long interaction length for K°'s compared to other hadrons. With the proposed design the accuracy of the measurement of missing $P_T$ is determined primarily by the energy resolution of the detector and the possibility of particles escaping out of the beam "holes" which are taken as 1.5 mr in the Monte Carlo.

For a typical background study, for example for $Z \to 2\nu$, the backgrounds from minimum bias events, two-jet events, W and t decays, and $Z \to$ all (except $\nu\nu$) were generated separately and combined, with each scaled to an integrated luminosity of $10^{36}$ cm$^{-2}$. Table III-1 shows the number of each type of event typically generated, the factor by which these had to be multiplied for an integrated luminosity of $10^{36}$, and the total events expected.

Table III-1

Numbers of events generated for each process and multiplication factor for an integrated luminosity of $10^{36}$ cm$^{-2}$.

| Process | Events Generated | Mult. Factor | Events/$10^{36}$ |
|---|---|---|---|
| MINBIAS | 800,000 | $5.0 \times 10^4$ | $4.0 \times 10^{10}$ |
| TWOJET($P_T > 20$) | 8,000 | $2.0 \times 10^4$ | $1.6 \times 10^8$ |
| TWOJET ($P_T > 130$) | 8,000 | 5.0 | $4.0 \times 10^4$ |
| TOP QUARK PAIRS ($50 > P_T > 1$ GeV/c, $M_t = 20$ GeV) | 8,000 | 50 | $4.0 \times 10^5$ |
| $W \to$ all | 8,000 | 5.7 | $4.6 \times 10^4$ |
| $Z \to$ all (no $\nu\bar{\nu}$) | 2,000 | 7.3 | $1.5 \times 10^4$ |
| $Z \to 2\nu$ | 3,000 | 1.0 | $3.0 \times 10^3$ |

The MINBIAS and TWOJET events had to be multiplied by large factors, since it is difficult to generate sufficient numbers of events. The apparent missing $P_T$ of the minimum bias events was determined mainly by the energy resolution of the detector. To save computer time, each of the MINBIAS events generated by ISAJET was put through the energy smearing algorithm 100 times, so that each ISAJET event was effectively used to simulate 100 minimum bias events. As a check to be sure that the relatively small number of large $P_T$ TWOJET events might generate a significant background which is missed because of statistics, two-jet events with $P_T > 130$ GeV/c were generated separately. This effectively meant that two-jet events with $P_T > 130$ GeV/c were double counted.

Quark jets, including heavy quarks, are generated in TWOJET. Below a $P_T$ ~20 GeV/c, the procedure used to generate the light quark jets in ISAJET is of doubtful validity. Low $P_T$ top quark pairs were therefore generated separately; t quark masses of 20 and 40 GeV were both run. Because the general TWOJET events contained $t\bar{t}$ pairs with $P_T > 20$ GeV/c, this meant that top quark jets with $P_T > 20$ GeV/c were double counted. The contribution of t quarks was generally more serious for $M_t = 20$ GeV, so the background estimates below assume $M_t = 20$ GeV.

## 2. Measurement of Missing Transverse Momentum

The existence of the neutrino was first surmised because of an apparent violation of energy-momentum conservation in β-decay. Such a violation is the most general signature for the production of new invisible particles, yet no modern detector at any electron or hadron collider has a significant capability to make use of this signature. A measurement of missing momentum also provides a measure of the momentum of high energy neutrinos such as those from $W \rightarrow e + \nu$ decays. Ideally a detector would be capable of measuring all

three components of the missing momentum. However, even with the proposed detector, which has calorimetry over the complete angular range down to approx. 1 mr of either beam, almost half the energy from a typical interaction is lost out the beam holes. It is however possible to make a fairly accurate measurement of the other two components of missing momentum, those transverse to the beam. With 1 mr beam holes the maximum transverse momentum that can be lost out the beam holes is 1 GeV/c (Fig. III-1). The typical contribution from this source is comparable to or smaller than the uncertainty in $\sum\vec{P}_T$ as determined by the calorimeters.

It is useful to estimate the accuracy with which the missing $P_T$ can be measured. If we take as a "typical" interaction, one which produces 100 20-GeV particles, each with a transverse momentum of 0.5 GeV/c, the error in $P_T$ for each particle is

$$(\Delta P_T)_i \cong \Delta P \sin\Theta = \Delta P(P_T/P) = .072 \text{ GeV/c}$$

where we assume the particle is a hadron and neglect the contribution due to the uncertainty in the angle so that $\Delta P/P = 0.65/\sqrt{20} = 0.145$. The overall error in $\sum P_T$ will be the incoherent sum of the errors for 100 such measurements, or $\Delta P_T \cong 0.72$ GeV/c. Figure III-2 shows the distribution of missing $P_T$ from the complete Monte Carlo calculation described above. The $\sigma$ of this distribution is approx 0.7 GeV/c, in agreement with our rough estimate. The tail on the distribution apparent for missing $P_T > 5$ GeV/c is due to rare large $P_T$ particles whose energy is "mismeasured" and events with neutrinos. Thus we conclude that it is possible to measure the missing $P_T$ with a typical accuracy of better than 1 GeV/c with the proposed detector. Fortunately the tails on the distribution can be greatly suppressed by cutting events which contain uninteresting charged leptons and by other cuts which help isolate events with the right topology. Specific examples of this will

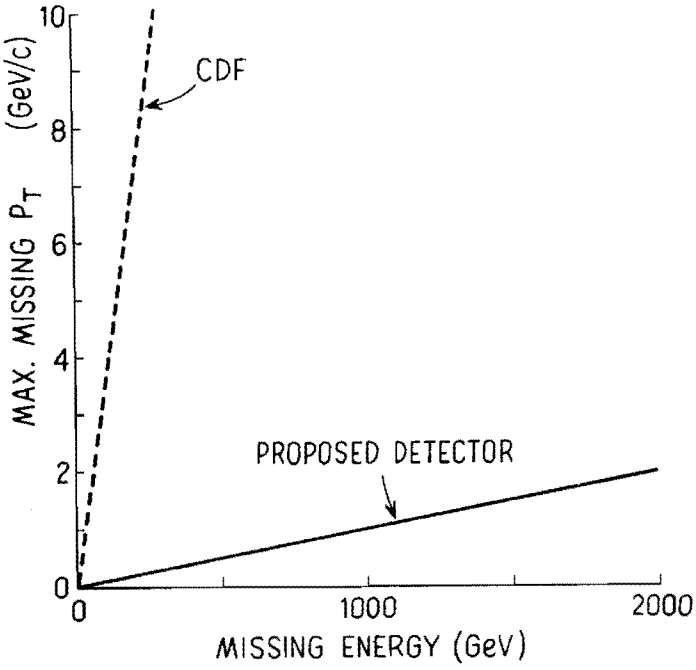


Figure III-1: Maximum missing $P_T$ vs missing energy due to particles exiting the beam holes for the proposed detector if $\theta > 1$ mr in both hemispheres is covered with calorimetry.

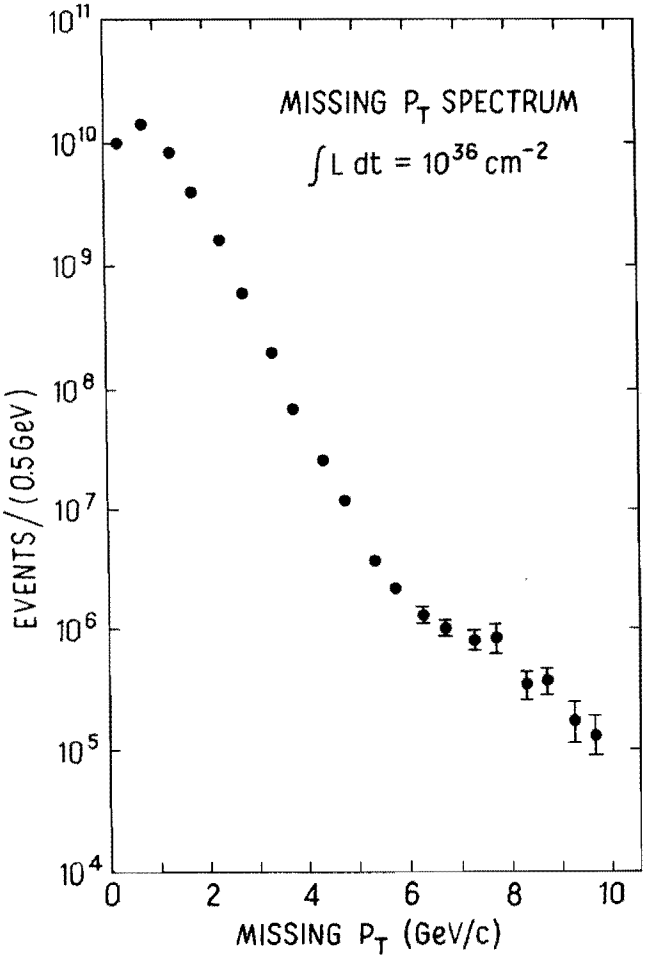


Figure III-2: Distribution of missing $P_T$ from the Monte Carlo program described in the text. The energy and angular resolution of the detector as well as particles escaping out the 1.5 mr beam holes are included. No charged lepton cuts have been applied.

be given in the detailed discussions below.

To compare the capabilities of the proposed detector with those of other detectors, we have made similar Monte Carlo studies for a detector like CDF. For these we assumed beam holes of 50 mr and an energy resolution of $0.65/\sqrt{E}$ for hadrons and $0.20/\sqrt{E}$ for electrons, the same as assumed for the proposed detector. According to H. Jensen[7], about 5% of the solid angle nominally covered with calorimetry is actually insensitive. For 5% of the particles we therefore assumed an energy resolution 3 times as large as given above. With a detector with these characteristics, for an integrated luminosity of $10^{36}$ $cm^{-2}$, over $10^5$ events with an apparent missing $P_T > 20$ GeV/c would appear due to two-jet events with one of the jets exiting a beam hole. This would be enough to swamp most of the interesting physics discussed below.

### 3. Measurement of the W Mass

We discussed briefly in Sect. I the method of determining the W mass from the position of the Jacobian peak in the $e^{\pm}$ momentum spectrum. This method will become difficult if the average transverse momentum of the W's is significantly higher than 10 GeV/c (See Fig. I-1.), which is on the low side of the theoretical estimates. It may also prove difficult if the production cross sections for heavy flavors are higher than expected. This possibility is suggested by the large cross sections for charm production observed at the ISR.

Since the neutrino from $W \rightarrow e + \nu$ typically has a momentum ~ 40 GeV/c, these decays will be accompanied by a very large missing $P_T$. This can provide an additional constraint on the decays and will allow us to make an accurate measurement of the W mass irrespective of the average $P_T$ of the W's. Because the missing transverse momentum is so large the x and y components of the neutrino momentum can be identified with the x and y components of the missing transverse momentum,

$$P_{\nu x} = -\sum P_{ix} \qquad \text{and} \qquad P_{\nu y} = -\sum P_{iy}$$

where the sums include hadrons, photons and electrons outside of 1.5 mr. The mass of the W is given by

$$\begin{aligned} M_W^2 &= E_W^2 - P_W^2 \\ &= (E_e + E_\nu)^2 - |\vec{P}_e + \vec{P}_\nu|^2 \\ &= [(P_{ex}^2 + P_{ey}^2 + P_{ez}^2)^{1/2} + (P_{\nu x}^2 + P_{\nu y}^2 + P_{\nu z}^2)^{1/2}]^2 \\ &\quad - (P_{ex} + P_{\nu x})^2 - (P_{ey} + P_{\nu y})^2 - (P_{ez} + P_{\nu z})^2 \end{aligned} \qquad (1)$$

The z-component of the neutrino momentum is effectively unknown. However, because the W's are typically quite slow ($\beta \approx 0.2$) and because $\langle P_{wx} \rangle \cong \langle P_{wy} \rangle \simeq \langle P_{wz} \rangle$, all of the terms in the square bracket in Eq. 1 are very nearly equal on the average, and the last three parentheses are small and approx. equal on the average. Therefore we can make a good estimate of the W mass, which is almost unbiased, by using only the x and y components in the above equation and multiplying by 3/2.

Then

$$\begin{aligned} M_W^2 \cong \frac{3}{2} \{ &[(P_{ex}^2 + P_{ey}^2)^{1/2} + (P_{\nu x}^2 + P_{\nu y}^2)^{1/2}]^2 \\ &- (P_{ex} + P_{\nu x})^2 - (P_{ey} + P_{\nu y})^2 \} \end{aligned} \qquad (2)$$

All of the quantities on the right-hand side can be measured with good accuracy and an estimate of the W mass can be made from each event.

We have tested this simple-minded algorithm with ISAJET events to establish how well the W mass can be determined and whether background from other sources of high $P_T$ electrons is a problem. To reduce background, we require that the electron have a transverse momentum > 15 GeV/c, and that there be a missing $P_T$ > 15 GeV/c. We also require that there be no other

charged lepton with momentum > 1.5 GeV/c. Cuts on the topology of the events similar to those described below for $Z \to 2\nu$ events could also be applied. However, the above cuts on the electron $P_T$ and missing $P_T$ were found to completely eliminate the background from heavy flavors. The only remaining background was from $W \to \tau + \nu_\tau$ events which was ≈6% of the $W \to e + \nu$. These can easily be estimated and corrected for. With the above cuts approx. 80% of the $W \to e + \nu$ events survive. The distribution of W masses calculated from Eq. 2 for $W \to e + \nu$ events is shown in Fig. III-3 for two choices of the average transverse momentum of the W's, $\langle Q_T \rangle$. The mean $M_W$ for these distributions is 77 GeV; the mass built into ISAJET is approx. 78 GeV. The $\sigma$ of the mass distributions is approx. 17 GeV, almost independent of $\langle Q_T \rangle$. For a run with integrated luminosity $10^{36}$ cm$^{-2}$, we expect > 3000 $W \to e + \nu$ events passing the cuts. From these events the W mass can be determined to a statistical accuracy < 0.4 GeV. Thus the accuracy of the W mass determination is likely to be limited solely by systematics, irrespective of the transverse momentum distribution of the W's. Once more information is available on the production of W's and Z's, any small systematic effects in Eq. 2 can be estimated and corrected for. The possiblity of systematic errors can also be investigated using $Z \to 2e$ events with either electron treated as a $\nu$.

The $P_T$ distribution of the W's can be determined directly from the $W \to e + \nu$ events. For each event

$$\vec{P}_W = \vec{P}_e + \vec{P}_\nu \tag{3}$$

so

$$P_{WT}^2 = (P_{ex} + P_{\nu x})^2 + (P_{ey} + P_{\nu y})^2 \tag{4}$$

All of the quantities on the right-hand side are known so that the transverse momentum distribution of the W's can be measured.

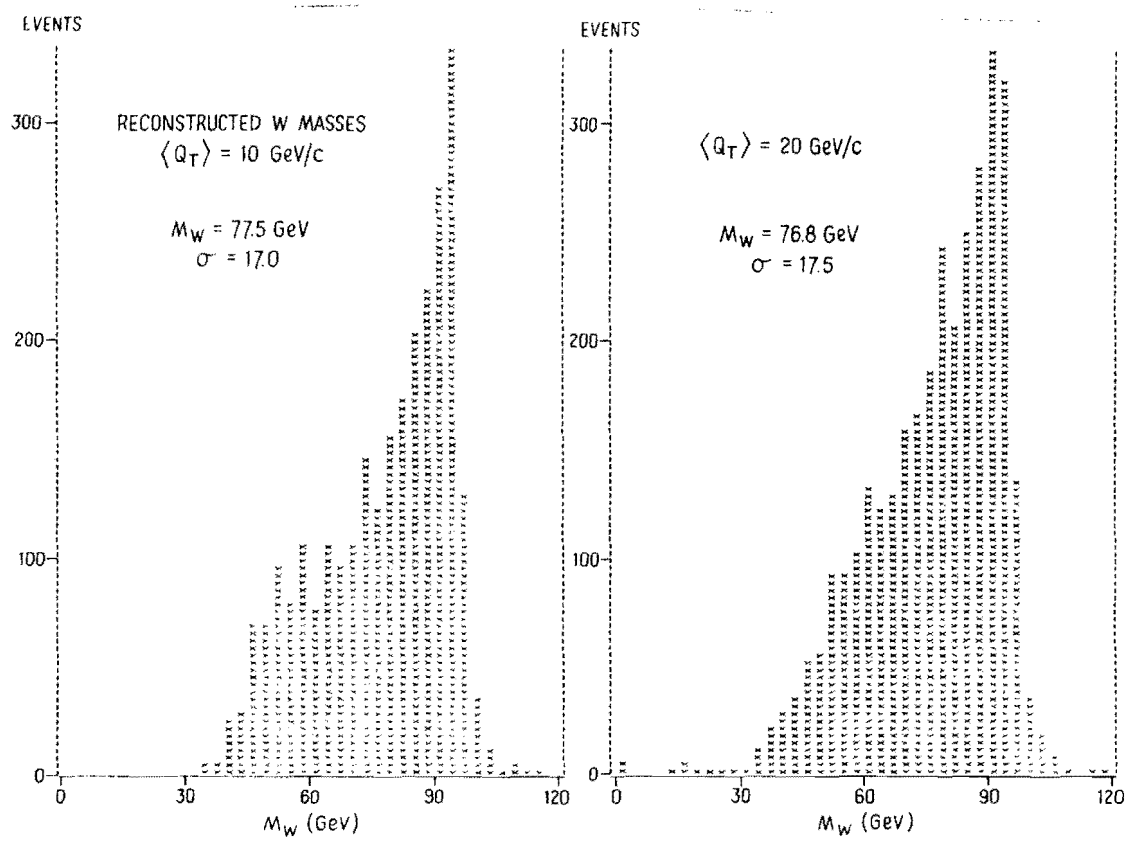


Figure III-3: Distribution of W masses as calculated from only the x and y components of the electron and neutrino momenta (Eq. 2) for two possible values of $\langle Q_T \rangle$, the average transverse momentum of the W's. The distributions have a width $\sigma \cong 17$ GeV.

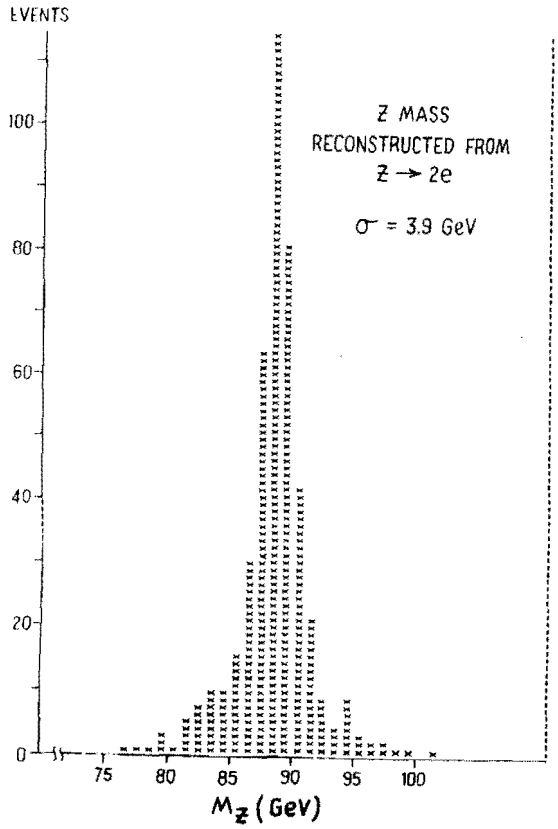


Figure III-4: Distribution of Z masses as reconstructed from Z → 2e events with the energy resolution of the detector included. The width σ of the distribution is approx. 3.9 GeV, the same width as the parent distribution from ISAJET.

## 4. Measurement of Z mass, $M_W/M_Z$, and $\rho$

The mass of the Z will eventually be measured to very good accuracy at $e^+e^-$ colliders. However, to minimize systematic errors in the ratio $M_W/M_Z$ it is important to measure $M_W$ and $M_Z$ in the same detector.

A measurement of the $Z^\circ$ mass with our detector is straight-forward using $Z \rightarrow 2e$ decays. Figure III-4 shows a Monte Carlo distribution of the measured Z masses, as reconstructed from $Z \rightarrow 2e$ decays. The resolution of the detector, as discussed above, is included. With an integrated luminosity of $10^{36}$ $cm^{-2}$ we expect $\approx$ 500 events. The $\sigma$ of the Z peak is approx. the width of the parent Z mass distribution generated by ISAJET, approx. ±4 GeV. Thus we would have statistical error in $M_Z$ of approx. ±0.19 GeV.

From the above we conclude that the statistical errors in $M_W$ and $M_Z$ will both be < 0.6%. The errors in both will be determined by the accuracy with which the energy calibration of the detector can be measured and maintained over long periods of time. With careful and detailed measurements in a test beam and continuous checking with light flashers and radioactive sources, we believe the calibration can be measured and maintained to approx. ±2%. This will determine the ultimate accuracy with which $M_W$ and $M_Z$ can be measured individually.

Fortunately the parameter which is most important theoretically is $\rho \equiv M_W^2/(M_Z^2 \cos^2\Theta_W)$. The systematic errors in $M_W$ and $M_Z$ due to the uncertainty in the energy calibration are very strongly correlated. $M_Z$ is determined from the momenta of two high $P_T$ electrons; $M_Z$ comes from the measurement of a high $P_T$ electron and the missing $P_T$ --which is determined by summing the separate momentum measurements of the electron and all other hadrons and $\gamma$'s from the interaction.--Thus it should be possible to measure $\rho$ to an ultimate accuracy of < 1% if $\cos^2\Theta_W$ is known from other experiments.

## 5. Measurement of $(Z \to 2\nu)/(Z \to 2e)$

As discussed in Sect. I this is an extremely important measurement because the number of neutrino species can be determined from it. If only three species exist, $\nu_e$, $\nu_\mu$, and $\nu_\tau$, this ratio is expected to be approx. 6.0. An accuracy of ± 20% in the ratio is adequate to establish that there are only 3 species.

As shown below, the accuracy with which this ratio can be measured depends to some extent on the transverse momentum spectrum of the Z's. This is because isolating the $Z \to 2\nu$ decays from the background is done on the basis of missing transverse momentum. For a $Z \to 2\nu$ decay the missing $P_T$ is equal to the $P_T$ of the Z so that the missing $P_T$ spectrum is the same as the transverse momentum spectrum of the Z's. Separating the $Z \to 2\nu$ events is generally easier if the average $P_T$ of the Z's, $\langle Q_T \rangle$, is larger. However, as discussed below, the principal background for the $Z \to 2\nu$ separation is $W^\pm \to \tau^\pm \nu_\tau$ with the $\tau^\pm$ decaying into hadrons and a neutrino. Because the average $P_T$ of the W's is almost certainly comparable to that of the Z's, the background tends to have the same average missing $P_T$ as the signal, irrespective of $\langle Q_T \rangle$. Thus the overall signal/background tends <u>not</u> to be a strong function of $\langle Q_T \rangle$.

As discussed in Sect. I-1 it is difficult to predict the transverse momentum spectrum of the Z's reliably. We estimated there that the average $P_T$ of the W's and Z's at $\sqrt{s}$ = 2000 GeV probably lies in the range 10 to 35 GeV/c. We have therefore run the Monte Carlos for three choices of $\langle Q_T \rangle$, approx. 10, 20, and 35 GeV/c.

The $Z^\circ \to 2\nu$ events will have a rather distinctive topology which greatly facilitates their identification. This is illustrated in Fig. III-5 which shows a polar plot of a typical $Z \to 2\nu$ event as seen looking along the beam axis. In the plot particles with $\Theta < 140$ mr relative to either beam are

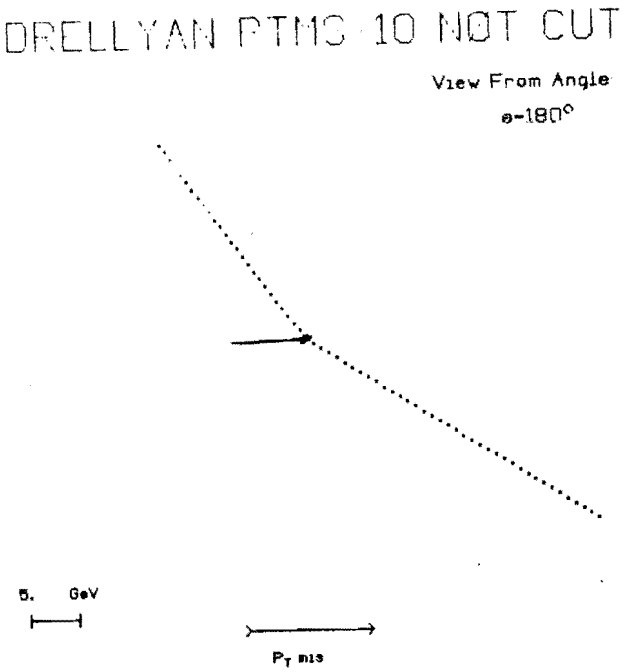


Figure III-5: A view of a $Z \rightarrow 2\nu$ event as seen looking into the beam. The length of each vector represents the transverse momentum of the associated particle. Charged particles are shown as solid lines. Dashed lines represent $\gamma$'s. Neutrinos are dotted. Particles within 140 mr of the beam are omitted for clarity. The missing $P_T$ is calculated from the transverse momenta of all hadrons, photons, and electrons outside of 1.5 mr from the beams.

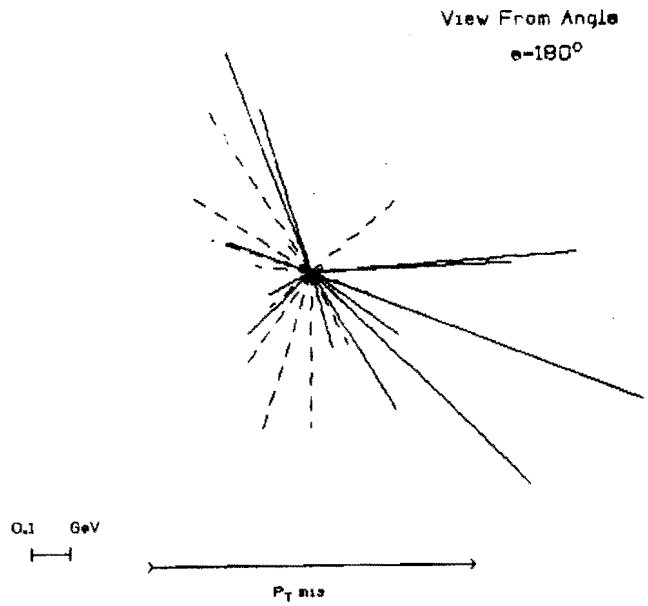


Figure III-6: Same as Fig. III-5 for a typical minimum bias event. Note the scale for the missing $P_T$ vector.

excluded to eliminate the beam jets. The length of each vector represents the $P_T$ of the particle. The (unseen) neutrinos are shown as dotted lines. The overall missing $P_T$ vector is also shown; this is also the $P_T$ of the parent Z. As expected from kinematics the gluon jet which recoils against the Z lies directly opposite the missing $P_T$ vector.

For comparison, we show in Figures III-6 to III-9, similar plots for typical background events. Figure III-6 shows a typical "minimum bias" event. Note that the missing $P_T$, in this case due to detector resolution and particles exiting the 1.5 mr beam holes, is very small. It is also not correlated in direction with any obvious grouping of particles. Figure III-7 shows a two-jet event. In this case the missing $P_T$ is larger, but bears no correlation with the direction of either jet. Figure III-8 shows an event containing a pair of top quark jets. The missing $P_T$ is aprox. 27 GeV/c but again shows no apparent correlation with the direction of a jet. Figure III-9 shows the most serious background for the $Z \to 2\nu$ separation. This contains the decay of a W to $\tau + \nu_\tau$ with the $\tau$ subsequently decaying into hadrons + $\nu_\tau$. The missing $P_T$ is quite large. However, the missing $P_T$ vector is not usually antiparallel to the gluon jet as in the $Z \to 2\nu$ events.

Thus the $Z \to 2\nu$ events have an almost unique topology, which we can use to reduce the background by a large factor. We have used ISAJET events to study the effect of various cuts. The cuts finally chosen, as discussed below, are probably not optimal, but serve to illustrate what can be done in a fairly straightforward fashion to isolate a clean $Z \to 2\nu$ sample. Eventually an optimization based on real data will be possible. This can probably be done most effectively with an algorithm which is taught to select $Z \to 2\nu$ events using $Z \to 2e$ events with the electrons replaced by $\nu$'s.

To describe the cuts we have imposed on the Monte Carlo events, it is

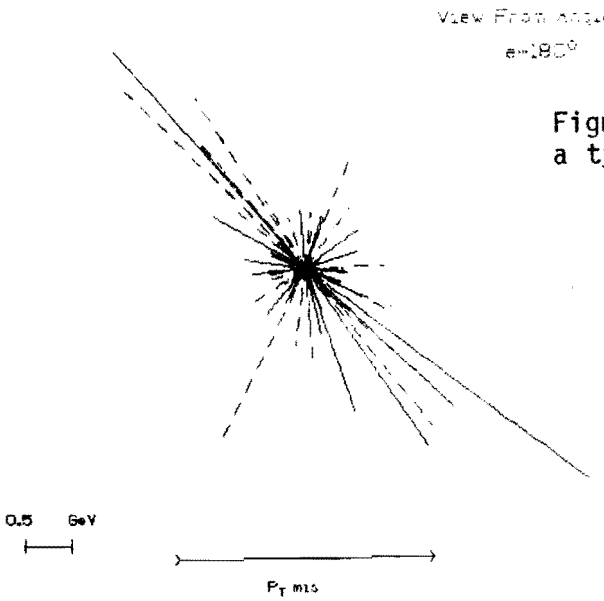


Figure III-7: Same as Fig. III-5 for a typical two-jet event.


Figure III-8: Same as Fig. III-5 for a typical event with a pair of top quarks produced. This event contains 2 electrons and 3 neutrinos.

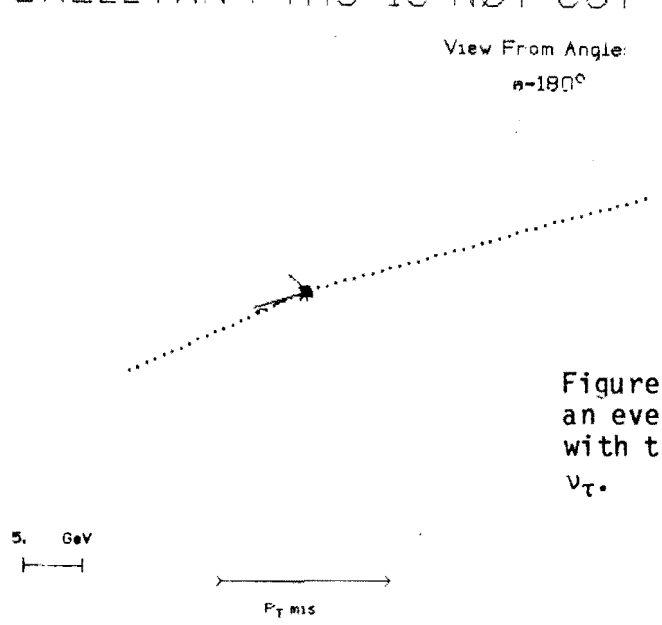


Figure III-9: Same as Fig. III-5 for an event with a W decaying into $\tau + \nu_\tau$ with the $\tau$ decaying into hadrons and $\nu_\tau$.

convenient to choose the x-y axis so that the missing $P_T$ is aligned with the +x axis as is done in Fig. III-5. We define the "missing $P_T$ hemisphere" as the region $-90° < \phi < 90°$ and the "jet hemisphere" as $|\phi| > 120°$. For the jet hemisphere we compute the three sums over all visible particles with $P_T > 1.5$ GeV/c,

$$S_1 = \sum P_{Ti} \cos \phi_i \tag{5}$$

$$S_2 = |\sum P_{Ti} \sin \phi_i| \tag{6}$$

$$S_3 = \sum P_{Ti} |\sin \phi_i| \tag{7}$$

where particles within 40 mr of the beams are excluded. $S_1$ is a measure of the total $P_T$ of the gluon jet. For $Z \to 2\nu$ events we expect it to be comparable in magnitude to the missing $P_T$. $S_2$ in the jet hemisphere is a measure of the alignment of the jet with the missing $P_T$ vector; $S_3$ is a measure of the flatness of the jet. In the jet hemisphere both $S_2$ and $S_3$ should be small compared to the missing $P_T$ for $Z \to 2\nu$ events. In the missing $P_T$ hemisphere, we expect few or no particles with $P_T > 1.5$ GeV/c since this is the hemisphere containing the Z. The multiplicity of particles with $P_T > 1.5$ in the missing $P_T$ hemisphere is therefore required to be zero unless the missing $P_T$ is > 50 GeV/c. The multiplicity of particles with $P_T > 1.5$ GeV/c in the jet hemisphere is also required to be nonzero and not too large in relation to the missing $P_T$.

Figures III-10 through III-13 compare the operation of these cuts for $Z \to 2\nu$ decays and for W decays, the most troublesome background. In each case the magnitude of the missing $P_T$ is plotted along the x-axis and the sums defined above along the y-axis. The cut imposed is shown as a straight line on the scatter plots. A cut on charged leptons with momentum >1.5 GeV/c has already been applied.

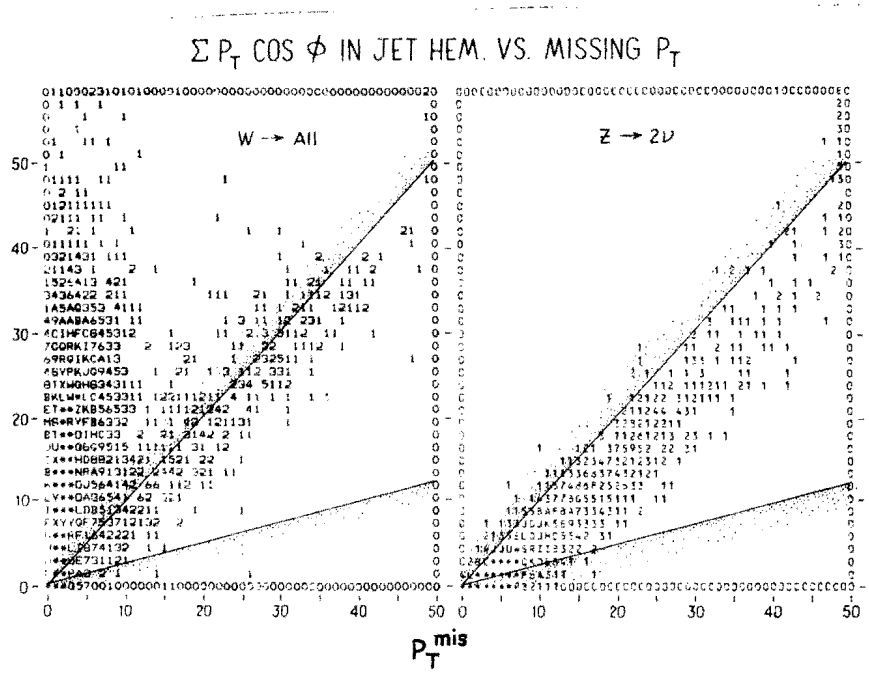


Figure III-10: $\sum P_{Ti}$ cos $\phi_i$ vs. missing $P_T$ for particles with $P_T > 1.5$ in the jet hemisphere for W → (all) compared to Z → 2ν [$\langle Q_T \rangle$ = 10 GeV/c]. Bins in the scatter plot are filled in the order 1, 2, . . . . A, . . . ., Z with * signifying an overflow. Events between the two lines are kept.

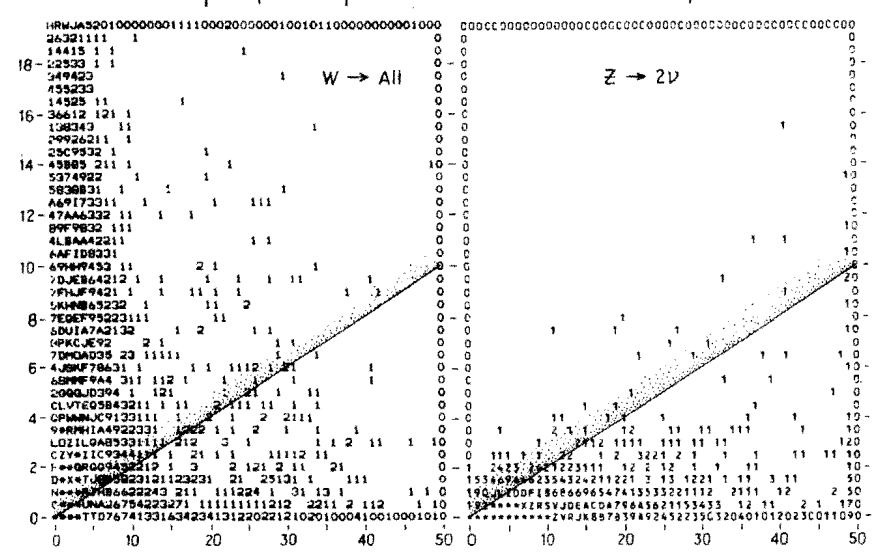


Figure III-11: $|\sum P_{Ti}$ sin $\phi_i|$ vs. missing $P_T$ for particles with $P_T > 1.5$ in the jet hemisphere. Events below the line are kept.

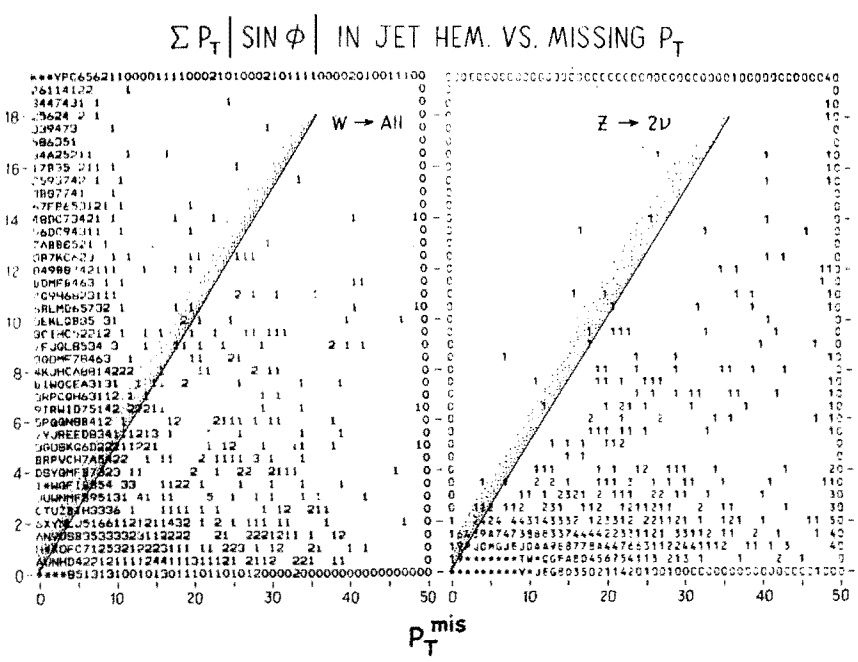


Figure III-12: $\sum P_{Ti} |\sin \phi_i|$ vs. missing $P_T$ for particles with $P_T > 1.5$ in the jet hemisphere. Bins in the scatter plot are filled in the order 1, 2, . . . ., A, . . . ., Z with * signifying an overflow. Events below the line are kept.

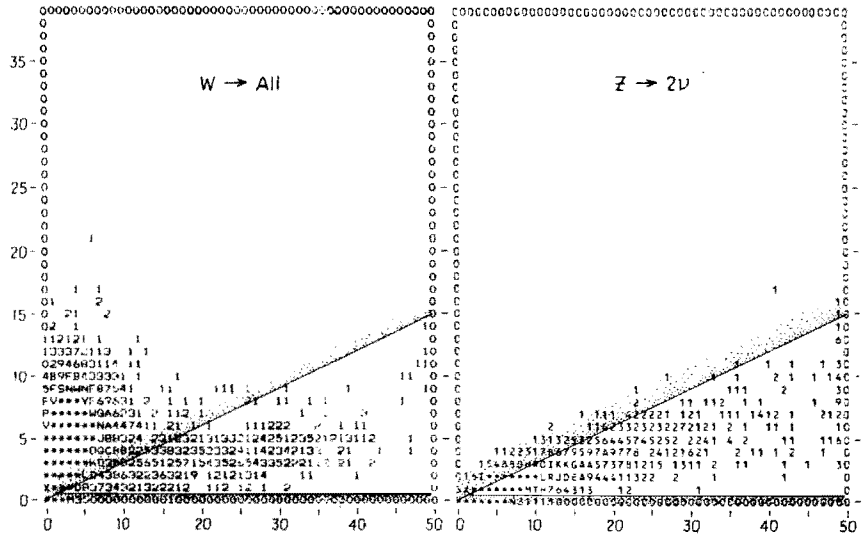


Figure III-13: Multiplicity of particles with $P_T > 1.5$ GeV/c in the jet hemisphere vs. missing $P_T$. Events between the lines are kept.

The gluon jet recoiling against the Z should also define a narrow cone in $\Theta$, the angle of each particle relative to the beam direction. To measure this quantitatively, for visible particles in the jet hemisphere with $P_T > 1.5$ GeV the angular spread between the highest and lowest momentum particles was computed,

$$\Delta\Theta = |\Theta_{PMAX} - \Theta_{PMIN}|$$

where $\Theta_{PMAX}$ and $\Theta_{PMIN}$ are the angles for the highest and lowest momentum particles. Fig. III-14 compares $\Delta\Theta$ vs. PMIN for $Z \to 2\nu$ and for $W \to$ (all) events. As might be expected the $\Delta\Theta$ distribution is much narrower for $Z \to 2\nu$ events.

The cuts are extremely effective for two-jet events. We find that no two-jet events with missing $P_T > 15$ GeV/c survive the cuts; all except $t\bar{t}$ events are completely eliminated. The background from $W \to$ (all) is reduced by a factor of 25, that from $t\bar{t}$ events is cut by a factor of almost 500, while $\approx$ 50% of the $Z \to 2\nu$ events survive. As a check against the possibility that very rare high $P_T$ jet events might generate significant background, these were studied separately. (See Table III-1.) These high $P_T$ events were completely eliminated by the cuts.

Figure III-15 compares the $Z \to 2\nu$ signal expected from the Monte Carlo with the total background for 3 values of $\langle Q_T \rangle$, the average transverse momentum of the Z's. A total integrated luminosity of $10^{36}$ is assumed. Even for $\langle Q_T \rangle = 10$ GeV/c the signal is well above the background for much of the missing $P_T$ range. As can be seen from Fig. III-15, the cuts imposed on the events tend to eliminate the signal as well as the background for missing $P_T$ below approx. 10 GeV/c. However the effects of the cuts can be calibrated by imposing the same cuts on $Z \to 2e$ events with the electrons treated as neutrinos. Figure III-16 shows the ratio of $Z \to 2\nu$ to $Z \to 2e$ as a function of

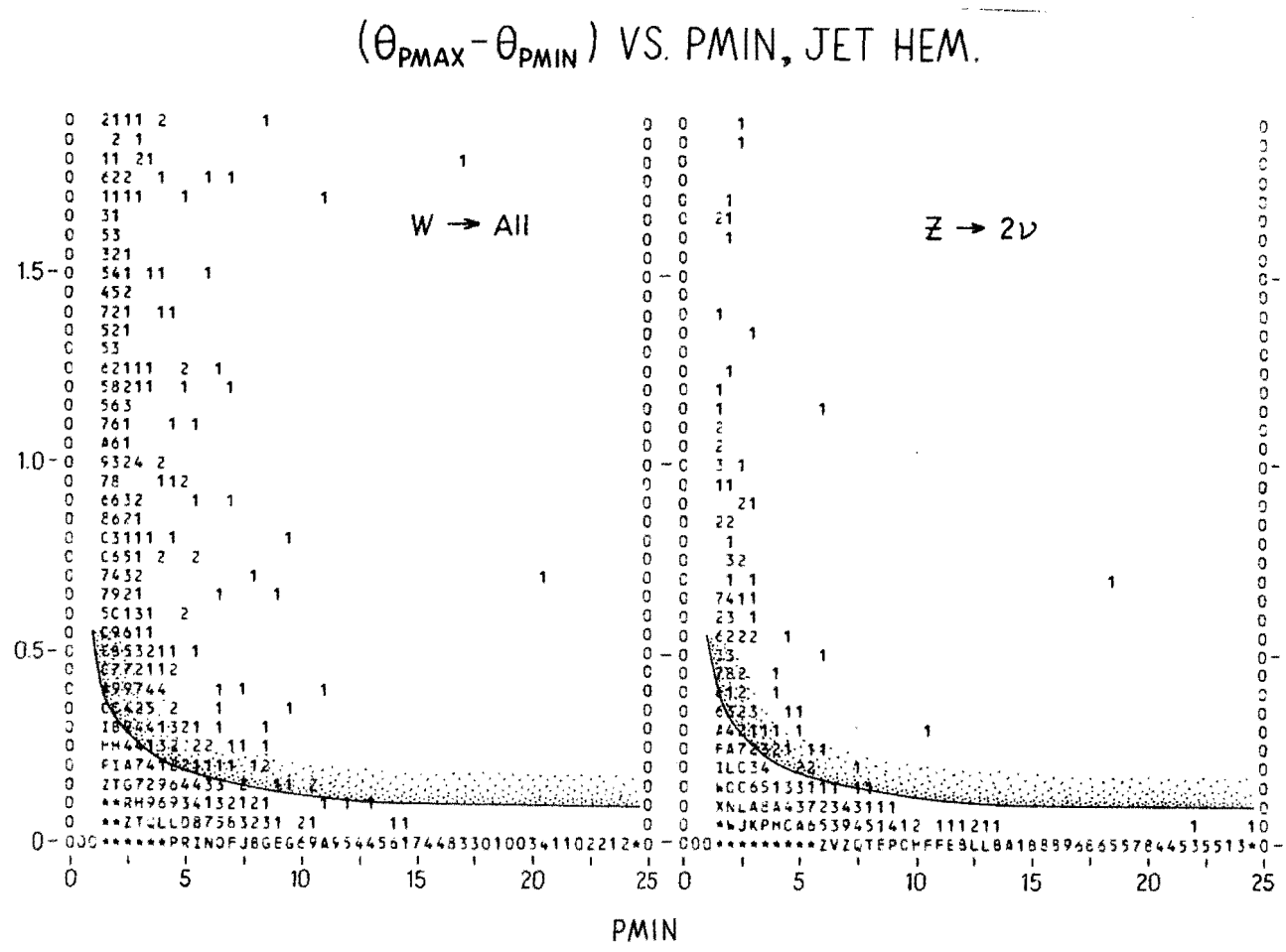


Figure III-14: $|\theta_{PMAX} - \theta_{PMIN}|$ for particles with $P_T > 1.5$ in the jet hemisphere vs. PMIN, the momentum of the lowest momentum particle. The left hand plot is for W → (all) events and the right is for Z → 2ν. Events below the curve are kept.

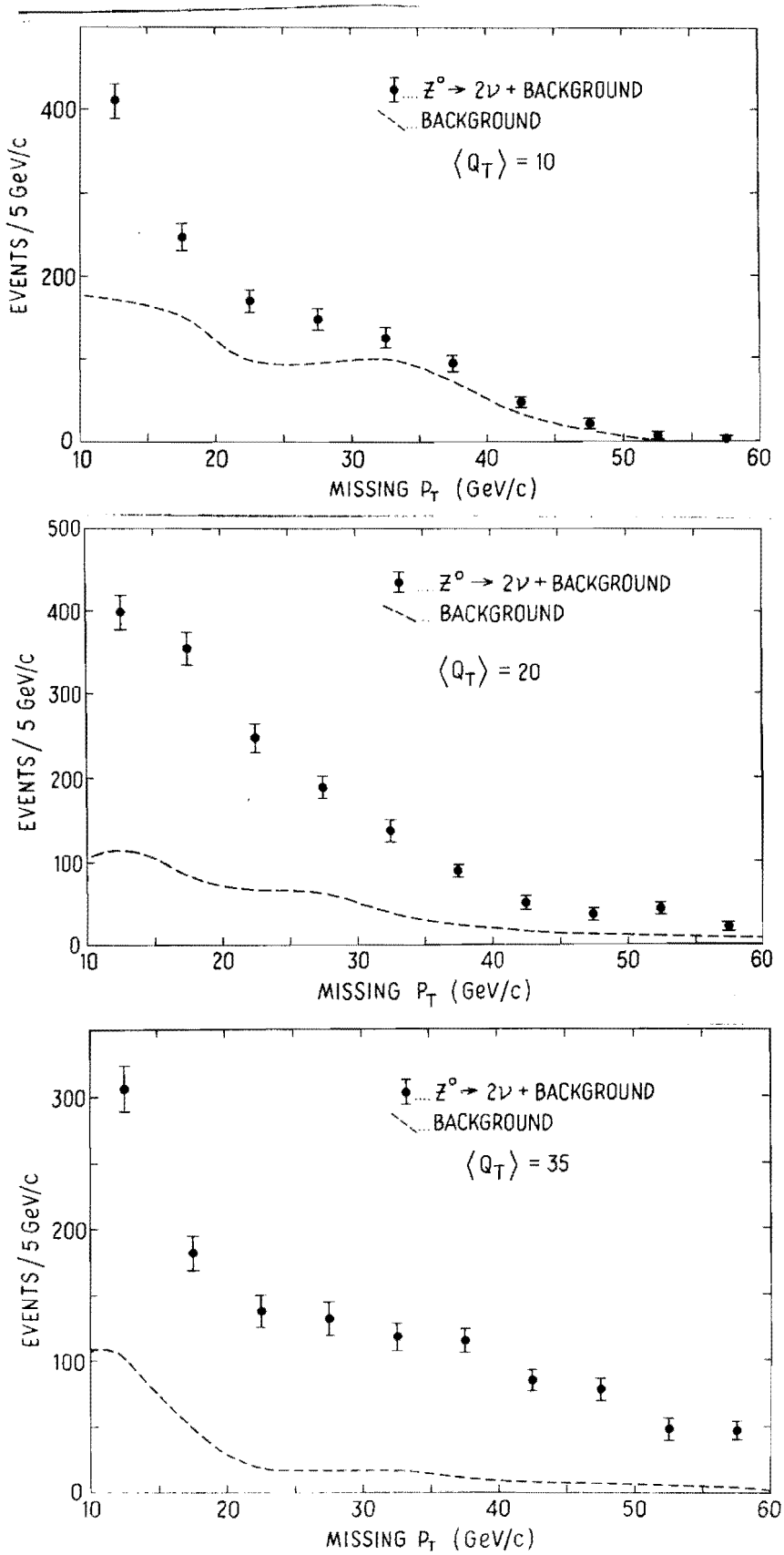


Figure III-15: $Z^\circ \to 2\nu$ signal compared to background for three values of $\langle Q_T \rangle$, the average $P_T$ of the Z's and W's. Below a missing $P_T$ of approx. 20 GeV/c the background is mainly from $t\bar{t}$. For larger missing $P_T$ it is mostly from $W \to \tau + \nu_\tau$. An integrated luminosity of $10^{36}$ cm$^{-2}$ was assumed.

missing $P_T$ for $\langle Q_T \rangle$ = 10 and $\langle Q_T \rangle$ = 20 GeV/c. This is calculated using the smoothed backgrounds sketched in Fig. III-15. The scale on the right shows the apparent number of neutrino species as calculated for each missing $P_T$ bin. Averaged over all missing $P_T$, this gives $(Z \to 2\nu)/(Z \to 2e) = 6.3 \pm 0.4$ for $\langle Q_T \rangle = 20$ and $6.1 \pm 0.5$ for $\langle Q_T \rangle = 10$. From this the number of neutrino species is approx. 3.1 with uncertainty of < 10%. This is as expected since 3 neutrino species were assumed in the Monte Carlo. Note that we will be able to study $(Z \to 2\nu)/(Z \to 2e)$ as a function of missing $P_T$. If the background is understood, this ratio is independent of missing $P_T$. This will give a very important check on the results.

At present little is known about the angular shapes and other characteristics of gluon jets. We have therefore tried to devise cuts which are relatively model independent and depend only on the general features of the $Z \to 2\nu$ events. If the gluon jets turn out to be more diffuse than ISAJET "predicts", the separation of the $Z \to 2\nu$ events will be correspondingly more difficult. However it seems just as likely that ISAJET may be pessimistic in this regard. In any case the background cuts will require careful studies.

In the Monte Carlos we have assumed a t quark mass of 20 GeV. This is the most pessimistic possibility. If the mass is greater the $t\bar{t}$ production will be smaller and the topology cuts become more effective. Even when the t quark mass is known the resulting missing $P_T$ spectrum may be difficult to calculate accurately. It may therefore not be possible to make a sufficiently reliable estimate of the background to the $Z \to 2\nu$ signal below $P_T^{miss} \approx 15$ GeV/c. Above $P_T^{miss} \approx 20$ GeV/c the background will be mainly from $W \to \tau\, \nu_\tau$. This should be straightforward to estimate with sufficient accuracy. If the average transverse momentum of the Z's is as low as 10 GeV/c and we have to rely on only $P_T^{miss} \gtrsim 20$ GeV/c we would only be able to determine the number

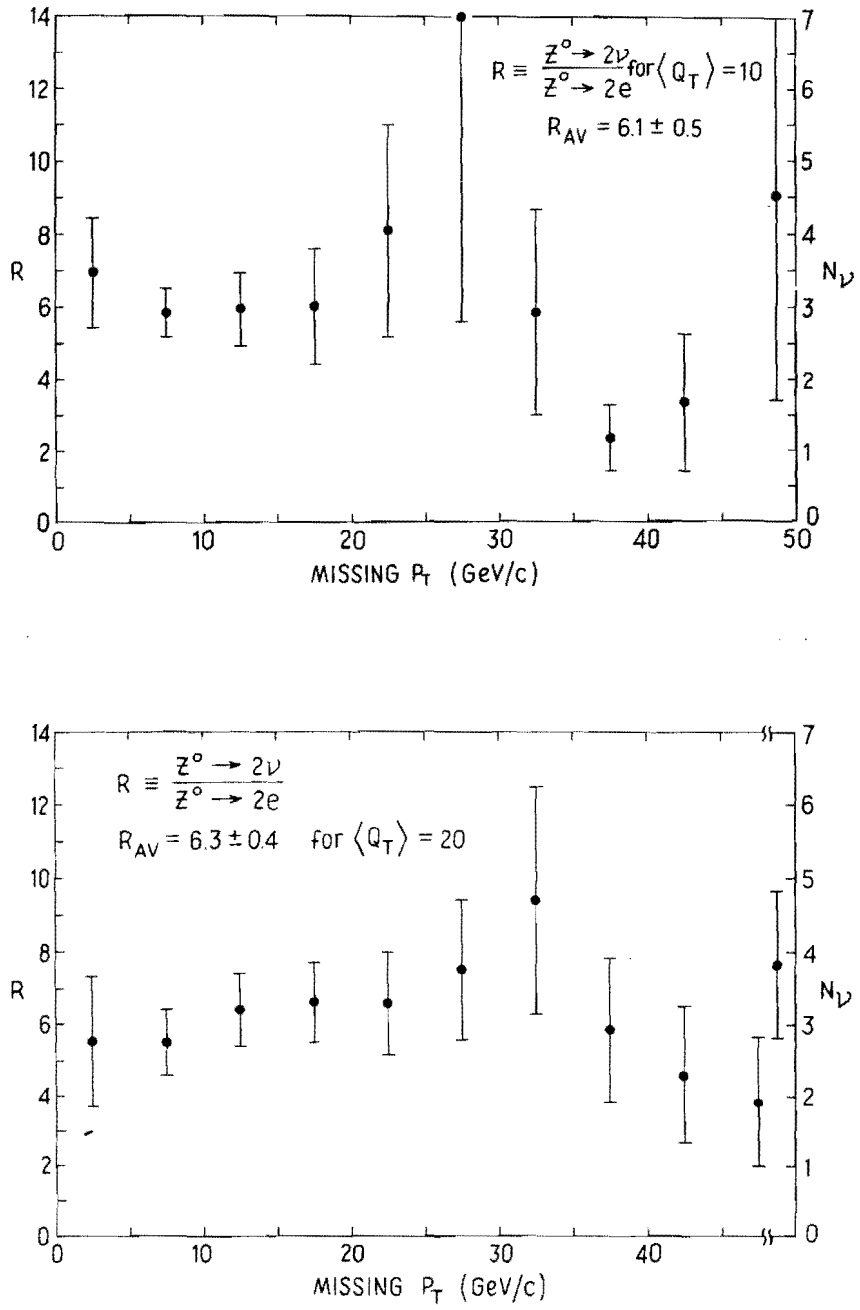


Figure III-16: The ratio of $Z \rightarrow 2\nu$ events extracted from the (signal + background) and background curves of Fig. III-15 and $Z \rightarrow 2e$ events with the same cuts applied. An integrated luminosity of $10^{36}$ cm$^{-2}$ was assumed. The scale on the right shows the apparent number of neutrino species $N_\nu$ for each missing $P_T$ bin. Ideally $N_\nu = 3.00$ for all missing $P_T$.

of neutrino species $N_\nu$ to an accuracy $\Delta N_\nu \cong \pm 0.6$, based on an expected $Z \to 2\nu$ signal of 200 events with missing $P_T > 20$ GeV/c for an integrated luminosity $\sim 10^{36}$ cm$^{-2}$.

It is worth emphasizing that the separation of the $Z \to 2\nu$ events from background ultimately has little to do with the energy resolution of the detector. Even if the tail of the missing $P_T$ distribution of minimum bias events extended much farther than expected, these events would generally be rejected on the basis of their topology --the missing $P_T$ vector would not generally be directed away from a colinear jet.--The same holds for the majority of the jet events. A high $P_T$ two-jet event might fake a large missing $P_T$ event due to measurement errors, but the event would usually fail to pass the cuts. Events with neutrinos are not as much of a problem as might at first be expected because the neutrinos are mostly produced fairly far down the decay chain and tend to have low $P_T$. The charged lepton veto greatly suppresses this background. As explained above, most of the background comes from $W \to \tau\nu_\tau$ events with the $\tau$ decaying into hadrons + $\nu_\tau$. This background is ultimately quite predictable, once data are available on W and Z production. The transverse momentum distribution of the W background events will be essentially the same as for the Z's. Once some data are available and W and Z production is generally understood, the background cuts described above can be tuned to give the best signal/background. We believe that the cuts described above, though very effective in reducing background, are far from optimal. Ultimately even better background rejection should be possible.

### 6. Search for Higher Mass W or Z

As discussed in Section I-1, there are a number of alternative models to the standard model which give a second W or Z with a mass higher than the

standard model. Kane and Perl[12] estimate the production cross section of a hypothetical Z' with mass 300 GeV to be ≈ 50 pb at $\sqrt{s}$ =2000 GeV. The branching ratio to 2e is comparable to that of the "standard" Z in models in which the Z' decays only into three generations of quarks and leptons. This would give about 1.5 events for an integrated luminosity of $10^{36}$. There should be no background; thus we would expect to be sensitive to a Z' with mass $\lesssim$ 300 GeV if the branching ratio to 2e is > 3%.

If a higher mass W' exists and decays to e + ν with an appreciable branching ratio, it will be possible to reconstruct the mass of the massive W' using the technique described above for the W. The distribution of reconstructed W masses in Fig. III-3 falls off rapidly above 100 GeV, so it should be possible to distinguish a massive W' from the standard W if the two masses differ by more than 20 GeV. As for the standard W and Z we might expect the production cross section for the W' to be several times larger than for the Z'. If the branching ratio for W' → e + ν is comparable to that for W → e + ν, we would expect ~ 12 events for a W' mass of approx. 300 GeV.

7. Search for Supersymmetric Particles (or other "Invisible" Particles)

As discussed in Sect. I-2, supersymmetric theories predict the existence of many new particles; the least massive hadronic states are likely to be the gluino $\tilde{g}$ and the scalar quarks $\tilde{\phi}$. These states are expected to be shortlived and decay to final states which include an "invisible" Goldstino $\tilde{G}$ or photino $\tilde{\gamma}$. For our purposes it is useful to consider the $\tilde{g}$ and $\tilde{\phi}$ as examples of particles which are strongly produced and decay into an invisible particle which carries off a large fraction of the momentum of the parent.

The simplest supersymmetric theories tend to predict masses for the $\tilde{g}$, $\tilde{\phi}$,

$\tilde{W}$, . . which are less than or comparable to $M_Z$. Gluinos are particularly attractive from an experimental point of view because they are produced with large cross sections and in many models they are expected to be the lightest of the supersymmetric hadrons since their masses are zero at the tree level. They decay to a gluon and Goldstino or a $\bar{q}q$ and a photino. The invisible $\tilde{G}$ or $\tilde{\gamma}$ lead to a missing $p_T$ which is ~ 0.5 $M_{\tilde{g}}$ for events in which a gluino pair or a gluino plus scalar quark are produced.

We have used the SUPERSYM option of ISAJET to Monte Carlo gluino and scalar quark production. This assumes production cross sections as calculated by Kane and Leveille.[8] The Monte Carlo is similar to that described above for W and Z production. The cuts on the jet topology cannot be used because the supersymmetric particles are produced in pairs so the missing $P_T$ vector is not aligned with a recoiling jet. The backgrounds are therefore higher than for W and Z production.

Figure III-17 shows the results of a Monte Carlo calculation of the missing $P_T$ for $p + \bar{p} \rightarrow \tilde{g} + \tilde{g} + X$ with $\tilde{g} \rightarrow g + \tilde{\gamma}$ for two choices of the gluino mass. These probably represent lower limits for the gluino signal because $\bar{p} + p \rightarrow \tilde{g} + \tilde{\phi} + X$ is not included in the calculation. The cross section for the latter process is expected to be large for reasonable values of the lightest scalar quark mass.[9]

In some models the gluino mass is much larger than the masses of the scalar quarks. To test these models, searches will have to rely on production of scalar quark pairs. The production cross section for these is considerably smaller than for pairs of gluinos of comparable mass. It is likely that there will be two or more scalar quarks with almost the same mass, in analogy with

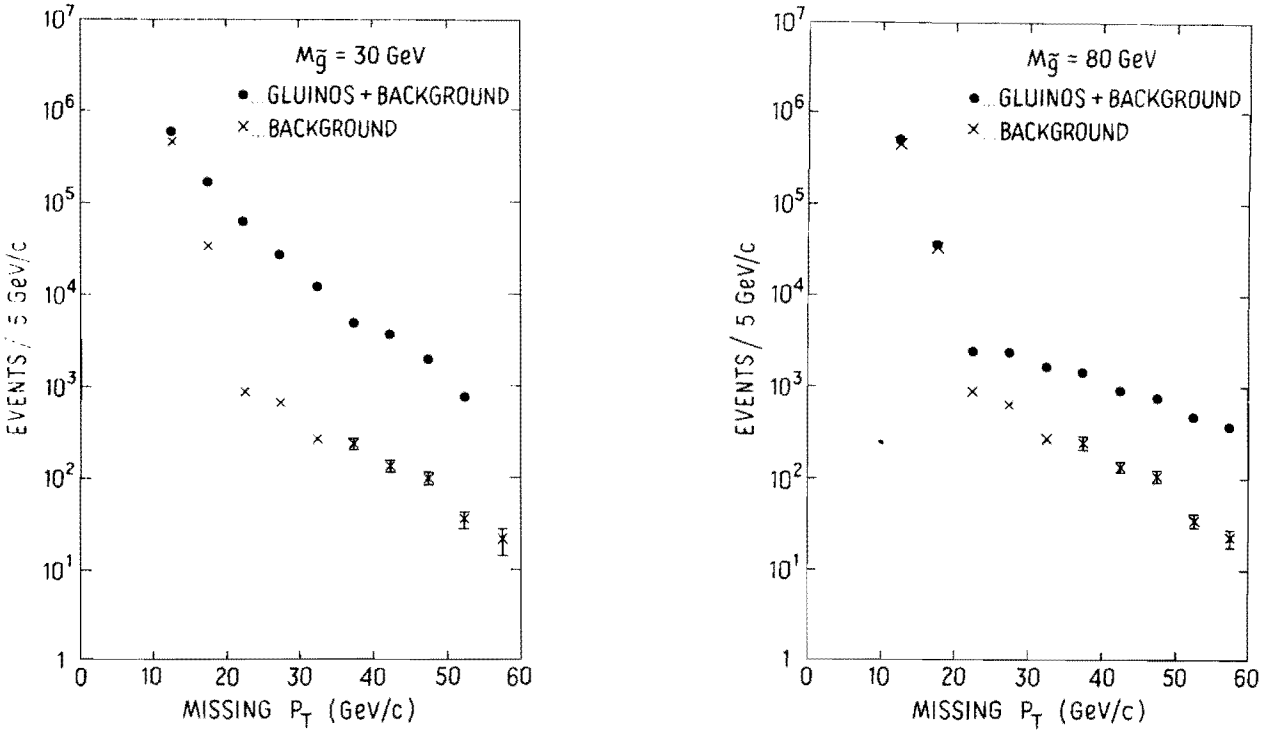


Figure III-17: Missing $P_T$ distribution expected from the Monte Carlo for gluino pair production with $\tilde{g} \rightarrow g + \tilde{\gamma}$. The background is mainly from W and $t\bar{t}$ production. A veto on charged leptons with P > 1.5 GeV/c is assumed.

the up, down, and strange quarks. The experimental signatures of all the scalar quarks will be essentially the same. If we assume there are 2 scalar quarks with masses of approx. 80 GeV, the total production cross section, as predicted using the SUPERSYM option of ISAJET with $\Lambda_{QCD}$ = 0.5 GeV, is 2000 pb. This gives 2000 events for an integrated luminosity of $10^{36}$ cm$^{-2}$. If we assume two body decays $\tilde{\phi} \rightarrow q + \tilde{G}$ for the scalar quarks the missing $P_T$ spectrum in Fig. III-18 is obtained. In this rather optimistic scenario the scalar quark signal is well above the background.

The only cut that has been applied in Fig. III-18 is that there be no charged lepton with P > 1.5 GeV/c. The background is from W and Z decays. It is likely that a large fraction of these background events will be recognizable and can be deleted in practice.

We conclude that gluino or scalar quark production would be detectable in the missing $P_T$ spectrum if the mass of the gluino is < 120 GeV or there are scalar quarks with mass $\lesssim$ 100 GeV. Hinchcliffe and Littenberg[9] have reached a similar conclusion. Comparable limits would apply for other massive particles which are produced strongly and decay with a large branching ratio to a noninteracting neutral particle and no charged lepton.

### 8. Leptoquark Search

Leptoquarks are predicted in technicolor theories as well as in composite theories. They are presumably produced in pairs and decay into a quark plus lepton. The leptoquarks of technicolor, because of their coupling to mass, are expected to decay preferentially into massive quarks. The dominant decays are likely to be to a top quark plus a neutrino[10]. Final states containing a t, $\bar{t}$, $\nu$, $\bar{\nu}$ give a spectacular signature: a missing $P_T$ on the order of half the mass of the leptoquark plus the t and $\bar{t}$ jets. Backgrounds should be very

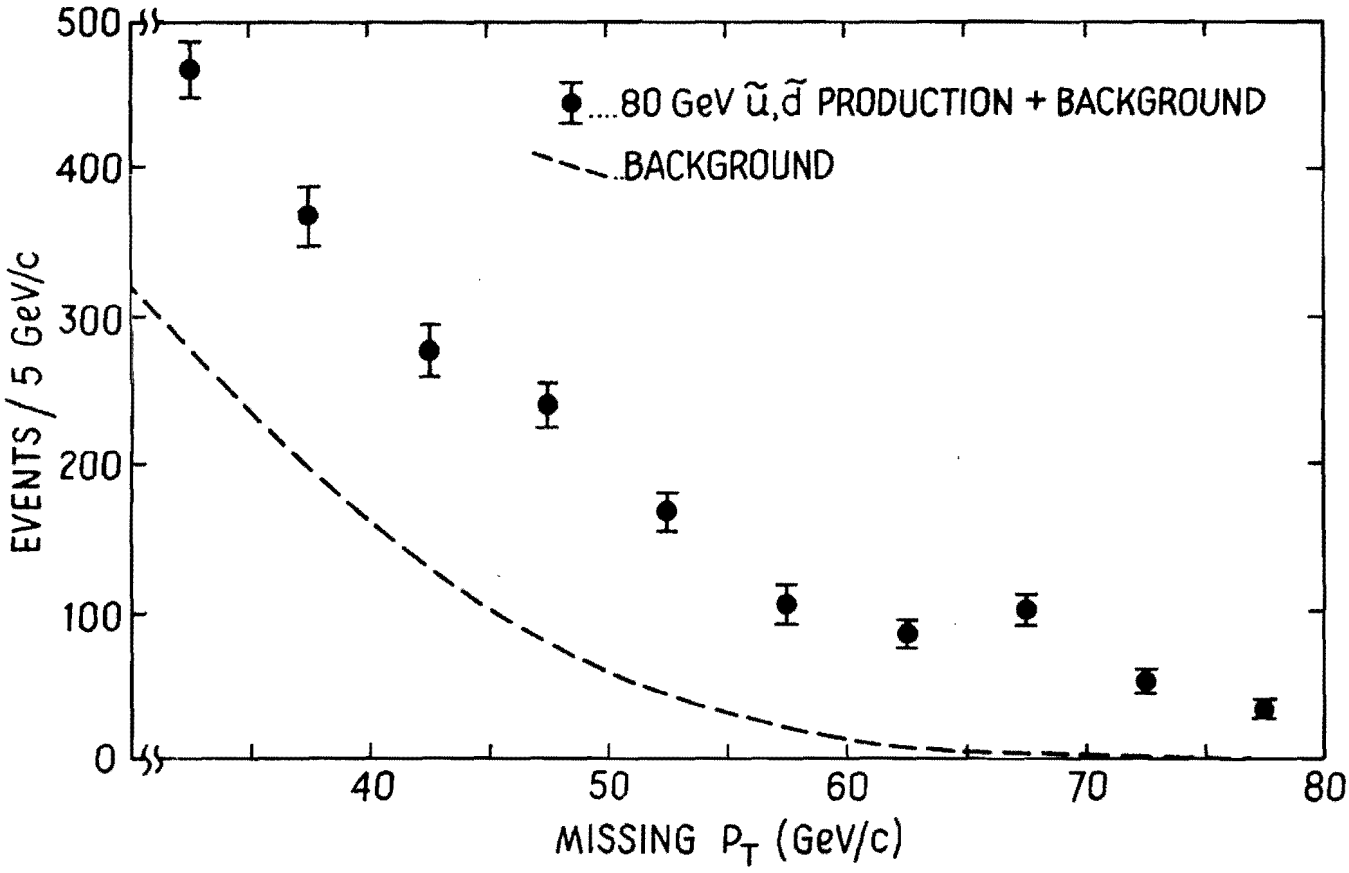


Figure III-18: Missing $P_T$ distribution expected from ũ plus d̃ pair production if their masses are both approx. 80 GeV and the decay is to a quark plus Goldstino. The dashed curve shows the expected background which is mostly from W and Z decays. A veto on events with charged leptons with P > 1.5 GeV/c is assumed.

small.

Leptoquarks in the composite theories carry both baryon number and lepton number and do not decay preferentially into heavy particles. Electroquark pair production will lead to comparable numbers of final states with the combinations $q\bar{q}\ e^+e^-$, $q\bar{q}\ e\nu$, and $q\bar{q}\ \nu\bar{\nu}$. Backgrounds for these states will be from $Z \to 2e$, $W \to e\nu$, and $Z \to 2\nu$. However, these can be reduced significantly by applying cuts to isolate the Z and W signals. Thus the $e^+e^-$ events from leptoquarks decays will not reconstruct to the Z mass and the vector sum of the two electron momenta will not be antiparallel to a gluon jet. The $\nu\nu$ events will have a large missing transverse momentum, which is not antiparallel to a gluon jet. Similarly for the $e\nu$ events the vector sum of the transverse momenta of the electron and neutrino (as reconstructed from the missing $P_T$) will not be antiparallel to a gluon jet as for a W, and the mass, calculated as described in Sect. III-3, will not generally be near the W mass.

Thus the signals for both composite and technicolor leptoquarks are expected to be quite clean. For techicolor leptoquarks with a mass of 150 GeV we expect a total of $\approx$ 50 events[11] for an integrated luminosity of $10^{36}$ $cm^{-2}$. Composite spin 1/2 leptoquarks should be produced with cross sections several times larger.[12] These should be sufficient to give a clearly detectable signal.

Many technicolor theories also predict ditechnileptons.[10b] These are color singlets with relatively small masses, perhaps only a few GeV. They can be pair produced in $\bar{p}p$ collisions and decay into spectacular final states containing six quark jets and two neutrinos (Fig. I-3). These should be easy to trigger on and identify using missing $P_T$ and the multijet topology. We have estimated production cross sections using the DRELLYAN option of ISAJET.

Drell-Yan production of the ditechnileptons can take place either through an intermediate $\gamma$ or $Z^\circ$ (Fig. I-3). For masses significantly less than $M_Z/2$, production will be dominated by $\gamma^* \rightarrow$ (ditechnilepton pair). The cross section will be approx. $(3/2)^2$ larger than for $t\bar{t}$ pair production. For ditechnilepton masses $\sim M_Z/2$, production is mainly through an intermediate $Z^\circ$. G. Kane[12] estimates the cross section will be $\gtrsim$ 10% of that for production of $t\bar{t}$ pairs of the same mass by this mechanism. Scaling Drell-Yan production cross sections for $t\bar{t}$ pairs from ISAJET, we estimate a cross section of 35 pb for a ditechnilepton mass of 45 GeV and 175 pb for a mass of 40 GeV. Thus we expect > 35 events for an integrated luminosity of $10^{36}$ cm$^{-2}$ if the mass of the ditechnilepton is < 45 GeV. Since backgrounds should be small we would be sensitive to masses < 45 GeV.

It is worth digressing here to discuss briefly how we might disentangle the physics if more than one of the above "new physics" signals are present in the data simultaneously. In fact each of the above scenarios has a unique signature. A new W', since it need not be produced in pairs, would have a gluon jet directly opposite the vector formed by combining the $P_T$ vector of the electron and the neutrino. Composite leptoquarks are distinctive because all three final states, $e^+e^-$, $e\nu$, $\nu\bar{\nu}$, are present simultaneously; the effective mass of $e^+e^-$system is not unique; and for the $\nu\nu$ final states there is no correlation between missing $P_T$ and a gluon jet, as there is for $Z \rightarrow 2\nu$. Technicolor leptoquarks will probably decay preferentially into final states containing a $t\bar{t}$ pair.

The supersymmetric particles $\tilde{g}$ and $\tilde{\phi}$ have perhaps the least distinctive signature. They are produced in pairs and there is no correlation between missing $P_T$ and a recoiling jet. The jet structure of the events with large missing $P_T$ should be a useful clue. The masses of the particles can be

estimated from the shape of the missing $P_T$ spectrum. The behavior of the cross section when $\sqrt{s}$ is varied would also be helpful in understanding the source.

## 9. Hadron-Hadron Interactions

One of the major differences between this detector and the CDF detector is that we go down to angles of about 1 mr whereas the CDF detector has calorimetry down to only 35 mr. Figures III-19 and III-20 illustrate the situation. Approximately half of the particles and 90% of the energy goes inside of 35 mr. Figure III-19(b) compares pseudorapidity $y^* = \eta = -\ln(\tan \theta/2)$ with rapidity y. To cover the complete range of rapidity it is desirable to cover angles well within 10 mr. In terms of pseudorapidity our detector will be sensitive out to about 7.3.

By having coverage of most of the solid angle there are many important aspects of the interactions that we can address with considerably less uncertainty than can a detector with more limited range. We note that the Fermilab Collider energy is as far above the present CERN collider energy as the Fermilab 400 GeV accelerator was above the AGS energy in terms of center of mass energies. Thus one should not at all imagine that the things done at CERN do not have to be redone at the higher Fermilab energy. There may well be new thresholds intervening. Indeed some cosmic ray measurements seem to indicate just such thresholds, as discussed below.

The inelastic cross section will need less correction with our small angle coverage. Our Monte Carlo (which does not include diffractive production) indicates that CDF would have about 2.5% of the events entirely below 35 mr while we would have only $0.5 \times 10^{-3}$ below 2.5 mr. Diffractive events would increase the loss rate for both of our detectors but the relative fractions might be expected to remain approximately the same. We expect to

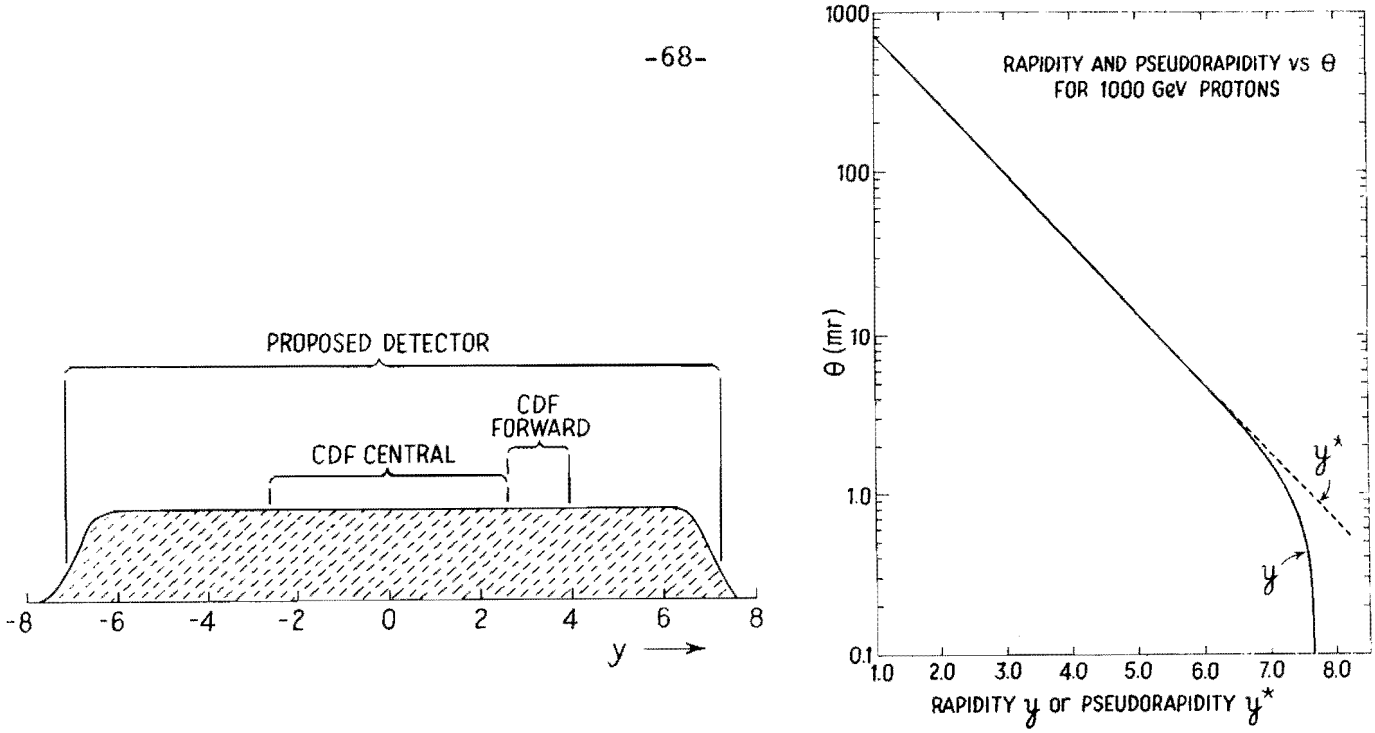


Figure III-19(a): Range of pseudorapidity covered by the proposed detector compared to that covered by the CDF with hadron calorimetry.
(b): Pseudorapidity vs. $\theta$ and rapidity vs. $\theta$ for 1000 GeV protons.

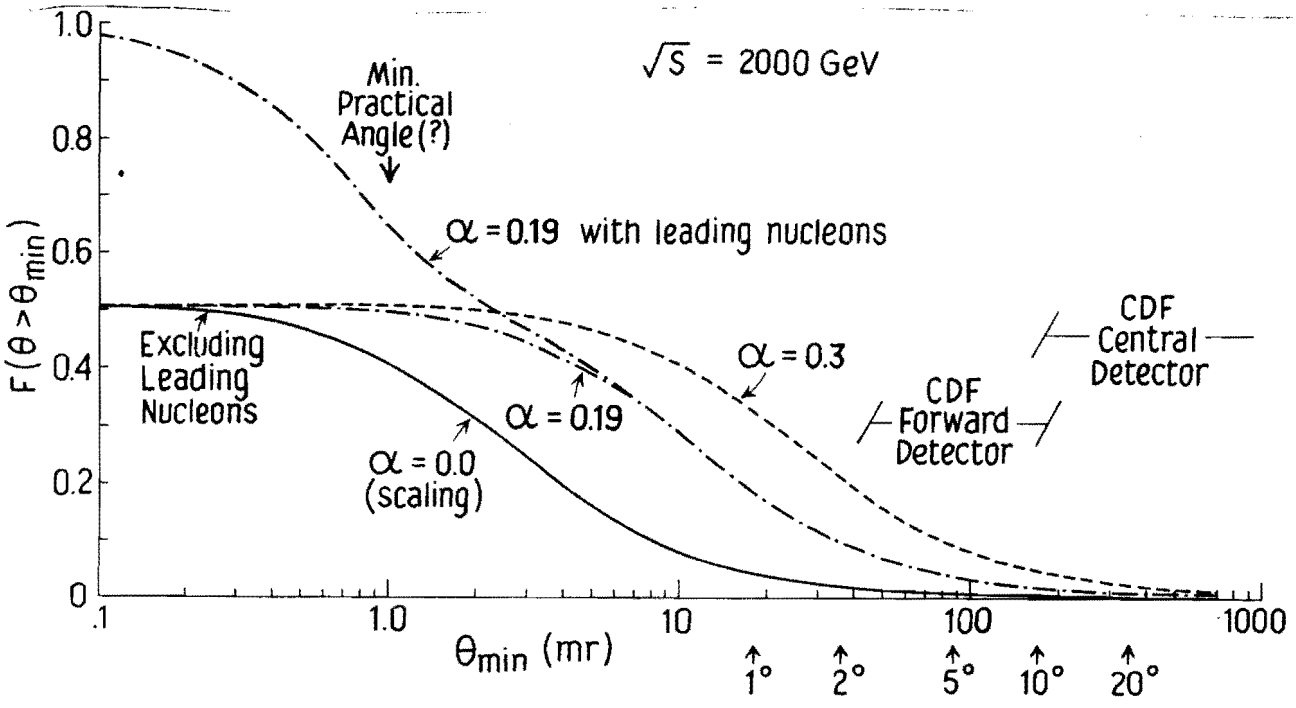


Figure III-20: Fraction of the total energy outside of $\theta_{min}$ for $\sqrt{s}$ = 2000 GeV, based on a Monte Carlo program of Gaisser et al. (Ref. 14). The parameter $\alpha$ is a measure of the violation of Feynman scaling. The case $\alpha = 0$ corresponds to exact Feynman scaling; $\alpha = 0.3$ corresponds to a large deviation from Feynman scaling; $\alpha = 0.19$ is a reasonable estimate from ISR and cosmic ray data. For the case $\alpha = 0.19$ only, the effect of including the leading nucleons is illustrated.

see more than half of the energy and over 90% of the produced particles.

Cosmic ray data from the Tien-Shan group suggest a sudden change in the absorption length above $\sqrt{s}$ = 500 GeV as shown in Figure III-21. Many or most of the anomalies reported in cosmic ray interactions above $10^{15}$ GeV may prove not to be real, given the uncertainties of atmospheric cascading, primary composition, limited statistics and detector constraints. Nevertheless charm decays, rising cross sections, and jets were all first and clearly seen in cosmic rays. We would ignore these data and its hints at our own peril. It is also notable that all of the anomalies are forward phenomena, as the forward energetic particles dominate the energy flow and consequently determine the behavior in air showers, emulsion chambers, and calorimetric detectors. Typical angles for secondaries from Centauro events, for example, are estimated to be ~ 100 mr at the Collider.[15] It is therefore essential to follow up these hints with a study of small angle phenomena at the Collider.

Obtaining the multiplicity will be difficult if one is limited to angles larger than 35 mr. Does the KNO scaling persist to Tevatron collider energies? Is there a break in the multiplicity versus $\sqrt{s}$ graph? Such a break is suggested by the Brazil-Japan cosmic ray group. [See Figure III-22 (taken from Ref. 13) which shows an apparent new threshold near $\sqrt{s}$ = 500 GeV.]

The importance of a measurement of the angular distribution of energy flow down to small angles has been emphasized by T. Gaisser.[14] Possible behaviors are illustrated in Figure III-20. This will contribute to the understanding of the general behavior of hadronic interactions at very high energies, and, as Gaisser[14] points out, contribute to the resolution of a fundamental astrophysical problem, the composition of primary cosmic rays above $10^{14}$ GeV.

The rapidity distributions are of general interest. The CERN rapidity

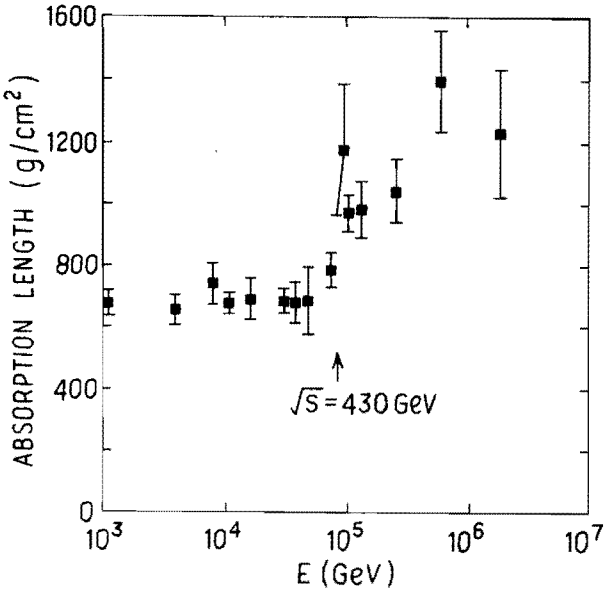


Figure III-21: Measured absorption length vs. lab energy from the Tien-Shan cosmic ray experiment (from Ref. 13).

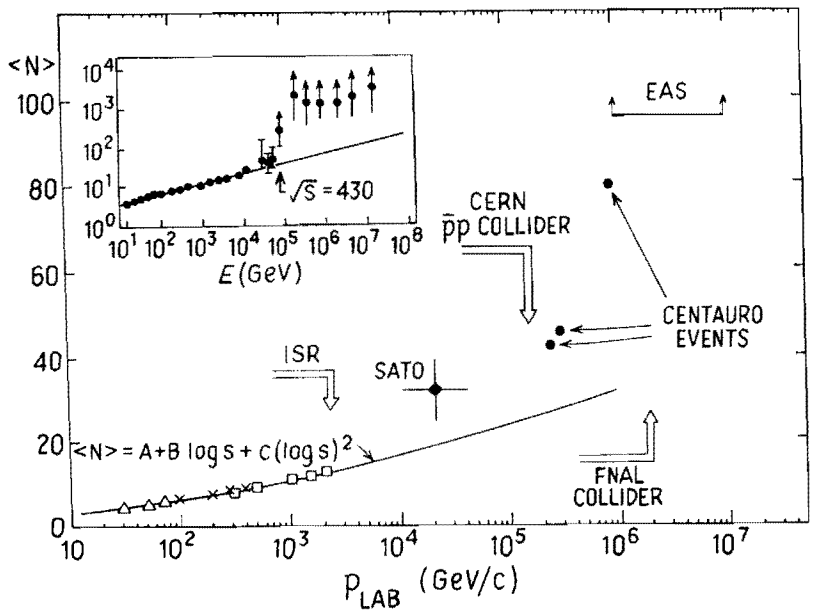


Figure III-22: Average charge multiplicity vs. lab momentum (from Ref. 13). The inset shows data from the Brazil-Japan cosmic ray experiment.

distributions did not seem to fill up the available space. How the rapidity distribution evolves by Fermilab energies is an important question. Again looking at this involves looking at the small angle particles to see the edge of the plateau.

It is clear that at the CERN collider jets can be seen at least at large $P_T$. The algorithms for separating out quark jets in the presence of beam jets are not yet developed, although fairly sophisticated algorithms for separating out massive quark jets exist for $e^+e^-$ events. If jets can be separated out well, then a small angle detector will greatly improve correlation studies. A hard collision may lead to a large angle jet on one side and a small angle jet on the other. These correlations can give important information on the production mechanisms. For example a "typical" quark in a nucleon with $x \cong 0.3$ which undergoes a hard scatter with $P_T \approx 5$ GeV/c will produce a jet at about 17 mr in the lab. This would be well inside of our detector and well outside the 35 mr limit of CDF.

## 10. Searches for New Flavors

If heavy jets corresponding to production of t quarks or other higher generation particles occur, then a combination of a missing $P_T$ trigger ($P_T$ will be missing due to neutrinos in the decay chain) with an examination of the jet may add considerable sensitivity to a search. For example, our Monte Carlo studies show that a cut on missing $P_T$, $P_T^{mis} > 10$ GeV/c, will enhance the fraction of jet events which contain a $t\bar{t}$ pair by a factor ~ 20 relative to jet events which do not.

The proposed detector with its very fine segmentation and good energy resolution should be competitive with other detectors in searches for heavy flavors. It is difficult to Monte Carlo heavy flavor production until more is

known about the characteristics of jets from high energy hadron interactions, so we have not made detailed studies of the backgrounds for heavy flavor searches. The best hope for accomplishing this physics may be to incorporate a minivertex detector which would allow events with charmed particles in the final state to be isolated. It seems inappropriate to plan on building a minivertex detector for use in the early running of the proposed detector. However there is plenty of room inside the central detector to install a minivertex detector, and we consider this to be a very attractive option for the future.

# IV. ACCOMMODATING THE PROPOSED DETECTOR IN THE DO AREA

## 1. Luminosity Considerations

It is important, particularly for the studies of hadron-hadron interactions discussed in Sect. III, to be able to cover the complete solid angle with calorimetry down to the smallest possible angles. With the very forward calorimeter design in Fig. II-1 it is possible to cover down to approx 1 mr if the calorimeters can approach to within 1.5 cm of the beam. This has a number of important advantages, particularly in studies of the energy flow (Fig. III-20) and in minimizing the missing $P_T$ due to particles going out the beam holes (Fig. III-1). This design assumes a clear space of ± 20 m. on either side of the interaction point. This entails having the low β quadrupoles just outside 20 m.

Low β designs for the BO area with a long clear space between the quads have been discussed extensively in the Superconducting Accelerator Design Report[1] and CDF Note No. 64.[2] The designs require that the two quads adjacent to the straight section on either end be made stronger. In order to be compatible with the use of the DO straight section for extraction, provisions to reverse these quads would be needed for DO. Fig. IV-1 taken from the Superconducting Accelerator Design Report compares the low-β long straight section with a normal straight section. A detailed study made for the CDF detector[2] shows that it is possible to have a $\beta^*$ of 5 m with a total clear space of 50 m. (See Fig. IV-2.) D. Johnson[3] has estimated that the luminosity at DO with $\beta^*$=3 m will be ~ $3 \times 10^{29}$ $cm^{-2}$ $s^{-1}$. We have therefore assumed $L \cong 1.8 \times 10^{29}$ for $\beta^* = 5$ m. With an average luminosity of $1.8 \times 10^{29}$ $cm^{-2}$ $sec^{-1}$ we could anticipate an integrated luminosity of $10^{36}$ $cm^{-2}$ in a 5 month run at 40% efficiency.

One way of achieving compatibility between the use of DO for extraction

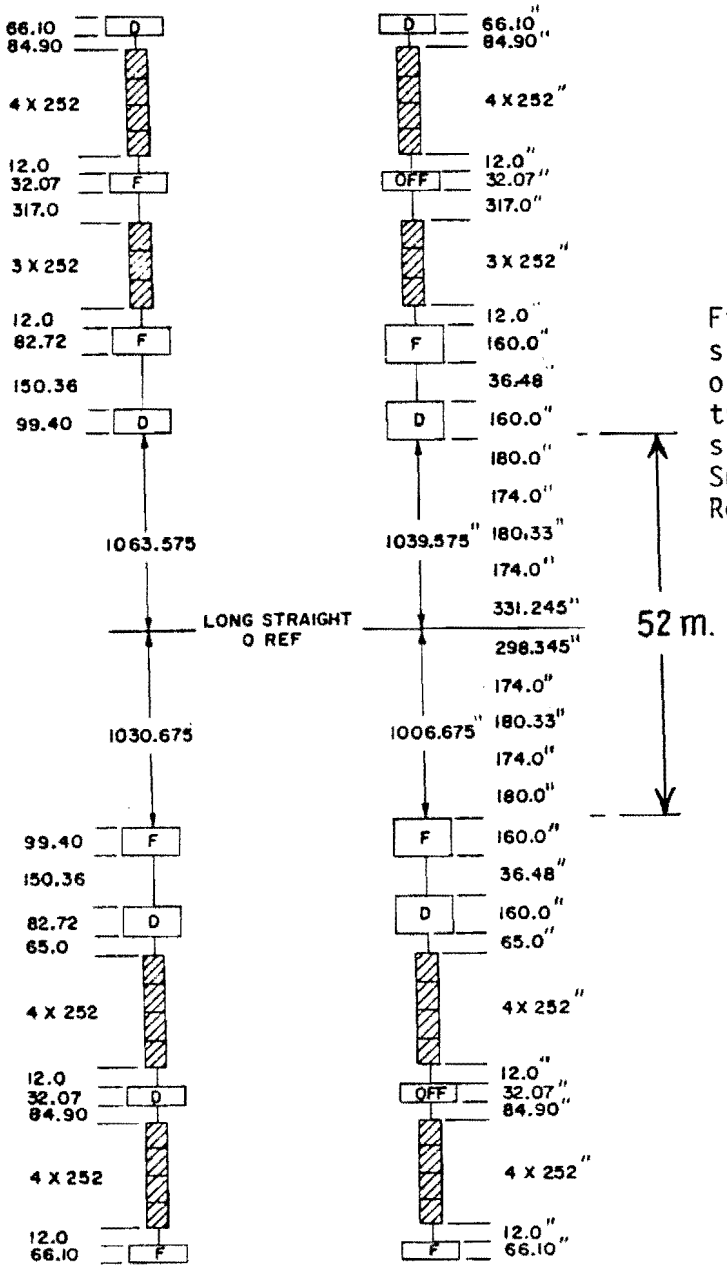


Figure IV-1: High luminosity long straight section compared to a "normal" one. When DO is used for extraction the two quadrupoles on either end of the straight section are reversed. [From Superconducting Accelerator Design Report[1]]

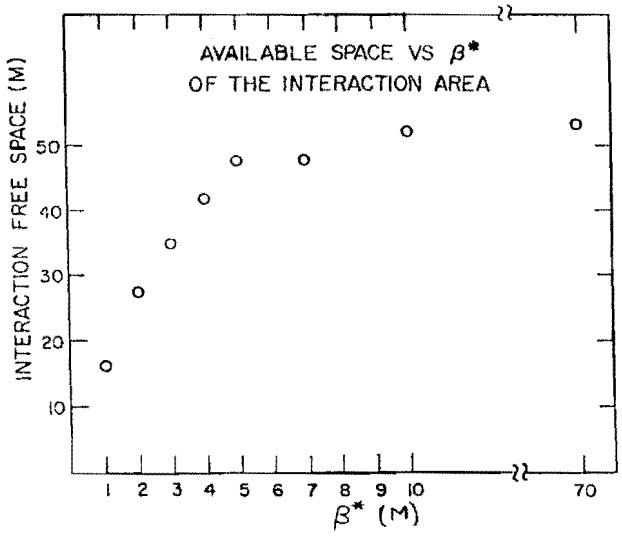


Figure IV-2: The variation of β* with clear space between the innermost quads for designs similar to that above for the high luminosity quads. [From Ref. IV-2]

and $\bar{p}p$ collisions is to divide each of the low $\beta$ quads into two elements which can separately be turned off or reversed by means of superconducting switches in the leads. This would require a modest effort to implement but the application should be straightforward.

According to D. Johnson[3] there is preliminary design for the low $\beta$ quads for DO which will give a free space of $\pm$ 10 m. The detector design we have considered in detail requires $\pm$ 20 m. We believe the DO area should complement the BO area. A unique feature of a new detector at DO would be calorimetry down to angles much smaller than CDF can cover (approx. 35 mr). Nevertheless we could live with a design with $\pm$10 m of free space. We have made some Monte Carlo studies to determine the effect of such a restriction. In general the hadron-hadron physics would suffer more than the physics based on a measurement of missing $P_T$. For example, the background to $Z \rightarrow 2\nu$ below $P_T^{mis}$ = 20 GeV/c would increase by approx. 30%; above $P_T^{mis}$ =20, there would be little change. (See Fig. III-15.) The average fraction of the energy contained in the detector decreases from ~ 0.56 for $\theta_{min}$ = 1.5 mr to ~ 0.47 for $\theta_{min}$ = 3 mr [Figure III-20].

We recognize that the example cited above in the Doubler Design Report referred to BO and may not apply directly to DO where the beam characteristics are different. We shall explore with the Laboratory staff the optimum design which achieves the best compromise between the minimum $\beta^*$, maximum clear space for the detector, cost, and flexibility.

## 2. Design of the Experimental Area

The proposed detector design is generally compatible with the preliminary design of the area presented by Wayne Nestander[4] except that more vertical

clearance is required. The proposed central detector design requires about 12' of vertical space above and below the beam.

We assume that the central detector and each of the forward calorimeters will be assembled with a self-contained piece of vacuum pipe. This will greatly facilitate the installation of the detector. It should be possible to move the assembled detector elements out of the assembly hall and install them in the Doubler ring in less than 2 days.

### 3. Desirability of a Bypass at D0

A bypass is planned at B0 to increase the separation between the Doubler and Main Ring vacuum pipes for the CDF. The D0 area is expected to house detectors with a generally shorter running time than CDF. A bypass which would allow work in D0 detectors while the main ring is in operation would be especially useful for D0.

Separating the main ring vacuum pipe farther from the Doubler would allow the forward and very forward calorimeters to be replaced by a single larger calorimeter as discussed below.

### 4. Concerns about Radiation Damage

The UA1 detector at CERN has had significant problems with radiation damage to their scintillation counters, particularly in their forward detectors. This emphasizes the need for careful control of proton beam scraping in the vicinity of D0 in both the Doubler and the Main Ring.

We have made a preliminary assessment of the resistance of various materials to radiation damage. Table IV-1 gives approx. threshold doses for radiation damage to materials of interest to detector builders. Lead glass counters and most semiconductor devices are the most susceptible. All of our PWC readout electronics would be on the outside of the calorimeters and should

Table IV-1 - Threshold Doses for Significant Radiation Damage (rad)

| | |
|---|---|
| Lead glass 5[a] | $3 \times 10^2$ r |
| Semiconductors (typical)[5b] | ~ $3 \times 10^3$ r |
| Acrylic plastics[5c] | $5 \times 10^6$ |
| Polystyrene plastics[5c] | $10^9$ r |

be reasonably well shielded. The electronics for the forward calorimeters might require additional shielding or the electronics could be moved further from the beams.

Acrylic-based scintillator and wavelength shifter bars are about three orders of magnitude more radiation resistant than lead glass. Polystyrene is quite radiation resistant and scintillators based on polystyrene are considerably more resistant than acrylic based.[6] If radiation resistance is a major concern we would probably choose the more expensive polystyrene-based scintillator for our calorimeters. The wavelength shifter bars in the endcap and forward calorimeters could probably be polystyrene-based or made so that they could be replaced fairly easily.

# V. OTHER CONSIDERATIONS

## 1. Possible Design Modifications

We expect details of the detector design to continue to evolve. A design with thinner iron plates in the first half of the hadronic section of the calorimeters is being considered. The mix of gas calorimetry and scintillation counters might change, particularly in view of the possibility of radiation damage. The use of uranium plates in the central calorimeter would be a very attractive option if large plates can be obtained at a reasonable cost. This would give a significant improvement in energy resolution and would give a more compact design. These options will be carefully studied.

If a bypass were built for DO the transverse dimensions of the very forward calorimeters could be enlarged so that the forward calorimeters could be eliminated. This would simplify the design and minimize background tracks in the farthest tracking chambers due to particles produced in the upstream calorimeters. (See Appendix A.)

We will do our best to accommodate other detectors which would run simultaneously or sequentially with ours. For example, other forward detectors, such as the one proposed by the Arizona group, can be accommodated by removing our end caps and forward detectors for part of the running. The central detector could still be used to provide these groups with data from the central region.

## 2. Possible Future Options

The ep group has suggested a design for a forward detector which incorporates a magnet to deflect forward-going particles so that the momentum of forward-going charged particles can be measured.[7] It may also be possible

to deflect the p and $\bar{p}$ beams enough to give a spatial separation between the beams and forward-going neutrals sufficient to allow calorimetry for neutral particles going off at 0°. This is a very attractive possibility if both hemispheres can be so equipped and if a design that is compatible with the physics goals discussed above can be achieved. If all solid angle can be covered with calorimetry it will be possible to measure the missing energy for each event. This measurement of the longitudinal component of the missing momentum would be an extremely valuable complement to the measurement of the two transverse components, if it can be determined to sufficient accuracy.

Another very valuable addition to the design would be a minivertex detector which would provide a tag on events containing charm or $\tau$ decays. This would be especially useful in identifying events that are more likely to contain heavy quark states. It should be relatively straightforward to add a minivertex detector to the design.

### 3. Cost Estimates

We have made preliminary cost estimates for the principal components in the central detector. These are summarized in Table V-1.

Table V-1 - Preliminary Cost Estimates (Central Detector)

| | |
|---|---|
| Iron, 480 tons of rolled steel plate: | $228K |
| Lead, 19 tons | 25K |
| Scintillator, 5504 pieces at $50/piece | 275K |
| Photomultiplier tubes: | |
| 1536 tubes at $65/tube | 100K |
| 1536 bases at $20/base | 31K |
| PWC electronics: | |
| 12608 channels at $7/channel | 88K |
| PWC's | 120K |
| Fabrication ???? | |
| | $868K |

We assume that the costs would be shared by NSF and DOE, mostly through university-based groups collaborating on the detector construction and use.

### 4. Manpower

The authors of this proposal are clearly too small a group to build and operate the proposed detector. We assume that if the proposal is approved, the collaboration would be expanded several fold. We assume the final collaboration would include a large fraction of the members of other groups who have submitted DO proposals. Physicists from national laboratories, particularly Fermilab, would be especially welcome.

## 5. Management of the Construction and Operation

We recognize that the organization of the design and construction of the detector, its operation, and the development of data analysis programs are each major undertakings. Collaborations composed principally of university groups have been quite successful in building and operating large detectors. One example is the HRS detector at SLAC, which was built by a collaboration of groups from the University of Michigan, Argonne, Indiana University, Purdue and other institutions. The IMB proton lifetime experiment was built and is being run by a collaboration from the University of Michigan, the University of California at Irvine, and Brookhaven.

# VI. CONCLUSIONS

In this proposal we have stressed the unique aspects of the proposed detector. The capability of measuring the two components of missing momentum perpendicular to the beams to an accuracy ~ 1 GeV/c opens up a whole new range of physics. This includes the suppression of background in studies of $W \to e + \nu$ decays, a measurement of the W mass to an accuracy $\lesssim$ 2%, a measurement of $(Z \to 2\nu)/(Z \to 2e)$, a measurement of $M_W/M_Z$ to an accuracy $\lesssim$ 1%, and searches for new particles such as gluinos, leptoquarks, and more massive gauge bosons. The new physics capabilities of the proposed detector are summarized in Table VI-1.

In order to achieve this capability the detector has been carefully designed to avoid cracks or dead regions and to cover angles down to 1 -2 mr from the beams with calorimetry. The ability to measure missing $P_T$ to this accuracy makes the proposed detector an ideal complement to CDF.

In addition, because the detector has calorimetry over a larger range of angles the detector can study the characteristics of hadron interactions over almost the entire range of pseudorapidity.

In this proposal we have not stressed the capabilities which the proposed detector would share with other detectors. With its very fine granularity, excellent angular resolution, and good energy resolution it will be competitive with or better than other detectors in most other phyics. This includes studies of jets, direct photon production, and searches for massive stable particles by time of flight.

Table VI-1

Summary of Unique Capabilities of Proposed Detector for New Physics

(Integrated luminosity ~ $10^{36}$ $cm^{-2}$)

- Measurement of $M_W/M_Z$ to approx. 1%
- Measurement of number of neutrino species from $(Z \to 2\nu)/(Z \to 2e)$
- Search for heavy gauge bosons W' and Z' with masses $\lesssim$ 300 GeV
- Search for gluinos and scalar quarks with masses $\lesssim$ 120 GeV
- Search for leptoquarks (technicolor or composite) with masses $\lesssim$ 150 GeV
- Search for ditechnileptons with masses $\lesssim$ 45 GeV

## REFERENCES AND FOOTNOTES

### SECTION I


1. W.J. Marciano and Z. Parsa, Proceedings of the DPF Summer Study, Snowmass (1982).
2. M. Veltman, Nucl. Phys B123, 89 (1977).
   M. Einhorn, D. Jones, and M. Veltman, Nucl. Phys. B191, 146 (1981).
3. M. Chanowitz, M. Furman, and I. Hinchliffe, Phys. Lett 78B, 285 (1978).
4. J. Banks, Phys. Rev. D25, 3027 (1982).
5. V. Barger, Proton-Antiproton Collider Physics - 1981, AIP Conf. Proceedings No. 85, AIP, 1982.
6. L.F. Abbott, E. Farhi, and S. Tye, Proceedings of the DPF Summer Study, Snowmass (1982).
7. G. Bunce et al., W, Z° Production at a pp Collider, Proceedings of the DPF Summer Study, Snowmass (1982).
8. (a) G. Altarelli, G. Parisi, and R. Petronzio, Phys. Lett. 76B, 351 (1978).
   (b) E.L. Berger, Proc. of the 3rd International Conf. on New Results in High Energy Physics, 1978, AIP Conf. Proc. No. 45.
9. B. Cox, Dimuon Production in Hadronic Interactions, Rapporteur Talk at XXI International Conf. on High Energy Physics, Paris 1982. FERMILAB-Conf-82/69-EXP.
10. E.L. Berger, Massive Lepton Pair Production, Review talk at APS Div. of Particles and Fields Meeting, Univ. of Maryland, 1982. ANL-HEP-CP-82-68.
11. (a) F. Halzen, A. Martin, and D. Scott, Phys. Rev. D25, 754 (1982).
    (b) A.D. Martin, Production of Z and W Bosons at the $\bar{p}p$ Colliders, Proton-Antiproton Collider Physics-1981. AIP Conference Proceeding No. 85 (AIP, New York, 1982).

12. G.L. Kane and M.L. Perl, Beyond the Standard Model, Proceedings of the DPF Summer Study, Snowmass (1982).

13. I.H. Dunbar, Nucl. Phys. B197, 189 (1982).

14. (a) B. Gittleman et al., Proc. of the DPF Summer Study, Snowmass (1982).
(b) H. Vogel and E. Lorenz, Proc. of DPF Summer Study, Snowmass 1982.

15. R.C. Ball et al., Supersymmetry Mass and Lifetime Limits from a Proton Beam Dump Experiment, UM HE 82-21, July 1982.

16. I. Hinchcliffe and L. Littenberg, Proc. of the DPF Summer Study, Snowmass (1982).

17. (a) K. Lane, Proc. of the DPF Summer Study, Snowmass, 1982.
(b) E. Farhi and L. Susskind, Phys. Rev. D20, 3404 (1979).
(c) S. Dimopoulos, Nucl. Phys. B168, 69 (1980).
(d) S. Dimopoulos, S. Raby and G.L. Kane, Nucl. Phys B182, 77 (1981).

18. G. Kane, private communication.

## SECTION II

1. L.W. Jones, Recent U.S. Work on Colliding Beams, Proc. of the International Conference on High Energy Accelerators, Dubna, 1963 (Atomizdat, Moscow, 1964).

2. R.C. Ball et al., Nucl. Instr. and Meth. 197, 371 (1982).

## SECTION III

1. F. Paige and S. Protopopescu, ISAJET: A Monte Carlo Event Generator for ISABELLE, BNL-29777.
F. Paige and S. Protopopescu, ISAJET: A Monte Carlo Event Generator for pp and $\bar{p}p$ Interactions, Proc. of the DPF Summer Study, Snowmass 1982.

2. F. Paige and L. Littenberg, private communication.

3. R. Baier et al., Z. Phys. C2, 259 (1978).

4. Jacques Leveille, University of Michigan, private communication.

5. G. Bellettini et al., Nucl. Instr. and Meth. 204, 73 (1982).

6. H. Abramowicz et al., Nucl. Instr. and Meth. 180, 429 (1981).

7. H. Jensen, presented at the DO Workshop, Fermilab, Nov. 1982.

8. G. Kane and J. Leveille, Phys. Lett 112B, 227 (1982).

9. I. Hinchcliffe and L. Littenberg, Proc. of the DPF Summer Study, Snowmass (1982).

10. (a) S. Dimopoulos, S. Raby and G. Kane, Nucl. Phys. B182, 77 (1981).
(b) S. Dimopoulos, Nucl. Phys. B168, 69 (1980).

11. Leptoquark pairs are expected to be produced with approx. the same cross section as scalar quarks of the same mass [G. Kane, private communication.] We have therefore used the SUPERSYM option of ISAJET for scalar quarks to estimate these cross sections.

12. G. Kane, private communication.

13. G. Goggi, CERN-EP/81-08.

14. T. K. Gaisser, Phys. Lett. 100B, 425 (1981).

15. G. Bauer et al, CDF Note No. 64, August, 1980.

## SECTION IV

1. A Report on the Design of the Fermi National Laboratory, Superconducting Accelerator, Fermilab Report, May 1979.

2. G. Bauer et al., Conceptual Design of a Forward Detector for the Antiproton-Proton Collider, CDF Note No. 64, August, 1980.

3. D. Johnson, presented at the DO Workshop, Fermilab, Nov. 1982.

4. W. Nestander, presented at the DO Workshop, Fermilab, Nov. 1982.

5. (a) J.S. Beale et al., Nucl. Instr. and Meth. 117, 501 (1974).

(b) S. Battisti et al., Radiation Damage of Electronic Components, CERN LABI I-RA/72-10 (1972).

(c) Chap. 3, Effects of Radiation on Materials and Components, J. Kircher and R. Bowman, eds., Reinhold Publ. Corp., N.Y.

6. T. Inagaki and R. Takashima, New Types of Plastic Scintillators, KEK Preprint 81-18, Nov. 1981.

J.C. Thevenin et al., Nucl. Instr. and Meth. 169, 53 (1980).

7. P. Coteus and U. Nauenberg, A Design for Small Angle (0-2 mr) Spectrometer for ep or $\overline{p}p$ Collisions at DO, presented at the DO Workshop, Fermilab, Nov. 1982.

APPENDIX A

# MEASUREMENT OF LEAKAGE FROM CCD FORWARD CALORIMETERS AND ESTIMATE OF RESULTING BACKGROUND IN TRACKING CHAMBERS

We have made measurements in the M5 test beam of the leakage from a calorimeter similar to those proposed for the CCD forward calorimeters. These measurements show that leakage from the calorimeters will not cause a significant background in the downstream tracking chambers. Our estimate is that the probability of finding a background track in one sector of a tracking chamber is $\lesssim 10^{-2}$ per $\bar{p}p$ interaction at $\sqrt{s}$ = 2000 GeV. On average, only one in 5 $\bar{p}p$ interactions will show any background tracks due to this source.

To evaluate possible background problems in the forward tracking chambers due to leakage from the calorimeters farther upstream, we have undertaken measurements in the M5 test beam. Data from these measurements together with a Monte Carlo program to simulate 2000 GeV $\bar{p}p$ interactions allow us to make a reliable estimate of the probability of finding background tracks in the forward tracking chambers.

## M5 MEASUREMENTS

To model the actual situation as accurately as possible, we have used a prototype of a forward calorimeter as a "target" and measured the probability of finding a secondary particle at an angle $\theta_s$ as a function of the impact position and beam momentum. The geometry is shown in Figure 1. Table 1 compares the calorimeter used in the tests with a forward calorimeter as discussed in this proposal. The main difference is that the prototype is

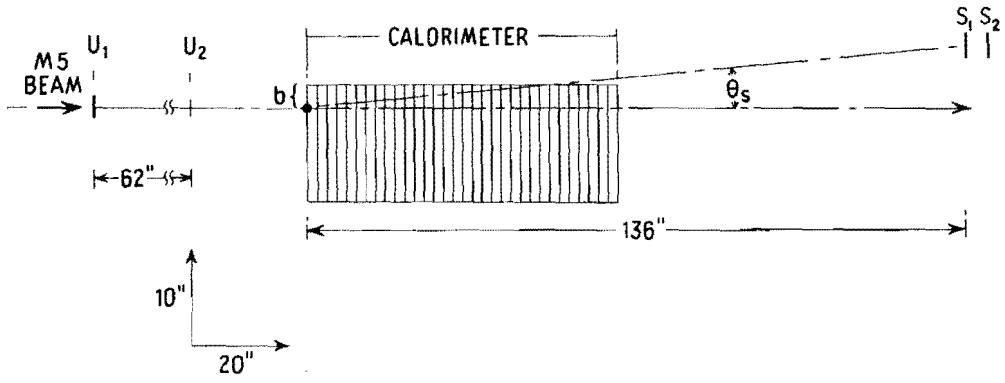


Figure A-1: Setup for M5 measurements.

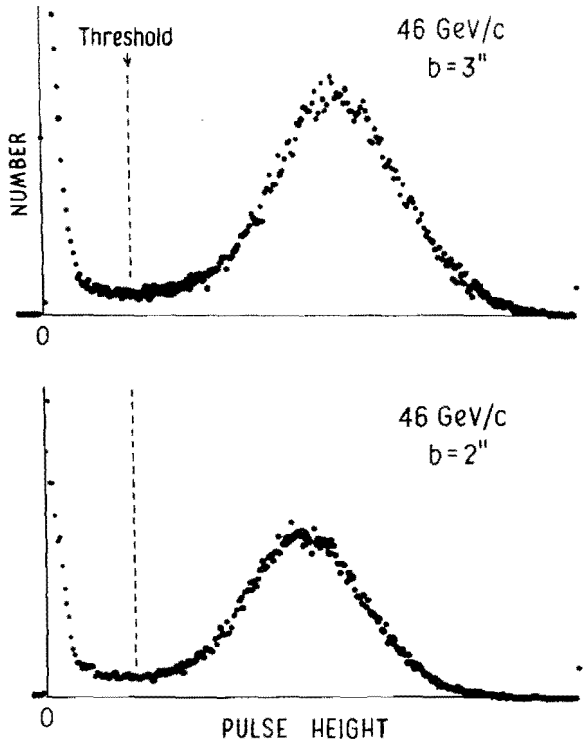


Figure A-2: Pulse-height spectra from the calorimeter for two impact parameters. The discriminator threshold is indicated.

TABLE 1

Comparison of Forward Calorimeter with Prototype used in M5 Measurements

| | Proposed Calorimeter | Prototype |
|---|---|---|
| Thickness of iron plates | 3.8 cm | 3.2 cm |
| Total iron | 137 cm<br>≅ 8 abs. length | 127 cm<br>≅ 7.4 abs. length |
| Lead plates | 11 cm<br>0.6 abs. length | None |
| Transverse dim. | ~ 100 cm | 30 cm x 30 cm |
| Total depth | 8.6 abs. length | 7.4 abs. length |

---

somewhat thinner in overall depth (7.4 abs. length vs. 8.6) and smaller in transverse dimensions. The M5 measurements will therefore give a somewhat pessimistic result for the leakage. The test calorimeter contained 40 scintillator sheets, each 1/4" thick, but only half of them were actually read out in the M5 measurements.

The incoming beam was defined by scintillation counters $U_1$ and $U_2$ (Fig. 1) plus a pulse from the calorimeter greater than 30% of the most probable pulse height for that beam momentum. The calorimeter pulse height requirement was important to eliminate triggers from muons in the beam and particles which interacted farther upstream and sent a spray of soft particles into the counters. Figure 2 shows pulse-height spectra from the calorimeter for two different impact points on the face of the calorimeter. The muon and low energy background gives the large peak at low pulse heights. The minimum pulse-height requirement is indicated; it is high enough to eliminate the low energy tail and low enough that it does not cause a significant bias in the measurements. Beam electrons could be selected by requiring pulses from gas

Cherenkov counter farther upstream. Rates with electrons were too low for detailed studies to be made, but sufficient data were taken to verify that leakage from incident photons would be no worse than for incident hadrons (as might be anticipated).

Particles leaking out the sides or downstream end of the calorimeter were detected with scintillation counters $S_1$ and $S_2$ which were put in coincidence with the counters in the beam. The requirement of both $S_1$ and $S_2$ eliminated counts from low-energy neutrons which are detected rather efficiently by a single scintillator, but not with wire chambers. The $S_1$ and $S_2$ counters were only 5 1/2" apart, so no significant directional requirement was placed on the particles detected. The high voltages on $S_1$ and $S_2$ were set so that pulse heights $\gtrsim$ 40% those from minimum ionizing particle would be sufficient. When the calorimeter was removed from the beam and the $S_1S_2$ counters put at beam height, the $S_1 \cdot S_2 \cdot U_1 \cdot U_2$ rate was > 80% of the $U_1 \cdot U_2$ rate. The $U_1$ and $U_2$ counters were 1" x 3"; the $S_1$ and $S_2$ counters were 2" x 3". All except $U_1$ had their long dimensions horizontal.

The probability of a particle incident on the calorimeter sending a secondary into the solid angle subtended by $S_1S_2$ is

$$P = S_1 \cdot S_2 \cdot U_1 \cdot U_2 \cdot CAL/(U_1 \cdot U_2 \cdot CAL)$$

This probability was measured as a function of:

(1) The impact parameter b which we define as the distance between the point the incident beam strikes the face of the calorimeter and the top of the iron plates. (See Fig. 1.)

(2) The scattering angle $\Theta_S$ which we define as the angle between the incident beam direction and the line joining the impact point and the center of S1.

(3) Beam momentum p.

To the extent practical, these parameters were varied over the range relevant

to the geometry of the proposed forward detectors.

Representative data from the measurements of P are given in Figure 3. As seen from Fig. 3, the probability rises rather rapidly with increasing $\theta_S$, particularly for small impact parameters, for $\theta_S$ in the range of interest ($\theta_S \lesssim 80$ mr). The probability rises rapidly with decreasing impact parameter and increasing incident momentum.

For orientation, it is worth pointing out that the solid angle subtended by $S_1S_2$ as seen from the front of the calorimeter is comparable to that subtended by one sector of a forward tracking chamber as seen from the upstream face of the preceding calorimeter. The low values observed for P ($P \lesssim .015$) suggest that leakage will not be a serious problem. Furthermore, as we discuss below, the average momentum of the particles which strike the end plug and forward calorimeters is < 50 GeV; the average number of hits on the upstream faces of the calorimeters is ≈ 18 per $p\bar{p}$ interaction, and the average impact parameter is 2.5". From Fig. 3, for a momentum of 50 GeV/c, the probability will be $P \lesssim 3 \times 10^{-3}$ per hadron incident on the calorimeter for all angles and impact parameters ~3" into a solid angle of $3.24 \times 10^{-4}$ sr. Each set of tracking chambers in the proposed forward detector subtends a total solid angle ~ $5 \times 10^{-3}$ sr as seen from the upstream face of the preceeding calorimeter. Thus the total number of particles per event in the tracking chambers from spray will be $\lesssim 3 \times 10^{-3} \times 18 \times (5 \times 10^{-3}/3.24 \times 10^{-4})$ ~ 1.0. A more detailed calculation, discussed below, shows that even this rather low figure is almost an order of magnitude overestimate.

Estimate of Overall Probability for CCD Forward Detector

In order to make a more accurate estimate of the number of tracks from spray off the calorimeters to be expected in a typical $\bar{p}p$ interaction, we have used a Monte Carlo simulation of $p\bar{p}$ interactions at $\sqrt{s}$ = 2000 GeV. The

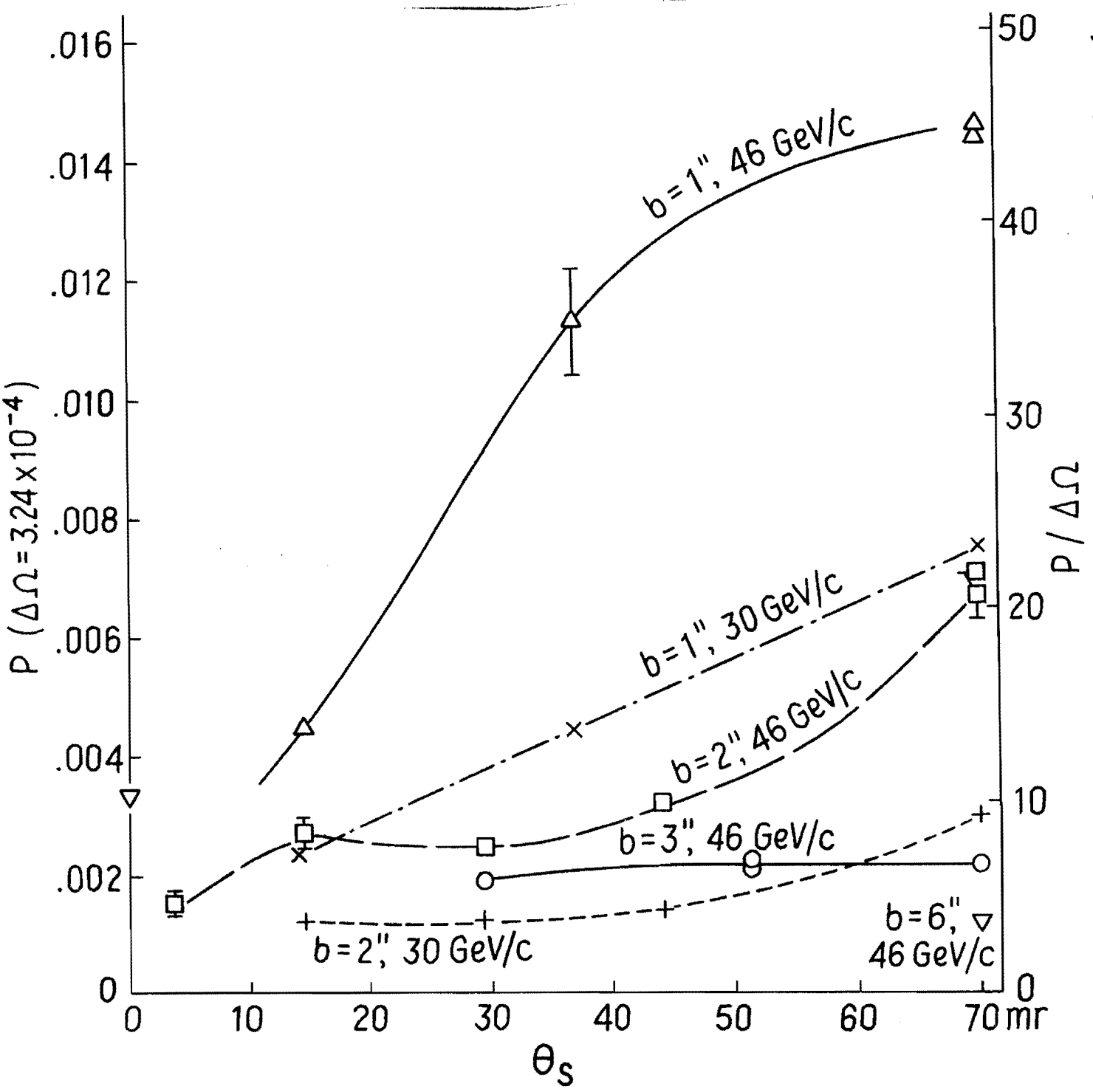


Figure A-3: Results of M5 measurements. The left-hand scale gives the probability of finding a particle in the $S_1S_2$ counters which subtended a solid angle of $3.25 \times 10^{-4}$ sr. The right-hand scale is the probability per steradian. The lines are drawn to connect points taken with the same beam momentum and impact parameter. The change in slope of the b=2", 46 GeV/c curve near $\theta_S$ = 15 mr is due to the transition from leakage out the back to leakage from the sides of the calorimeter.

secondary particles ($\pi$'s, K's, or photons) are followed from the interaction point. If a secondary hits a calorimeter, the probability of it sending spray into a tracking chamber downstream is calculated from a fit to the M5 data. The probability is summed over all particles produced in each $\bar{p}p$ interaction.

The Monte Carlo simulation used a program written by R. Ellsworth and T. Gaisser[1] to generate the $\bar{p}p$ interactions. This is based on an extrapolation of $p_T$ and $x_F$ distributions found at lower energies and includes violations of Feynman scaling seen in the lower energy data. Total energy is conserved approximately so that in practice at $\sqrt{s}$ = 2000 GeV the energy carried off by the secondaries adds up to within 0.1% of 2000 GeV.

Figure 4 shows an expanded view of the proposed forward detector layout. We have considered separately the T2 tracking chambers and each of the T3 chambers. In the Monte Carlo, the probability of producing spray in, for example, the T2 chambers is summed for each particle that strikes the upstream face of CAL1. The probability is calculated from a parameterization of the M5 data as a function of impact parameter b, angle $\Theta_S$, and particle momentum p as defined above.

Fig. 5 shows the distribution of $\Theta_S$ values from the Monte Carlo for all the tracking chambers combined. Most of the values of $\Theta_S$ are < 80 mr and so are in the range covered in the M5 measurements (Fig. 3). Fig. 6 shows the distribution in impact parameter for secondaries hitting CAL1 or CAL2. The mean impact parameter is 2.5". The M5 measurements covered 1" < b < 6". Fig. 7 shows the momentum distribution for secondaries which hit CAL1 or CAL2. Most of the secondaries (>70%) have momenta < 20 GeV; a few (~17%) have momenta > 50 GeV. Thus most of the time the M5 data have to be extrapolated to lower momenta.

Figures 8 and 9 show typical results from the Monte Carlo. Figure 8

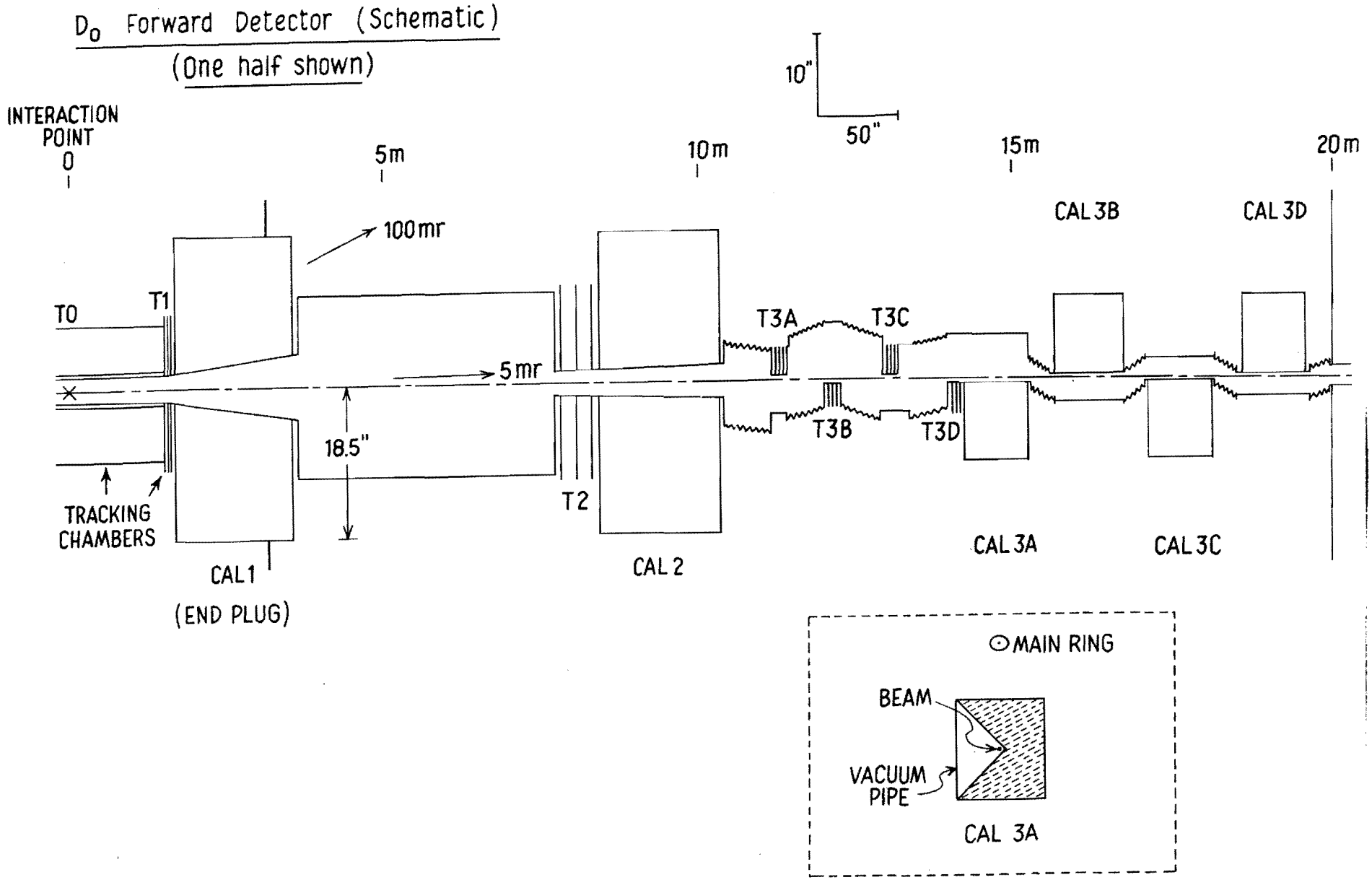


Figure A-4: Proposed geometry for the end cap and forward calorimeters.

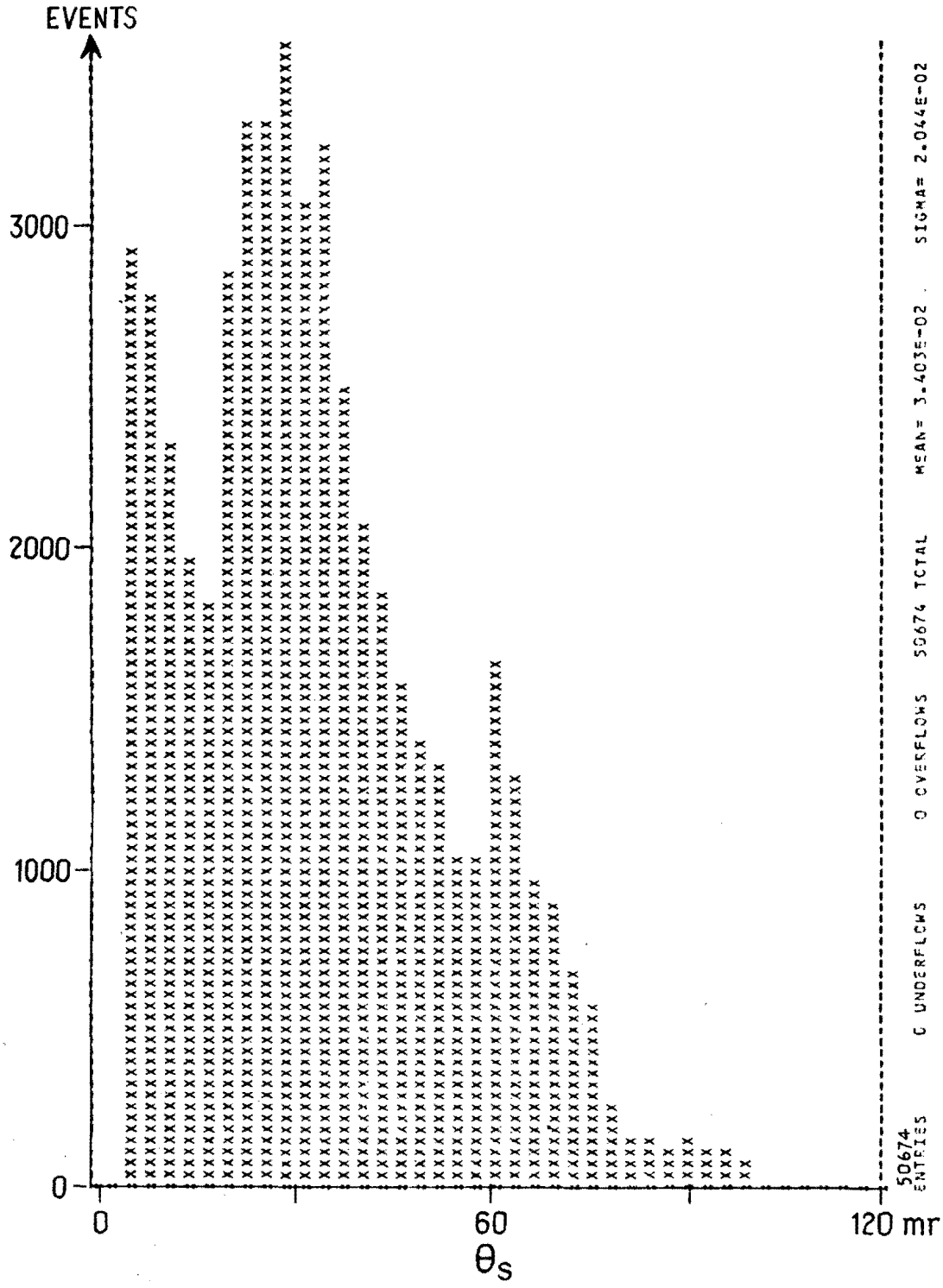


Figure A-5: Distribution of values of $\theta_s$ used in the Monte Carlo program.

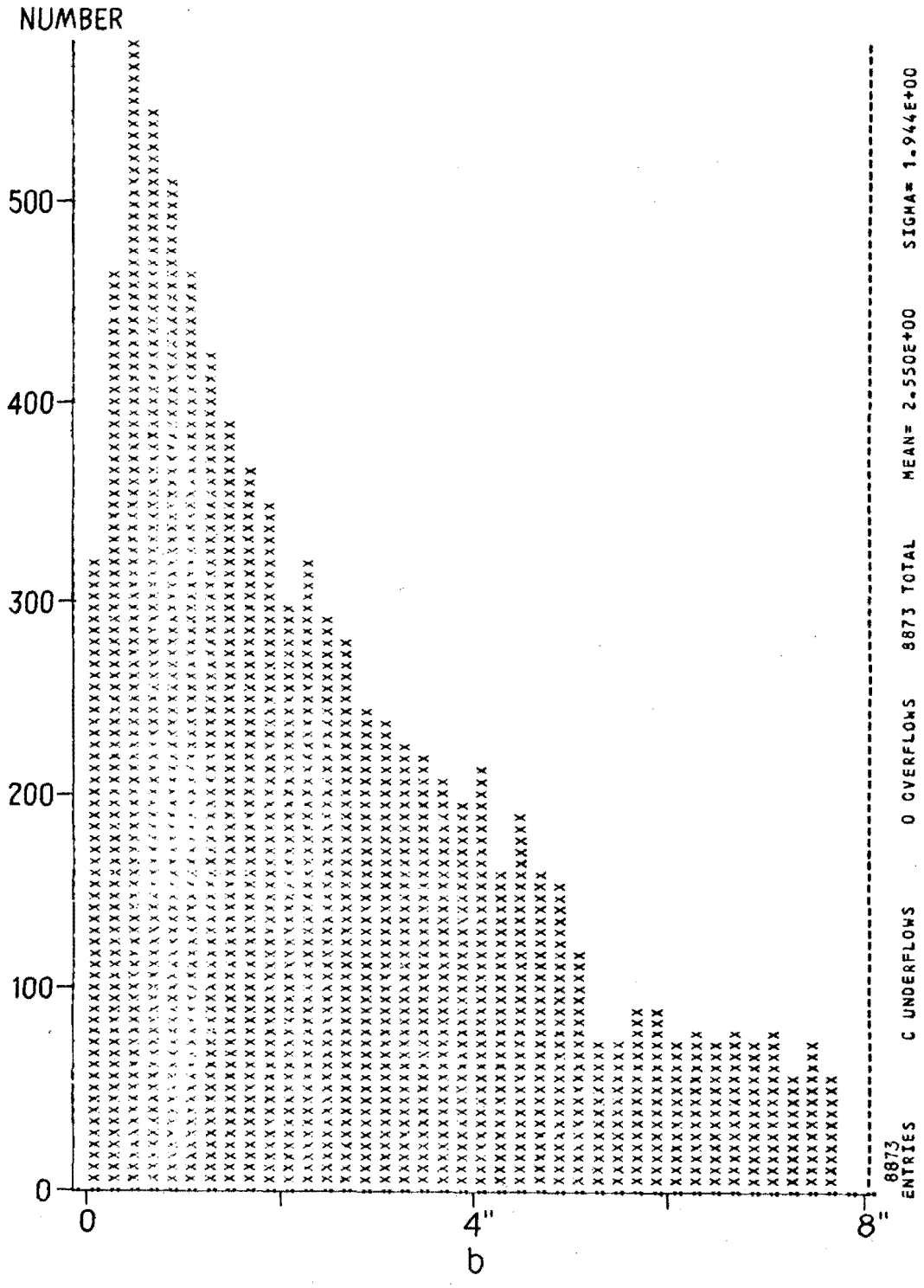


Figure A-6: Distribution of impact parameters for particles striking CAL1 or CAL2 from Monte Carlo.

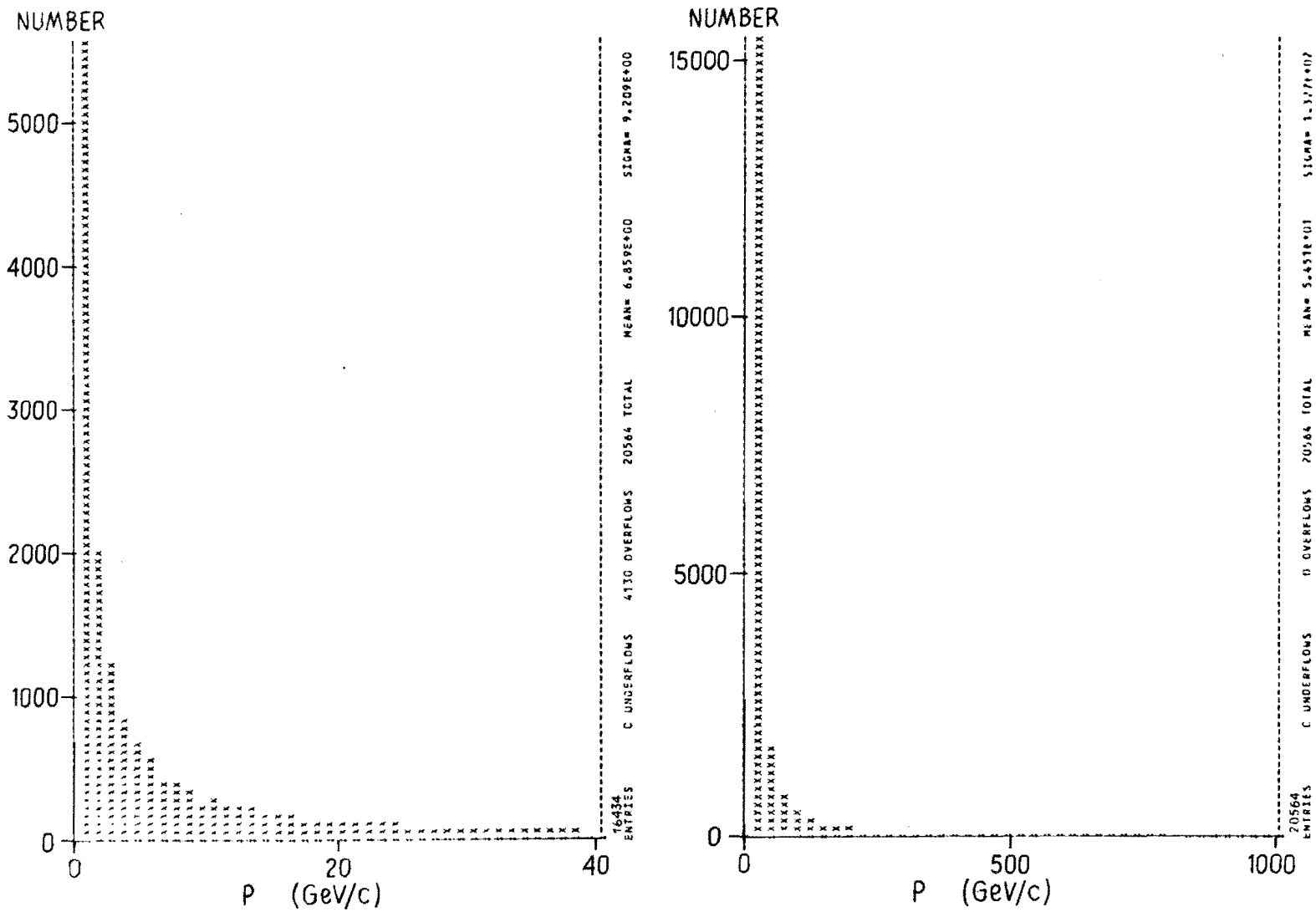


Figure A-7: Momentum distribution of particles striking CAL1 or CAL2 (on two different scales).

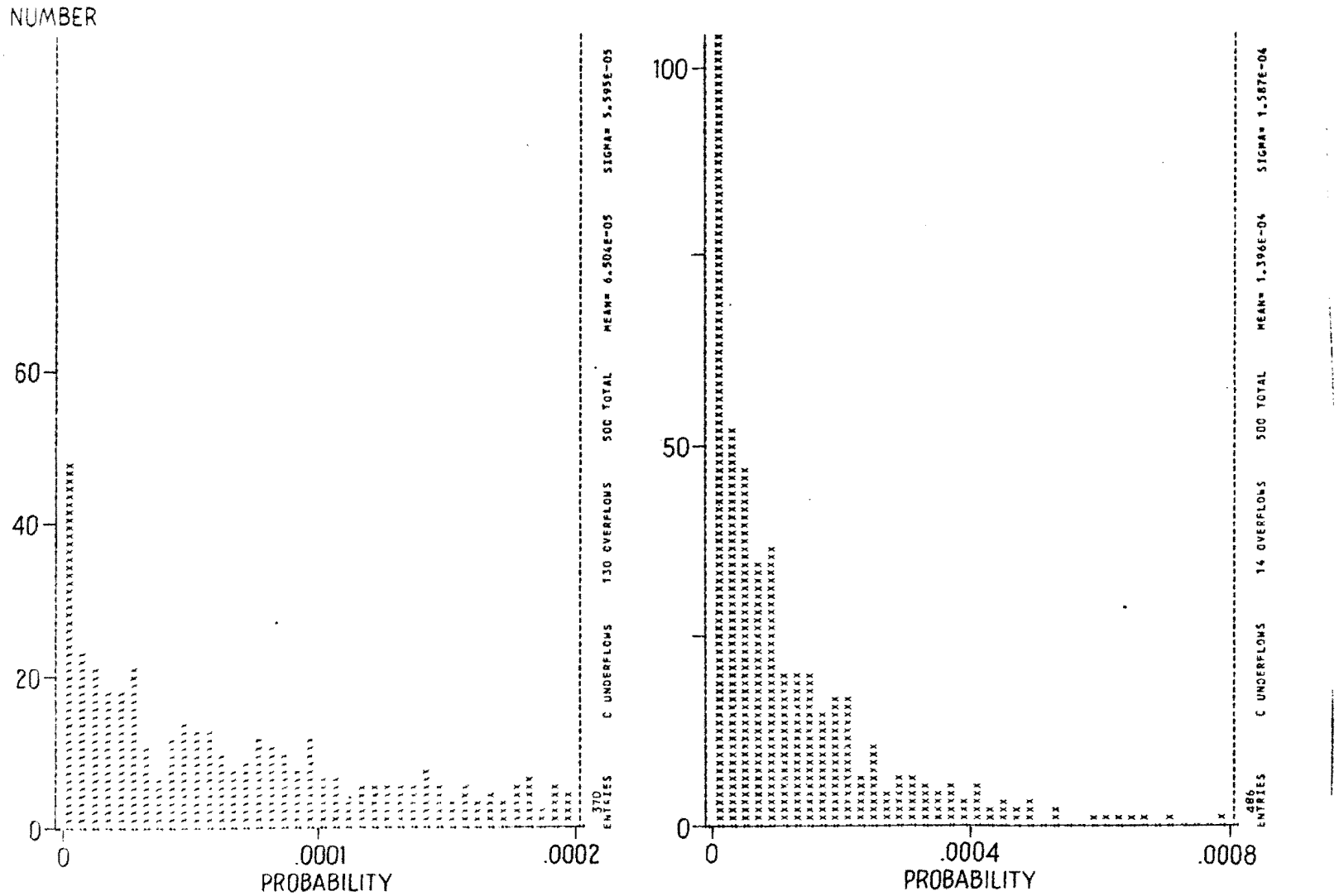


Figure A-8: Distribution of probabilities of sending spray into one sector of the T2 tracking chambers for 500 simulated 2000-GeV interactions. The same distribution is shown for two different scales on the x-axis.

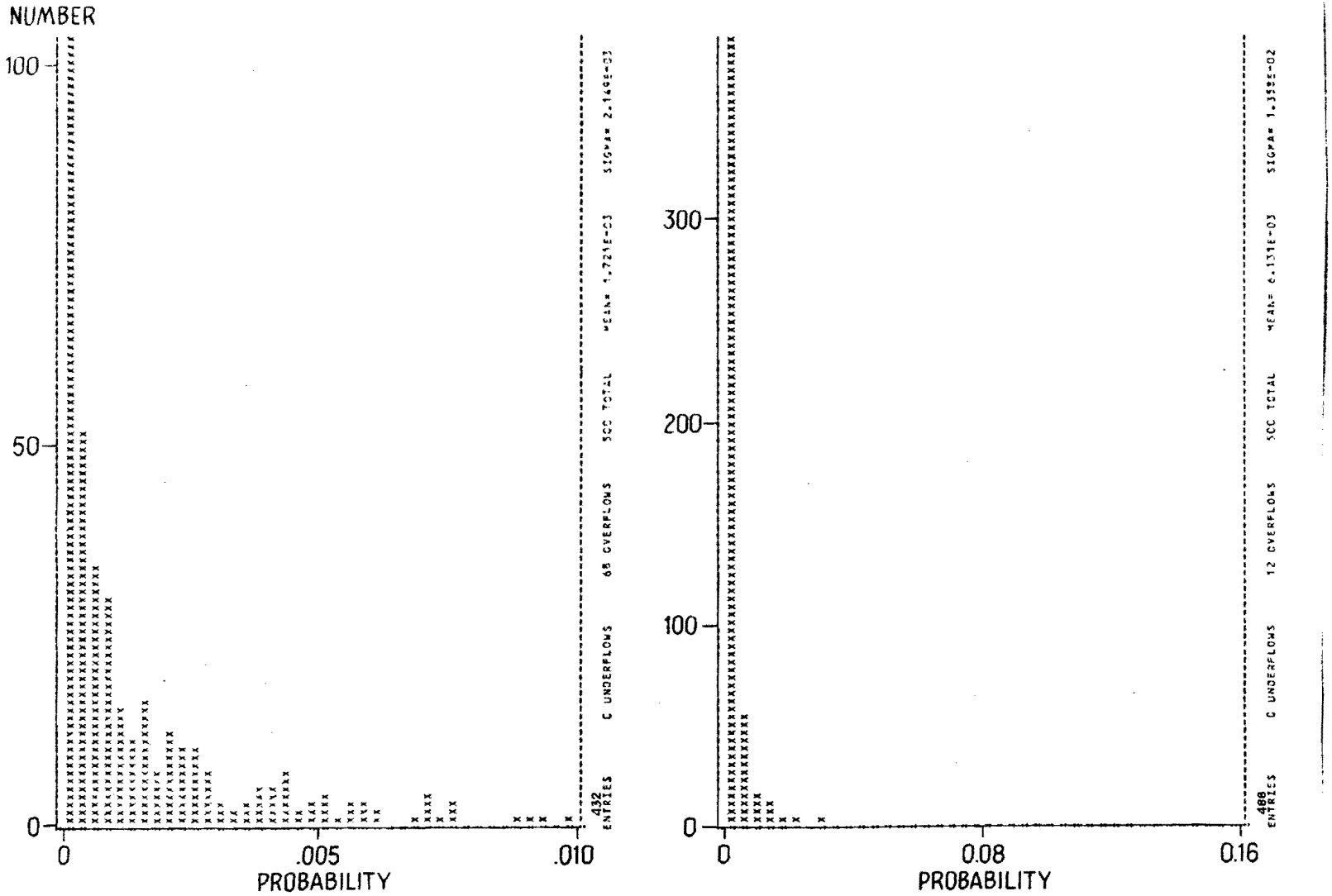


Figure A-9: Distribution of probabilities of sending spray into one sector of the T3B tracking chambers for 500 simulated 2000-GeV interactions. The same distribution is shown for two different scales on the x-axis.

shows the distribution in the probability of seeing a background track in one sector of the T2 tracking chambers for 500 $\bar{p}p$ interactions. Fig. 9 shows the same distribution for the T3B chambers. Table 2 gives the (approximate) mean probability per sector for each set of tracking chambers.

TABLE 2

Mean Probabilities for Each Set of Tracking Chambers

| Tracking Chamber | Probability of Stray Track per Sector per $\bar{p}p$ Interaction |
|---|---|
| T2 | $2.0 \times 10^{-4}$ |
| T3A | $1.3 \times 10^{-2}$ |
| T3B | $6.1 \times 10^{-3}$ |
| T3C | $3.6 \times 10^{-3}$ |
| T3D | $2.7 \times 10^{-3}$ |

Summing over all sectors of T2 and T3 we estimate that on the average there will be approx. 0.2 background tracks per $\bar{p}p$ interactions. Even this low number is probably high. It was clear in the M5 measurement that much of the leakage was out the back, not the side, of the calorimeters. The calorimeters in the proposed forward detector are deeper than the one used in M5. (See Table 1.) We also plan to back them up with passive shielding.

As seen from Figures 8 and 9, the probability of having a background track in a sector from a $\bar{p}p$ interaction is generally very small, $P' < 10^{-3}$, but the probability distribution has a long tail. For T3B this tail goes out to $P' \sim 10^{-1}$ (Fig. 9). This reflects the momentum distribution which has a similar tail (Fig. 7). This means that in practice, most $\bar{p}p$ events will have a very low probability of producing spray in the tracking chambers, but occasionally a high momentum secondary hitting near the inner edge of a

calorimeter will produce a "large" number of background tracks (i.e. - one or two in an entire tracking chamber, as seen from Fig. 9).

[Since the M5 data only covered incident momenta from 15 GeV/c to 46 GeV/c, it was necessary to extrapolate the probability to other momenta (mostly lower). For the above, we used $P = cp^2$ as suggested by the M5 data. As a check, we also tried $P = cp^{1.0}$. With this dependence the numbers in Table 2 increased by a factor of about 1.8.]

Conclusions

On the basis of our M5 data and a Monte Carlo calculation to simulate the general features of 2000 GeV $\bar{p}p$ interactions, we conclude that background in the tracking chambers due to leakage out the sides and back of the proposed forward calorimeters is not a significant problem. On the average, each $\bar{p}p$ event will contain << 1 stray track from this source. Stray tracks which do not come from the $\bar{p}p$ interaction point are trivial to recognize and discard. They only become a problem if they are so numerous that they swamp the tracking chambers.

## References

1. T.K. Gaisser, Phys. Lett. 100B, 425 (1981); Fermilab Pub. 80/104, December 1980.

ADDENDUM TO P-724 May 16, 1983

## Summary

Many questions were posed by the Program Advisory Committee and the answers given here are rather lengthy. We therefore start with a brief summary of our main conclusions.

Most of the questions specific to P-724 had to do with characteristics of the detector which have been incorporated into the Monte Carlo discussed in our proposal. We believe the characteristics assumed for the detector in the Monte Carlo were reasonable. In some cases they were perhaps slightly pessimistic such as the assumption of an energy resolution $\sigma_E/E = 0.20/\sqrt{E}$ for photons and electrons. We also are hoping that through the use of uranium plates, rather than iron and lead, in the calorimeter we will be able to improve the hadron energy resolution significantly compared to the $0.65/\sqrt{E}$ that was assumed in the proposal.

Our proposal discusses a great number of important physics questions that can be addressed with the proposed detector. The PAC's questions regarding P-724 are phrased in a general way. In order to be specific we have assumed the questions referred to the separation of $Z^\circ \to 2\nu$ events from background. This is one of the most difficult physics objectives we discuss in our proposal; it is also probably the most important and one of the most susceptible to a realistic Monte Carlo simulation. This process therefore represents a very plausible test of a detector for the DO area.

We have made the following Monte Carlo studies:

(i) What is the effect of increasing the minimum momentum above which charged leptons can be vetoed from 1.5 to 5.0 GeV/c? This has to do with Questions 1 and 2 of the PAC.

(ii) What is the effect of worsening the rms hadron energy resolution $\sigma_E/E$ from $0.65/\sqrt{E}$ to $1.30/\sqrt{E}$? This has to do with Questions 3 and 4.

(iii) What happens if the size of the beam holes is increased from 1.5 mrad to 5.0 mrad? [Question 5].

The results of these Monte Carlo studies are summarized in Figure I-1 which compares the background to $Z \to 2\nu$ for each of the above situations with that expected for the characteristics assumed in the proposal. Generally speaking, the effect of each of the above is to increase the background

significantly for $P_T^{mis}$ below 10 GeV/c. Above 10 GeV/c there is little or no effect. Figure I-1 also shows for comparison the signal and background for the "standard" assumptions. The $Z^\circ \to 2\nu$ signal is not significantly affected by the above changes except that (i) gives a 5% increase in signal because of the lower probability of vetoing a $Z^\circ \to 2\nu$ event because it happens to contain a charged lepton with $P > 1.5$ GeV/c.

Thus we conclude that none of these more pessimistic assumptions will cause a serious worsening of the $Z^\circ \to 2\nu$ background. Of course, other aspects of the physics we hope to do may be seriously affected. For example, if the beam holes were enlarged to 5 mrad, much of the forward hadron-hadron physics would be lost or badly compromised.

In regard to Question 6, we show that it is possible to use only two very forward calorimeters rather than the 4 split ones in our proposal. This leads, however, to a slight loss in the containment of energy for hadrons which strike the calorimeter near the beam pipe.

Our background estimates for $Z^\circ \to 2\nu$ explicitly contain t, b, c, . . production (Question 7) and decays. The decay $W^\pm \to \tau^\pm\nu$ is also explicitly considered and constitutes the largest background source. Background from $W^\pm \to L^\pm\nu$ where $L^\pm$ is a heavier lepton would be comparable or less than that from $W \to \tau\nu$. We note that Frank Paige, an author of ISAJET, believes it is not possible to measure $Z \to 2\nu$ at ISABELLE, and we agree that this would be extremely difficult because of the smaller average $P_T$ of the Z's and smaller production cross section.

Because we propose a calorimeter with much finer spatial resolution than UA1 or UA2 the background for electrons resulting from the overlap of charged tracks with one or more $\pi^\circ$'s is expected to be at least two orders-of-magnitude smaller (Question 8).

We expect that through the use of yellow filters and careful design the variation in pulse height over the length of our calorimeter scintillators will be quite small (Question 9).

In Part II of this Addendum we discuss the questions for all DO proponents. In the response to the Question c, we point out that ours is probably the only detector, existing or proposed, that can trigger on events with large missing $P_T$ ($P_T^{mis} > 6$ GeV/c). With the addition of a microvertex detector we could trigger on events which contain charmed particles or $\tau$ leptons, though this is not planned for the first stage of operation.

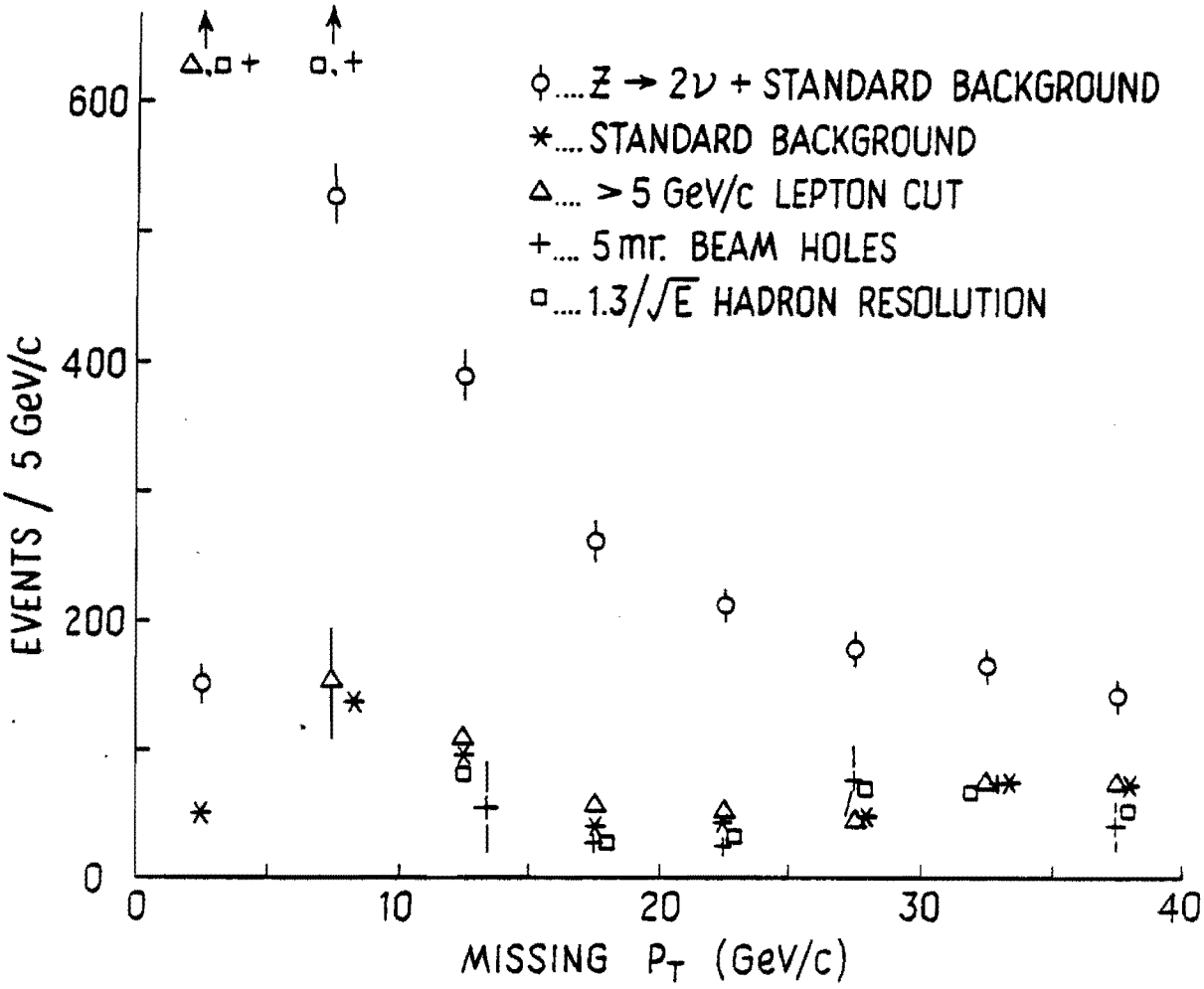


Figure I-1: Comparison of $Z^\circ \rightarrow 2\nu$ signal plus standard background with total background for different assumptions concerning the detector characteristics. The error bars shown for the (signal + background) are the estimated statistical errors for a run with integrated luminosity $10^{36}$ cm$^{-2}$. The error bars shown for the background points are the statistical errors in the Monte Carlo studies. All sources of background including jet events, heavy flavor production and decay, and W decays are included. An average $P_T$ for Z and W production of 20 GeV/c was assumed.

In the response to Question e, we show that we could detect a heavy lepton produced in $W \to L + \nu_L$ which decays into hadrons + $\nu_L$. The signal will appear as events with $P_T^{mis} > 25$ GeV/c and no charged lepton with momentum > 1.5 GeV/c. The signal/background is approx. 1:1 with most of the background coming from $W \to \tau + \nu_\tau$. The neutral partner of a massive charged lepton is also likely to show up in the $(Z^\circ \to 2\nu)/(Z^\circ \to 2e)$ ratio.

In the response to Question f, we show that we can identify a sample of $t\bar{t}$ events with < 6% background and an expected yield ~500 events for a $10^{36}$ $cm^{-2}$ run ($M_t$ = 40 GeV). Identification is done on the basis of the missing $P_T$ and the requirement of two or more high $P_T$ electrons. The mass of the t can be determined to ≈5% accuracy using the transverse mass calculated from the missing $P_T$ and the electron momentum only.

Our detector should be as good or better than any existing or proposed detector for studying direct photon production. The most important characteristic of the detector for this physics is fine segmentation in the electromagnetic detector, not unusually precise electromagnetic energy measurements.

We also show (Question h) that if heavy quarks are produced diffractively with a cross section ~1 mb x $(M_c^2/M_Q^2)$ we will be able to obtain a clean sample of $\sim 10^5$ identified $t\bar{t}$ events in a standard run. This identification relies only on missing $P_T$ and the detection of high $P_T$ electrons.

PART I - QUESTIONS FOR P-724

1. Your cut at 1.5 GeV/c lepton momentum seems highly optimistic. The Committee would like a more detailed discussion of how your goals would be compromised with a more pessimistic consideration of the likelihood of losing leptons, especially as they are likely to be associated with hadrons.

The Monte Carlo studies for our proposal were made well before results on $W \to e + \nu$ from UA1 and UA2 were available. On the whole we believe we did a remarkably good job of anticipating the problems (and solutions thereof) in isolating the W signal. This includes our emphasis on the importance of missing $P_T$ and the use of the transverse mass (p. 44 of our proposal). Even the 15 GeV/c cuts we used on the $P_T$ of the electron and the missing $P_T$ were identical to those used in the UA1 analysis. We did not, however, anticipate the problems the CERN detectors would have in isolating a clean electron signal. However, as we discuss below, our detector with its much finer segmentation should do much better.

It should be emphasized that the 1.5 GeV/c cut we used in the $Z^\circ \to 2\nu$ Monte Carlo serves a much different function than the 15 GeV/c cut in the $W \to e + \nu$ analysis. The $P_T$ spectrum of electrons from $W \to e + \nu$ peaks about 40 GeV/c so little signal is lost and much background suppression is gained by imposing a relatively high cut on the $P_T$ of the electron. In the $Z^\circ \to 2\nu$ analysis the cut is imposed to reduce the background at largish missing $P_T$ from events which include heavy flavor production and decay. The optimal "threshold" momentum for the charged lepton cut is that which maximizes the $Z^\circ \to 2\nu$ signal-to-background and minimizes the number of $Z^\circ \to 2\nu$ events which are accidentally vetoed. [Since the same cuts are applied to $Z^\circ \to 2e$ events, accidental vetos do not affect the $(Z^\circ \to 2\nu)/(Z^\circ \to 2e)$ ratio, only its statistical error.] With an ideal detector and a cut on events with charged leptons > 1.5 GeV, we estimate from the Monte Carlo that approx. 9% of the $Z^\circ \to 2\nu$ events will be vetoed because they happen to contain a high $P_T$ electron or muon in the gluon jet or the beam jets. Typically the $Z^\circ \to 2\nu$ events contain ~25 hadrons, including $\pi^\circ$'s with $P > 1.5$ GeV/c and not within 30 mrad of the beam. Thus it would be unlikely that, with a very fine-grained calorimeter, there would be a significant loss of $Z^\circ \to 2\nu$ events because of an overlap between a $\pi^\circ$ and a charged particle. This has been verified by a Monte Carlo calculation. (See Question 8.)

Table I shows a rough comparision of the granularity near 90° of the calorimeter we propose with those of UA1, UA2, CDF, and the other major detectors proposed for DO. Since the probability of an accidental overlap varies as the area of the circle of confusion, the overlap probability should be $\sim 10^{-2}$ smaller for our detector than the others. Our detector is also much more finely segmented in depth. This makes it more likely that an accidental overlap can be detected from the longitudinal energy deposition profile.

In order to evaluate the effect of raising the charged lepton veto threshold, we have run the Monte Carlos with the threshold raised to 5 GeV/c. For simplicity in what follows we assume an average $P_T$ of the Z's and W's of approx. 20 GeV/c in the Monte Carlos. This is on the low end of the range predicted by E. Berger for the Fermilab Collider, 20 to 30 GeV/c.

In Figure I-1 we compare the background from the "standard" Monte Carlo (lepton veto for P > 1.5, $0.65/\sqrt{E}$ energy res. for hadrons, and 1.5 mrad beam holes) with the background if the lepton veto is raised to 5 GeV/c. We see there is a substantial increase in background for $P_T^{mis} < 10$ GeV/c, but little effect above 10 GeV/c. The signal and background for the standard case are also shown. [Note that the background has been reduced somewhat relative to the curves in the proposal because of an improved set of cuts.] If the 5 GeV/c lepton cut is used, the signal increases about 5% due to the lowered probability of $Z^\circ \to 2\nu$ events being lost because they contain a charged lepton with momentum above the veto threshold.

We conclude that raising the threshold for the charged lepton veto by over a factor of three causes only a modest increase in background. In addition, as discussed above, a cut above 1.5 GeV/c will probably be possible. (Additional discussion is given below in the response to Question 8.)

Table I - Comparison of CCD Calorimetry with Other Detectors

| | CCD | UA1 | UA2 | CDF | LAPDOG* | P-726* |
|---|---|---|---|---|---|---|
| Coverage | > 0.06° | > 0.2° | > 40° | > 2° | >5° | >0.5° |
| Holes or dead regions | 0 | ~10° (top & bottom) | ~6% | ~6% | Large** | Small |
| Granularity (Central region) | Wires ±0.5° Scintillator ≈±3° x 45° Cathode pads ≈4.5° | ≈5° | ≈6° | ≈3.5° | Pb Glass - ≈2.8° x 45° Pads ≈±4° (?) | ≈±4° x 6° |
| Total Thickness (Central region) | > 7 $\lambda_{abs}$ | > 5.8 λ | 4.5 λ | 5 λ | ? | 5 λ |
| Energy Res. (σ) | | | | | | |
| Hadronic | $0.65/\sqrt{E}$ | $0.8/\sqrt{E}$ | $\sim 0.32/E^{1/4}$ | $0.65/\sqrt{E}$ | ? | |
| E.M. | $0.15/\sqrt{E}$ | $0.15/\sqrt{E}$ | $0.14/\sqrt{E}$ | $0.15/\sqrt{E}$ | $\sim 0.05/\sqrt{E}$ | $.007 + .011/\sqrt{E}$ |
| Z mass res. (Z → 2e) [Intrinsic Width ≅ 3 GeV] | ≈2.3 GeV | | | ≈2.3 GeV | ~0.8 GeV | ~0.5 GeV |

* These numbers are generally based on the original proposal and may not include updates or changes.

** Includes hole near Θ=30° covering 2π in φ plus coils and coil supports, and possibly a thick iron magnetic shield around M.R. vacuum pipe.

2. Assuming that one eliminates every event with an electron or muon candidate with $P_T$ > 1.5 GeV/c, it might eliminate a large number of the interesting events. How sensitive is the missing $P_T$ distribution to the magnitude of this cut?

We emphasize that the charged lepton cuts, where appropriate, will be applied in the analysis, not in the trigger. For some physics such as t quark searches and $W \to e + \nu$, one would want to require the presence of one or more electrons or muons. For other physics such as $Z^\circ \to 2\nu$ and gluino searches the absence of charged leptons is the desired characteristic.

We discuss above in Question 1 the effect of raising the charged lepton veto threshold from 1.5 GeV/c to 5 GeV/c on the $Z^\circ \to 2\nu$ background. With the 1.5 GeV/c lepton veto about 9% of the $Z^\circ \to 2\nu$ events would be lost because they contain a charged lepton > 1.5 GeV/c. This has been included in the rates given in the proposal. An additional 1% would be lost due to accidental overlaps of a $\pi^\circ$ and charged track. (See Question 8.)

We estimate from our Monte Carlo that if the charged lepton veto were eliminated entirely, the background to $Z^\circ \to 2\nu$ for missing $P_T$ > 10 GeV/c would increase by approx. a factor of 3. This would make the $(Z^\circ \to 2\nu)/(Z^\circ \to 2e)$ measurement significantly more difficult, but it would probably still be feasible. (See Figure 1.)

3. How sensitive is the missing $P_T$ distribution to the total energy resolution? $.65/\sqrt{E}$ may be optimistic for the overall in situ performance.

In the Monte Carlo simulations discussed in the proposal we use for the hadron energy resolution $\sigma_E/E = 0.65/\sqrt{E}$ where $\sigma_E$ is the standard deviation of the distribution which was assumed to be Gaussian. This is consistent with published data for calorimeters with 5 cm iron plates. (Ours are assumed to be 3.75 cm.) See, for example, G. Bellettini et al., NIM 204, 73 (1982) and H. Abramowicz et al., NIM 180, 429 (1981). This is also the resolution assumed for the central calorimeter in CDF. (See Table I.) The UA1 group quotes a resolution of $0.80/\sqrt{E}$ for hadrons and $0.15/\sqrt{E}$ for electrons and $\gamma$'s.

To test the sensitivity of the $Z \rightarrow 2\nu$ background on the assumed energy resolution we have rerun the Monte Carlos with an energy resolution for hadrons of $\sigma_E/E = 1.30/\sqrt{E}$. The results are shown in Figure I-1. We see that even this drastic worsening of the energy resolution only affects the background below $P_T^{mis} \cong 10$ GeV/c.

4. Do expected non-Gaussian tails in your calorimeter response seriously compromise the sensitivity to large missing $P_T$ events?

The answer to the previous question shows that even a large component with twice the expected resolution would not be a problem. We have also repeated the Monte Carlo calculations of the background for the $Z^\circ \to 2\nu$ signal with the "standard" Gaussian distribution for the hadron energy resolution modified to include a long tail. If we put 5% of the hadrons in a Gaussian distribution with $\sigma_E/E = 3.3/\sqrt{E}$, or five times wider than the $0.65/\sqrt{E}$ normally assumed, we find a background which is almost indistinguishable from the "standard" background in Fig. I-1. A tail containing 5% of the hadrons which falls like $(\Delta E)^{-3}$ causes the background below $P_T^{mis}$ = 10 GeV/c to increase, but leaves the background at higher $P_T^{mis}$ unaffected.

Basically the reason a non-Gaussian tail is unlikely to cause a problem is because we are interested mainly in events with missing $P_T$ > 10 GeV/c. For an apparent missing $P_T$ this large to occur due to the mismeasurement of the energy of a single particle, its $P_T$ must be > 10 GeV/c. Single particles with this large a transverse momentum are very unusual; we estimate from ISAJET that < 1 in $10^5$ of the particles have $P_T$ > 10 GeV/c. The errors in the energy measurements of multiple particles add incoherently (in a well-designed calorimeter), and it is very unlikely that two or more particles will each have sufficiently large $P_T$ and simultaneously have sufficiently large energy errors to simulate an event with $P_T^{mis}$ > 10 GeV/c. We believe the most likely source of large missing $P_T$ is therefore going to be physics, i.e. - events with high transverse momentum neutrinos or other invisible particles. We also believe the physics backgrounds to the new physics we hope to study have been simulated as accurately as possible in our Monte Carlos.

As an extra precaution, our calorimeter design includes both scintillation and gas calorimetry. This redundant information allows a check of one measurement against the other.

We have given considerable thought to mechanisms which might cause tails in the energy response of our calorimeter. Obvious instrumental sources such as cracks and areas of low response have been carefully considered in the design and will be a major concern in the actual construction.

A possible source of a tail is hadron punchthrough. We have therefore designed a calorimeter which is unusually thick compared to existing and proposed detectors (Table I). Remaining punchthrough has been put into our Monte Carlo.

Another possible source of a tail is the (semi-) leptonic decay of particles before they are absorbed in the calorimeter. The most likely source is $K^{\pm}$ decays because of their short lifetime and large leptonic branching ratio. For a $K^{\pm}$ decay to give a missing $P_T > 10$ GeV/c (due to its decay neutrino) it must have a $P_T > 20$ GeV/c. Particles with this large a $P_T$ are extremely rare. We estimate from ISAJET that only $\sim 5 \times 10^5$ $K^{\pm}$ with $P_T > 20$ GeV/c will be produced in a 1 $pb^{-1}$ run. Of these only ~1000 will decay before being absorbed. Approximately 99% of these will have a detectable $\mu^{\pm}$ and will be vetoed in the $Z \rightarrow 2\nu$ analysis.

Our highest priority for a detector "upgrade" is to use uranium plates in the calorimeter instead of lead/iron. This would improve the hadronic energy resolution considerably and therefore significantly reduce the contribution to the apparent missing $P_T$ due to energy measurement errors. To determine how much we can improve the resolution, we plan to build a test calorimeter with uranium plates. Delivery of the uranium is expected before the end of the summer.

5. Can you verify by Monte Carlo calculation whether the very forward calorimeters are in fact required for missing $P_T$ physics?

We estimate that without the very forward calorimeters we would cover angles down to approx. 5 mrad from the beams. [See Fig. A-4 of our proposal.] This can be attained without moving any calorimeters. We have therefore rerun the $Z^\circ \to 2\nu$ and background Monte Carlos with 5 mrad beam holes. The background, shown in Fig. I-1, rises dramatically for missing $P_T < 8$ GeV/c, but is unaffected for $P_T^{mis} > 10$ GeV/c. [For some points the 5 mrad background appears to be smaller than the standard (1.5 mrad beam hole) background. This is almost certainly due to statistical fluctuations in the Monte Carlos. For practical reasons it is difficult to generate a sufficiently large number of background events to make statistical fluctuations negligible.]

We emphasize that a 5 mrad beam hole would have a serious impact on hadronic physics at small angles. The ability to study hadrons down to very small angles would be a unique capability. The installation of the very forward calorimeters could be delayed to a second stage if the Laboratory believes their installation for the first run introduces too many difficulties.

[See also next question for further discussion.]

6. P-724 might reduce criticism of its forward calorimeters if a way could be found to put both left and right sections of a given set of calorimeters at the same longitudinal position. Do you have any idea how this can be done?

In Figure I-2 we show a design with the left and right halves of the very forward (VF) calorimeters at the same longitudinal position. These calorimeters are split into two halves longitudinally, one of which can be moved to the left, the other to the right to close in on the beams once they are stable. This design is more compact than the one shown in our proposal and requires fewer flexible bellows. It is also somewhat easier to construct. It is slightly poorer in containing particles which spray from the inner edges of the upstream VF calorimeter. A small fraction of the spray going off at angles ~30 mrad from the upstream VF calorimeter passes through the central hole of the second and is lost as far as the energy measurement is concerned. However, our M5 measurements show that the probability of finding spray at a given angle falls off rapidly with decreasing angle for angles $\lesssim$ 40 mrad. [See Figure A-3 in our proposal.]

If it is necessary to build the detector in a space of ±10 to ±12 m between the low-$\beta$ quadrupoles a design with only one set of forward calorimeters is more appropriate. An example is shown in Figure I-3. In this design $\Theta_{min} \cong 3$ mrad. This supposes that the inner wall of the vacuum chamber can be moved to within 1.5 cm of the stable beams and the sensitive volume of the detector starts within 0.5 cm of the inner wall.

Roughly speaking, there is a continuum of forward calorimeter designs depending on the available clear space. If ±L is the free space in meters between the low-$\beta$ quads, the minimum angle which can be reached if the forward calorimeters are movable is $\Theta_{min} \cong 0.02/(L-5)$. If the calorimeters are not moved (no flexible bellows), $\Theta_{min} \cong 0.05/(L-3)$ where we assume a 7.5 cm inner diameter for the vacuum pipe through the forward detectors. We assume that the forward calorimeters will be assembled around an integral section of vacuum pipe. Installation would therefore be very straightforward.

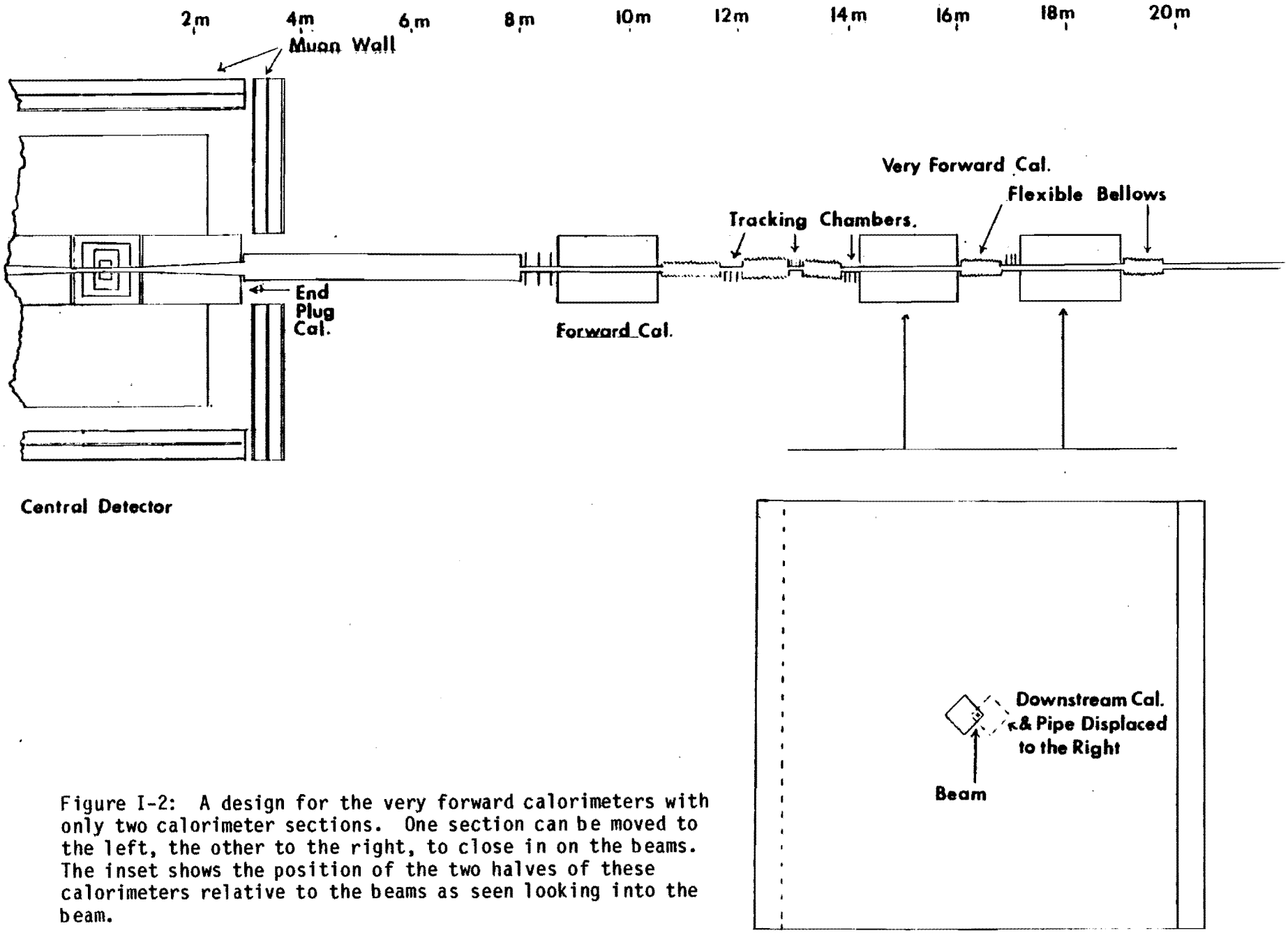


Figure I-2: A design for the very forward calorimeters with only two calorimeter sections. One section can be moved to the left, the other to the right, to close in on the beams. The inset shows the position of the two halves of these calorimeters relative to the beams as seen looking into the beam.

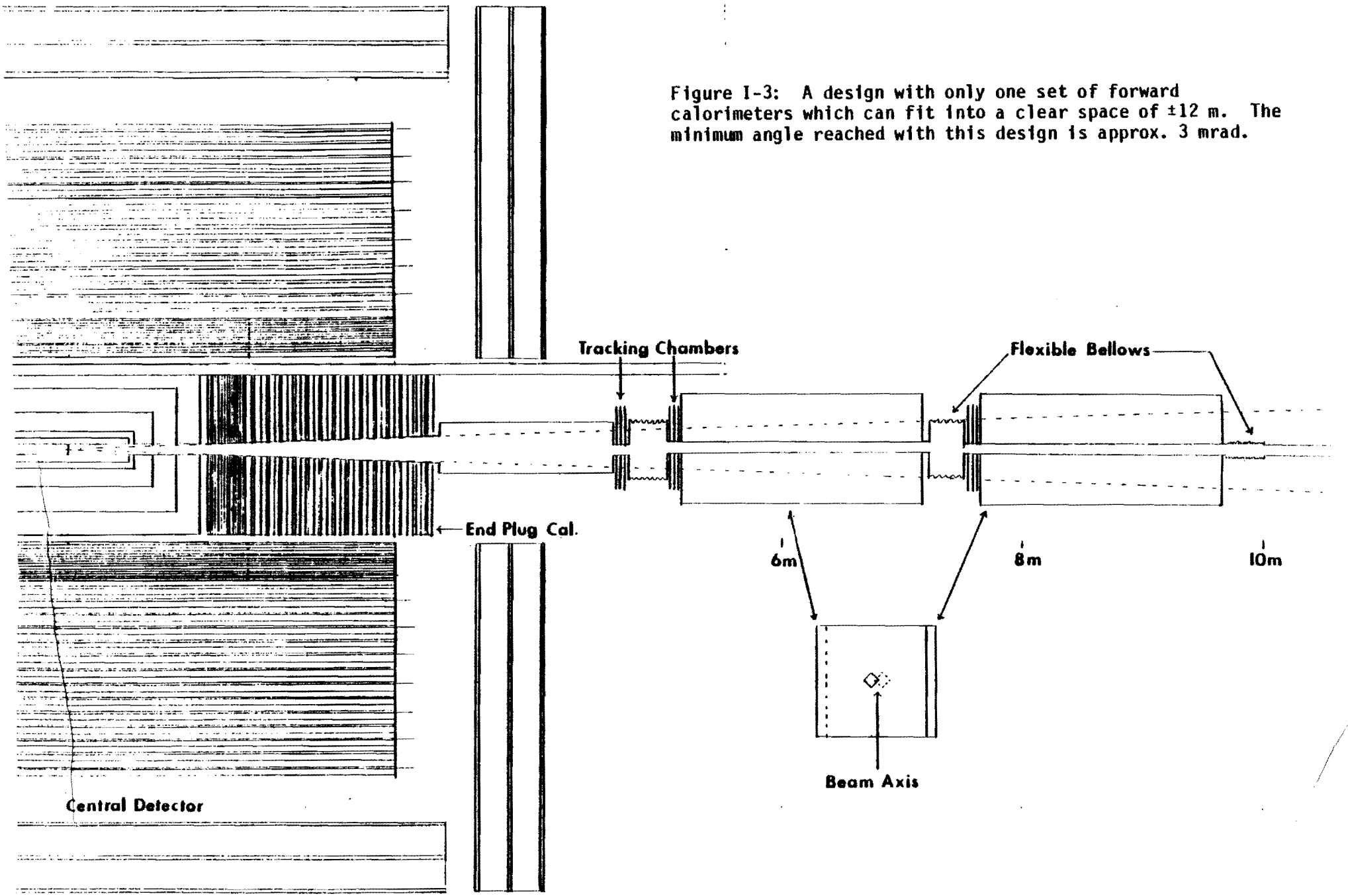


Figure I-3: A design with only one set of forward calorimeters which can fit into a clear space of ±12 m. The minimum angle reached with this design is approx. 3 mrad.

7. Could you please give a realistic estimate of the background to the $Z^\circ \to \nu\nu$ signature, in particular the effects of heavy quark or lepton production. (The authors of ISAJET doubt that this process is measurable.)

We believe we have included all of the predictable backgrounds in the estimates given in our proposal and updated in Figure I-1. The background estimates include minimum bias events, two-jet events, W and t production and decay, as well as instrumental effects such as detector resolution and punchthrough. New physics such as heavy lepton or gluino production could increase the background slightly. However, the background cuts we impose to reduce the background for $Z^\circ \to 2\nu$ events are very effective against backgrounds from particles produced in pairs (e.g. - $t\bar{t}$, $\tilde{g}\tilde{g}$, $L^+L^-$). This is basically because the missing $P_T$ vector for these events is unlikely to be opposite a jet and there is usually more than one recognizable jet (not counting the beam jets).

There are at least two reasons why our background estimates for $Z^\circ \to 2\nu$ may actually be pessimistic. One is that we have assumed a t mass of 20 GeV/$c^2$, essentially the lowest allowed value. We have verified that if the t mass is significantly higher the resultant background to $Z^\circ \to 2\nu$ would be significantly lower because of the smaller production cross section and the increasing effectiveness of the background cuts. Our Monte Carlo predicts approx. 0 events from this source if $M_t$ = 40 GeV. We are also confident that by more sophisticated techniques for extracting the signal from the background we can improve the separation of $Z^\circ \to 2\nu$ from the largest background source $W \to \tau + \nu_\tau$. We have already found we can significantly reduce the background at large $P_T^{mis}$ shown in Fig. I-1 by a Fisher discriminant analysis [CCD Memo 1, R. Ball and I. Leedom, March 1983.] We also know that much more powerful techniques for multivariate analysis are available, but we haven't had time to implement them.

As far as the feelings of the authors of ISAJET on the feasibility of a measurement of $Z^\circ \to 2\nu$, we have had numerous conversations with Frank Paige regarding ISAJET. His opinion, as stated to us, is that he does not believe the $Z^\circ \to 2\nu$ measurement could be made at the CBA. He has no incentive to worry about its feasibility at the Fermilab Collider. As far as we know Frank has no opinion on the feasibility of a $Z^\circ \to 2\nu$ measurement at Fermilab. We agree with Frank that the measurement would be very difficult or impossible

at $\sqrt{s}$ = 800 GeV because of the much lower average $P_T$ of the Z's and the lower production cross section.

We are rather confident of our background estimates because the largest background is $W \to \tau + \nu_\tau$ whose cross section should be quite predictable relative to $Z^\circ \to 2\nu$. The $t\bar{t}$ production is a less serious but important background. If the mass of the t is ~20 GeV/$c^2$ and the cross sections for central production of $t\bar{t}$ built into ISAJET are much too small, the $t\bar{t}$ background could become more of a problem. A large cross section for diffractive production of heavy flavors would not be a problem because we could easily place angular cuts on the $\theta$ angle of the jet which balances the missing $P_T$.

8. Please calculate in detail the background for electrons resulting from the overlap of charged tracks with one or more $\pi^\circ$'s.

Generally speaking our detector would be much better in this regard than any existing or proposed detector because of the much finer granularity in the calorimeter (Table I). An electron shower vertex in our detector can be localized to $< \pm 0.5$" in the electromagnetic detector. For a good electron the incoming charged track can be required to hit within $\pm$ 0.5" of this vertex. Since this background goes as the area of the "circle of confusion" we will be $\sim 10^2$ times better in this regard than UA1 and UA2 (Table I). In addition, we have much better segmentation in depth. A fake electron due to an overlap of a charged hadron and a $\pi^\circ$ will generally carry to greater depths in the calorimeter since the lead is only approx. 0.5 abs. length. Thus the fakes will usually be distinguished by a long "tail" extending into the iron plates.

A detailed answer to this question can only be given in terms of a specific physics objective. We have therefore made a Monte Carlo study of the probability that a $Z^\circ \to 2\nu$ event will be lost because it contains a fake electron with $P > 1.5$ GeV/c which is not within 40 mrad of the beams. In this analysis we assumed that charged hadrons with $P > 4$ GeV/c would be distinguishable from e's because of their energy deposition in the hadron calorimeter, and so could not contribute to fake electrons. We looked for a charged hadron and a $\gamma$ within $\pm 0.7^\circ$ of each other (Table I) whose combined momentum exceeded 1.5 GeV/c. With $Z^\circ \to 2\nu$ events generated by ISAJET we find $< 1\%$ of the events are lost due to fake electrons from such overlaps.

9. To what extent will multiple hits in the same scintillator in the calorimeters compromise the correction for pulse height variation as a function of distance from the photomultiplier?

We do not believe this is a problem because of the much more detailed energy information from the PWC's interleaved with the scintillators. However, we believe it is extremely important to make these scintillators as uniform as possible. We believe we can make them quite uniform for several reasons:

1) In E613 we had veto counters which were 78" long, carefully made with good scintillator, and viewed by a phototube on one end only. Except for a region < 4" long near the light pipe they were uniform to ±5% over the entire length. No yellow filters were used between the light pipe and phototube. The counters in the CCD calorimeter are 108" long and about 0.2" thick compared to 0.5" for the E613 counters.

2) The scintillators in the UA1 "gondolas" are 0.06" thick and 160" long. These scintillators had to be formed in a semicircular shape by heating the scintillator to let it slump into the desired shape. It is under considerable localized pressure because of the lead plates interleaved with the scintillator. Despite all these potential causes of reduced light transmission the measured attenuation length for these counters is approx. 80". We believe this was achieved without the use of yellow filters.

3) We have made tests which show that the attenuation length in scintillator can be increased a factor of 5 or 10 by inserting a yellow filter ahead of the phototube. In our detector we view the scintillator directly through adiabatic light pipes with good area matching so that we will have very good light collection in the central detector scintillators. Thus we expect ~10 times as many collected photons per GeV than a typical calorimeter with wavelength shifter bars. We can therefore afford to give up 90% of the light if necessary through the use of a deep yellow filter and still have plenty of light.

4) Various groups have used a technique to improve the uniformity of long counters by selectively blackening the inside surface of the wrapping so that the wrapping on the near end is much less reflective than the far end. This works best on thin counters because it relies on absorbing the near ultraviolet light before it gets wavelength shifted into the visible.

We are therefore confident that with good scintillator, careful design and construction, and the techniques described above, we can achieve a uniformity of better than ±10% over the useful length of the counters.

## PART II - QUESTIONS FOR ALL DO PROPONENTS

a. Please comment on any other present or potential commitments which might impact on your ability to perform your proposed experiment in a timely fashion.

Members of the Michigan group have provisionally joined the LEP-3 collaboration. They have, however, stipulated that if the DO proposal is accepted their involvement in LEP-3 will be small or nonexistent.

The University of Illinois at Chicago group have a commitment to E557/E672 which will run this winter. E672 will have another run in late 1986.

John LoSecco at Cal Tech is currently involved in the IMB proton lifetime experiment.

b. How will the performance of your detector depend on the length of the beam-beam interaction region? Do you need low beta?

The design we consider optimal is discussed in the proposal (page 73). This design would allow a clear space of ±20 m between the low beta quads. We estimate that with this design it will be possible to achieve a $\beta^*$ of approx. 5 m. [See Fig. IV-2 of our proposal.] This should give a luminosity ~ $1.8 \times 10^{29}$ $cm^{-2}$ $s^{-1}$ and an integrated luminosity of $10^{36}$ $cm^{-2}$ in a 5-month run at 40% efficiency.

We could, of course, design the detector to fit into ±10 to ±15 m of clear space. The physics implications of this design are discussed previously in the response to Question 5. As noted in our response to Question 6, if the forward calorimeters are moved closer to the stable beams the minimum angle we can reach with calorimetry is $\Theta_{min} \cong 0.02/(L-5)$ where ±L is the clear space in meters. If the calorimeter positions are fixed $\Theta_{min} \cong 0.05/(L-3)$.

c. Could you please estimate the errors on the measurement of missing transverse momentum? How does the loss of particles at small angles affect this measurement?

The spectrum of missing $P_T$ predicted for our detector from a complete ISAJET-based Monte Carlo is shown in Fig. III-2 of our proposal. The distribution has a width ~0.7 GeV/c.

The effect of the loss of particles at small angles has been discussed in the response to Question 5.

We note that our detector design is the only one which emphasized the importance of missing $P_T$ from the beginning. We also believe that our detector is the only one which will be able to trigger on missing $P_T$. This is a prerequisite to be able to study many "new physics" questions like gluino production and $Z \rightarrow 2\nu$ decays. Such events will be accompanied by modest transverse energies, and so will be difficult to trigger on with a conventional $E_T$ trigger. We estimate that with a missing $P_T$ trigger set for a threshold of $P_T^{mis} > 6$ GeV/c, the trigger rate will be approx. 1 Hz at a luminosity $\sim 2 \times 10^{29}$ cm$^{-2}$ s$^{-1}$.

d. How well do you reconstruct the interaction vertex? Are lifetime measurements for heavy quarks and leptons conceivable?

With the more-or-less conventional tracking chambers we plan to install in the first stage we anticipate a vertex resolution ~0.3 mm. The lifetime of a conventional sequential lepton with a mass of 30 GeV/$c^2$ is expected to be $\sim 10^{-19}$ s. The lifetimes of states containing t quarks are also expected to be comparably short [M.K. Gaillard and L. Maiani, in Quarks and Leptons, Cargese 1979, Plenum Press. New York]. Direct lifetime measurements for these states therefore seem very unlikely. Nevertheless we feel it is extremely important to have the highest practical accuracy for measuring the vertex position and identifying tracks from particles which decay close to the vertex. The ultimate goal is to be able to trigger on events which contain charmed particles or $\tau$ leptons. These should be rich in new physics such as $t\bar{t}$ production, Higgs particles, etc. We therefore intend to install a micro-vertex detector at a later stage when the technology is more developed.

e. Suppose $W^+ \to L^+\nu_L$ and $Z^\circ \to L^+L^-$ where L is a new heavy lepton. How well does your detector determine the characteristics of L?

Of the two modes suggested, the $W^+ \to L^+\nu_L$ mode seems the most promising for the detection and identification of the L because of the higher rate. For definiteness we assume $L^\pm$ is a conventional sequential lepton with a mass ~40 GeV/$c^2$. We expect ~ $4.6 \times 10^4$ W events in a 1 $pb^{-1}$ run. [See Table III-1 in our proposal.] Of these ~3500 will decay into $W^\pm \to L^\pm\nu_L$. The dominant decay mode of the $L^\pm$ will be $L \to q\bar{q}\,\nu_L$ (≈2400 events). We have done a Monte Carlo study of this decay using a modification of ISAJET. We find that the missing $P_T$ spectrum from these events is quite hard since the $\nu_L$ from $W \to L\nu_L$ tends to follow the direction of the W. Unlike $W \to e + \nu$ and $W \to \mu + \nu$ events the $W \to L + \nu$ events are not often accompanied by a muon or electron with $P > 1.5$ GeV/c. A charged lepton veto for $P > 1.5$ GeV/c will therefore eliminate most of the background from $W \to e\nu$ and $W \to \mu\nu$ and reduce that from events with t quarks. The main backgrounds will be from $W \to \tau + \nu_\tau$ and $Z^\circ \to 2\nu$. The latter can be eliminated by discarding large missing $P_T$ events with a single jet with total momentum equal and opposite the missing $P_T$ vector. The number of $W \to \tau + \nu_\tau$ events will be comparable to the $W \to L + \nu_L$ signal. The missing $P_T$ spectrum from the $W \to \tau + \nu_\tau$ events will be quite accurately predictable from the $W \to e + \nu$ events, so this background is readily calculable.

The missing $P_T$ spectrum from the Monte Carlo is shown in Fig. II-1 with and without the $L^\pm$ (i.e. - signal plus background vs. background). The background from $t\bar{t}$ and $W \to t + X$ is included with the assumption that $m_t = 20$ GeV/$c^2$. We see that for missing $P_T > 25$ GeV/c the signal/background is approx. 1 to 1. We have not had time to prove it, but we believe that much of the background can be eliminated by looking at the topology of the events. The $W \to L + \nu_L$ events with large $P_T^{mis}$ usually show a striking multijet topology with no jet aligned with the missing $P_T$ (Figure II-2). The angular distribution of the L's as determined from the hadron jets will also show the angular distribution characteristic of W leptonic decays. [See, for example, Fig. I-2 of our proposal.] This will help to identify the source of the large $P_T^{mis}$ signal.

The details of the scenario will vary somewhat with the mass of the heavy lepton, but we believe we would have a good chance of detecting it and determining its characteristics if $M_L < 70$ GeV/$c^2$. We note that if the $L^\pm$ is like the known charged leptons, with a low-mass neutral partner, we will be

alerted to its presence from the $(Z^\circ \to 2\nu)/(Z^\circ \to 2e)$ ratio. This, plus the excess of events with large missing $P_T$ and no e or $\mu$ above the cutoff, will be strong evidence for a new generation of leptons. [Note that the $W \to L + \nu$ events would not constitute a large background to $Z \to 2\nu$ because the topology cuts which greatly reduce the $W \to \tau + \nu_\tau$ background will be even more effective against $W \to L + \nu$.]

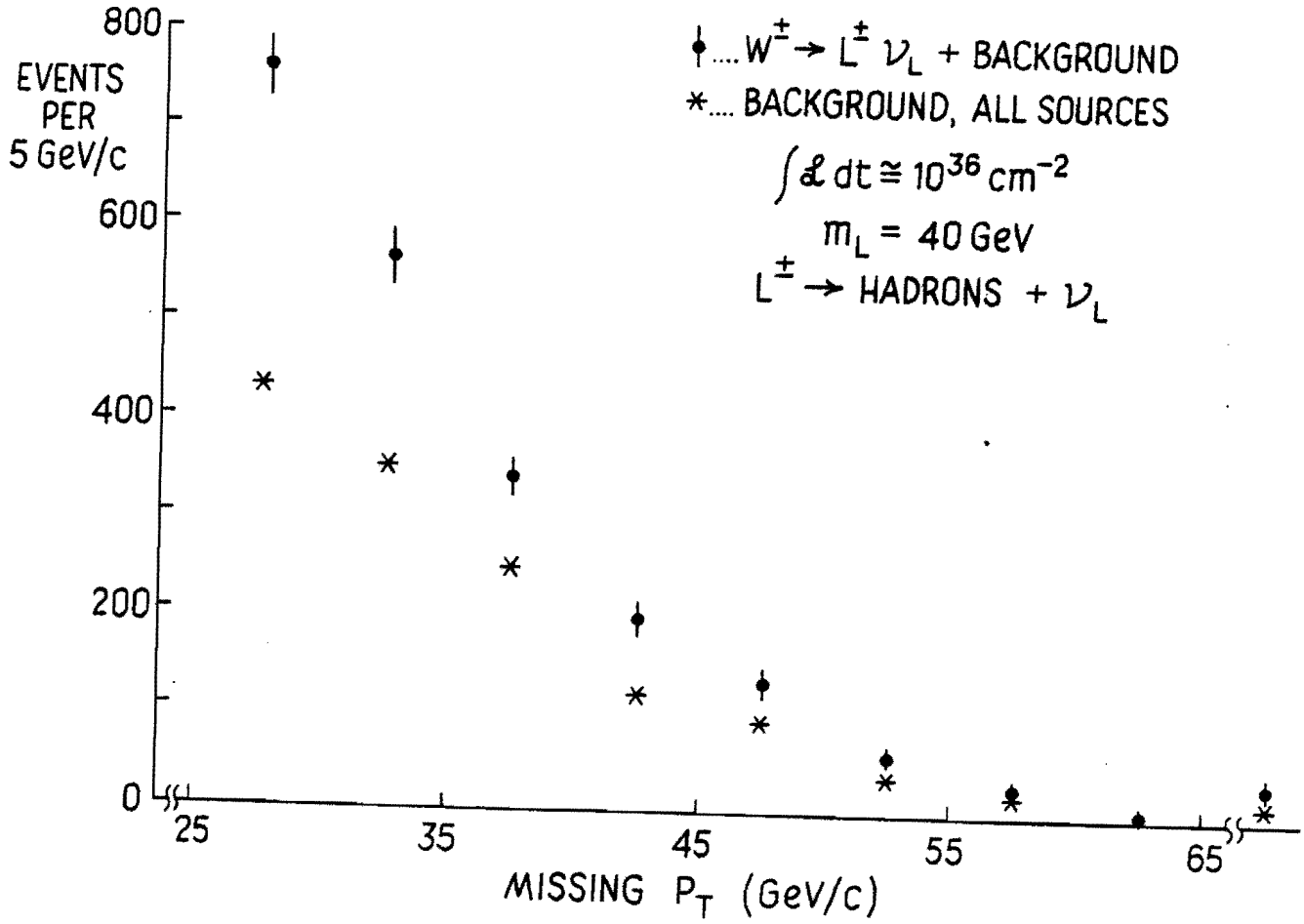


Figure II-1: Missing $P_T$ distributions expected if a sequential charged lepton with $M_L \sim 40$ GeV exists compared to that without. A veto of events with $e^\pm$ or $\mu^\pm$ with $P > 1.5$ GeV/c has been imposed.

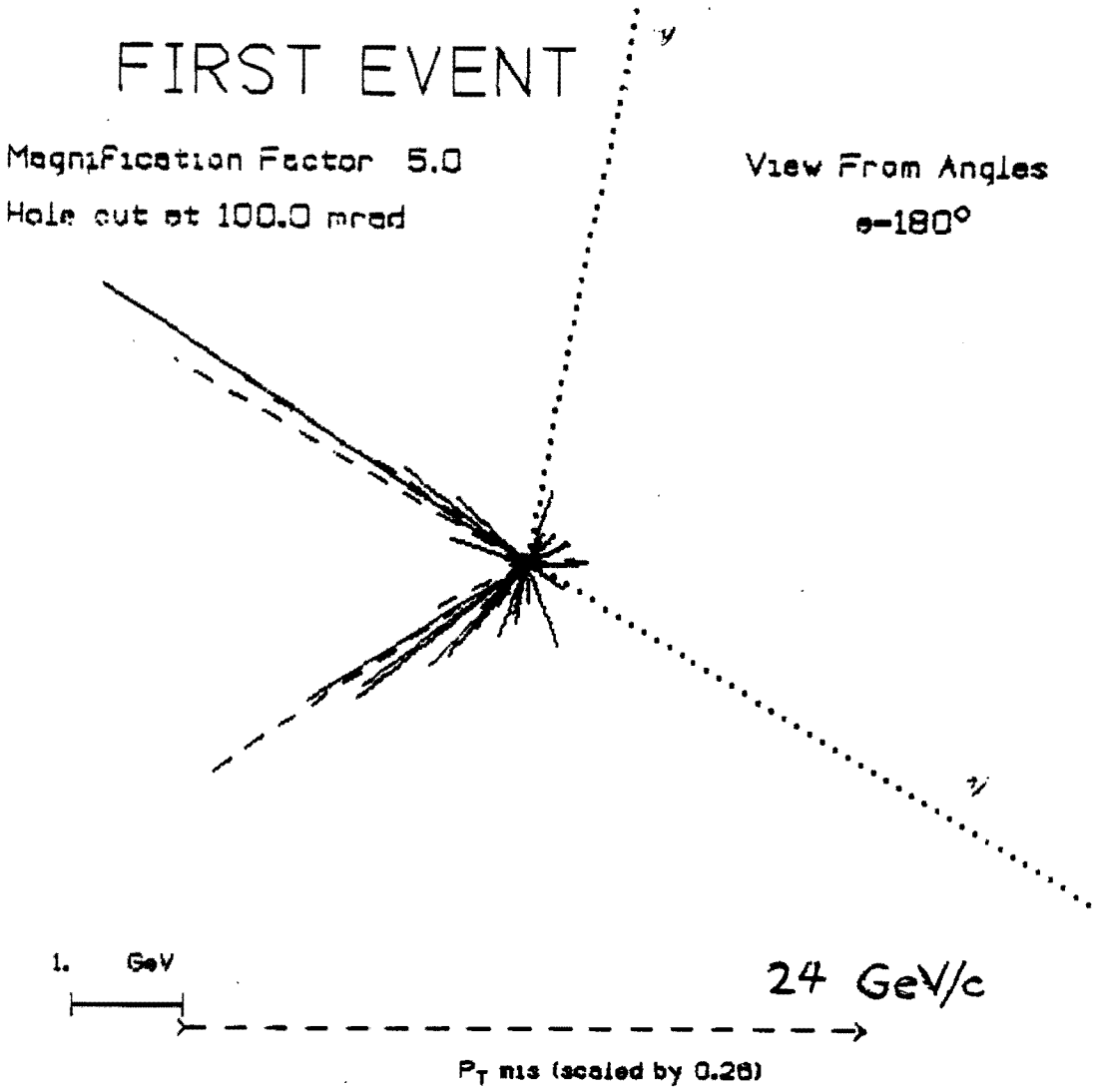


Figure II-2: A $W^- \to L^- + \nu_L$ event as seen looking into the beam. The $L^-$ is assumed to decay into $\bar{c} + s + \bar{\nu}_L$. The length of each vector in the plot is proportional to the $P_T$ of the particle. Neutrinos are shown as dotted lines, $\gamma$'s as dashed lines, and other particles as solid lines. The missing $P_T$ vector for the event is shown below it.

f. Assume $gg \to Q\bar{Q}$ with Q = c, b, t (20 GeV) is a subprocess for heavy quark production. How well does your detector a) distinguish different flavors of jets, b) measure the angular distribution of the subprocess, c) measure associated multiplicities, and d) measure $P_T$ of the subprocess?

We believe that by and large our detector would be as good or better than any existing or proposed detector for this physics. However, we believe that many of these questions cannot be tackled without considerably more experience with real data. No one, as far as we know, has yet identified the flavor of any jet. Our experience with ISAJET is generally discouraging. The jets from heavy quarks tend to be diffuse and overlapping. It remains to be seen what real heavy quark jets look like, though ISAJET has done well in predicting the cross section and general features of high $P_T$ jets.

We also believe that reasonably accurate measurements of jet masses may be very difficult. The CERN Collider data (and ISAJET) suggest that even large $P_T$ jets are accompanied by a nearly isotropic distribution (in angle) of low $P_T$ particles. These are fairly numerous and cannot be assigned to any particular jet, but their exclusion may lead to large errors in the reconstructed jet masses. The best measurement of the t quark mass is likely to come from the lepton momenta and missing $P_T$ as described below.

The missing $P_T$ capability of our detector will give us an extra constraint on heavy flavor production events which nearly always contain neutrinos with moderately large momentum. Even though these events often contain more than one neutrino, usually one dominates so the missing $P_T$ tends to be a good measure of the $P_T$ of the largest $P_T$ neutrino. An example of the importance of this is given below in the measurement of the mass of the t quark. As mentioned earlier, the addition of a microvertex detector would allow the identification of at least some of the events containing charm. The technique discussed by Anne Kernan at the Moriond $p\bar{p}$ Workshop for detecting $D^* \to D\pi$ is also of considerable interest in this regard.

To test the ability of our detector to identify events with t quarks and measure the t mass, we have done a Monte Carlo study of $t\bar{t}$ events produced by ISAJET. For definiteness we take the t quark mass to be $\approx 40$ GeV/$c^2$. The t and $\bar{t}$ will generally produce several detectable charged leptons and a fairly large missing $P_T$ in their cascade of decays $t \to b \to c \to s \to u, d$. This suggests looking for events with two or more identifiable charged leptons and a moderately large missing $P_T$.

We have therefore looked at $t\bar{t}$ events with 2 or more electrons, one with $P_T$ > 5 and the other with $P_T$ > 2 GeV/c and with no detectable muon. Figure II-3a shows a scatter plot of $\sum P_T$ for all events with > 2 electrons each with $P_T$ > 2 vs. missing $P_T$. Figure II-3b shows the same scatter plot for events containing $b\bar{b}$, $c\bar{c}$, . . . pair production. We see the two scatter plots are quite different. The cut shown ($\sum P_T$ of electrons > 12, $P_T^{mis}$ > 6) will eliminate the background events and keep most of the $t\bar{t}$ events. We have also verified that there is <6% background from W decays (except those containing top quarks). In a run with an integrated luminosity of 1 $pb^{-1}$ we expect $1.8 \times 10^4$ $t\bar{t}$ events if $m_t$ = 40 GeV/$c^2$. From the Monte Carlo we estimate that approx. 460 of these will pass the charged lepton and the missing $P_T$ cut described above. (≈5000 will pass if $m_t$ = 20 GeV/$c^2$).

Thus we can isolate a very clean sample of events containing t quarks (though with rather low efficiency). Barger, Martin, and Phillips [MAD/PH/100] have shown that if the transverse mass of the electron and neutrino defined as $m_T^2 = (P_T^e + P_T^\nu)^2 - [(P_x^e + P_x^\nu)^2 + (P_y^e + P_y^\nu)^2]$, is calculated, the end point is $(m_t - m_b)$. In this case there is more than one neutrino involved so we cannot identify the x and y components of the missing $P_T$ with $P_x^\nu$ and $P_y^\nu$. However this is usually a good approximation. A good estimate of $m_t - m_b$ can therefore be obtained from the $m_T$ distribution as calculated from the momentum of the highest $P_T$ electron in the event and the missing $P_T$. The distribution in $m_t$ from the Monte Carlo for events which pass the cuts is shown in Figure II-4. With some guidance from a Monte Carlo, it will be possible to determine $m_t$ with respectable accuracy.

We therefore conclude that a detector with the capability of measuring missing $P_T$ with good accuracy will be able to cleanly separate events containing t production and measure the t mass to ~5% accuracy.

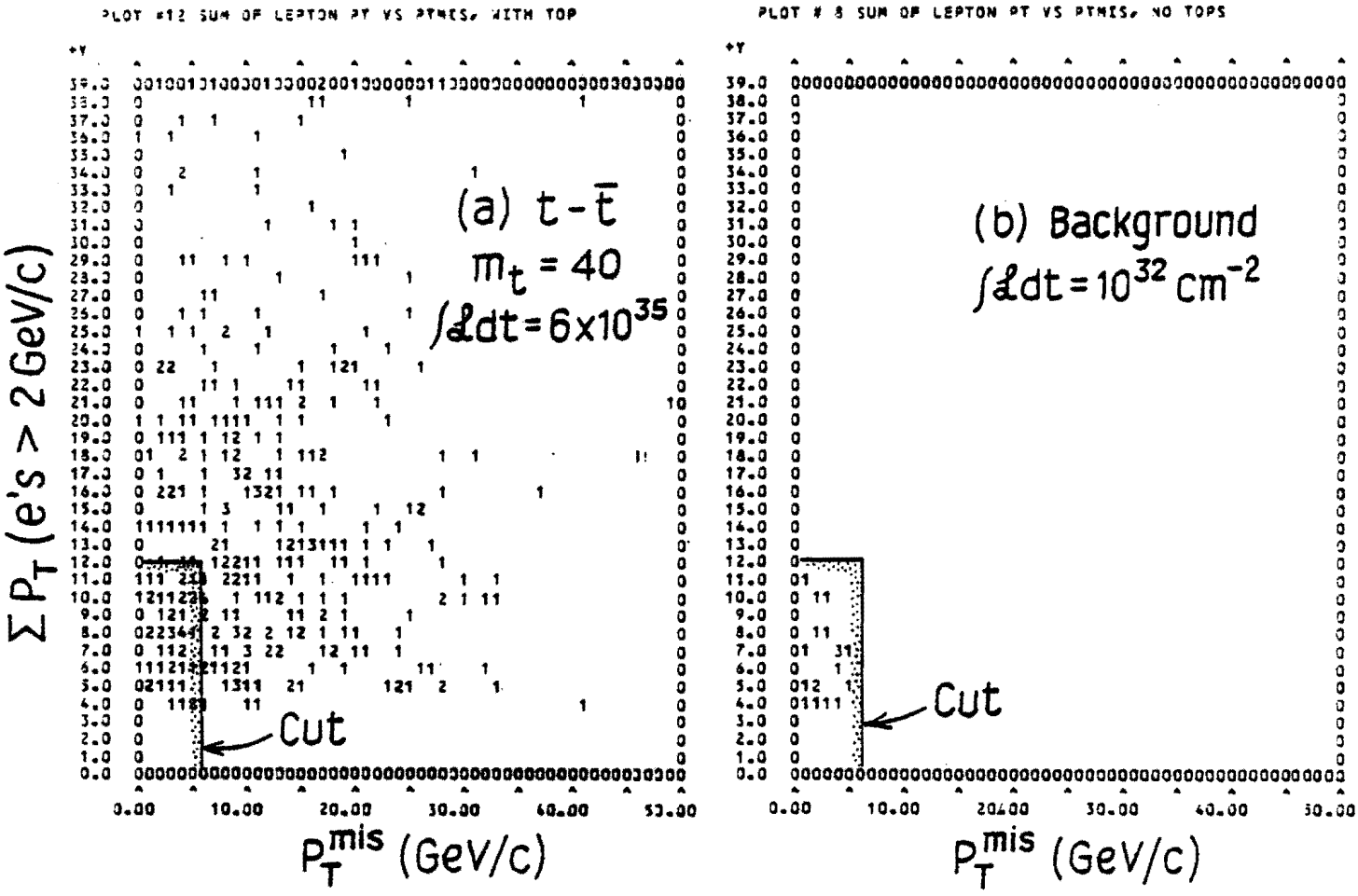


Figure II-3: Scatter plots of $\sum P_T$ for all electrons with $P_T$ > 2 GeV/c vs missing $P_T$ for (a) $t\bar{t}$ events and (b) background events from b, c, u, d quark production. Only events with two electrons with $P_T$ > 2 GeV/c and no detectable muon are plotted. A background ~6% of the signal from W decays is not included. Note different integrated luminosities for the two plots. A t mass of 40 GeV is assumed.

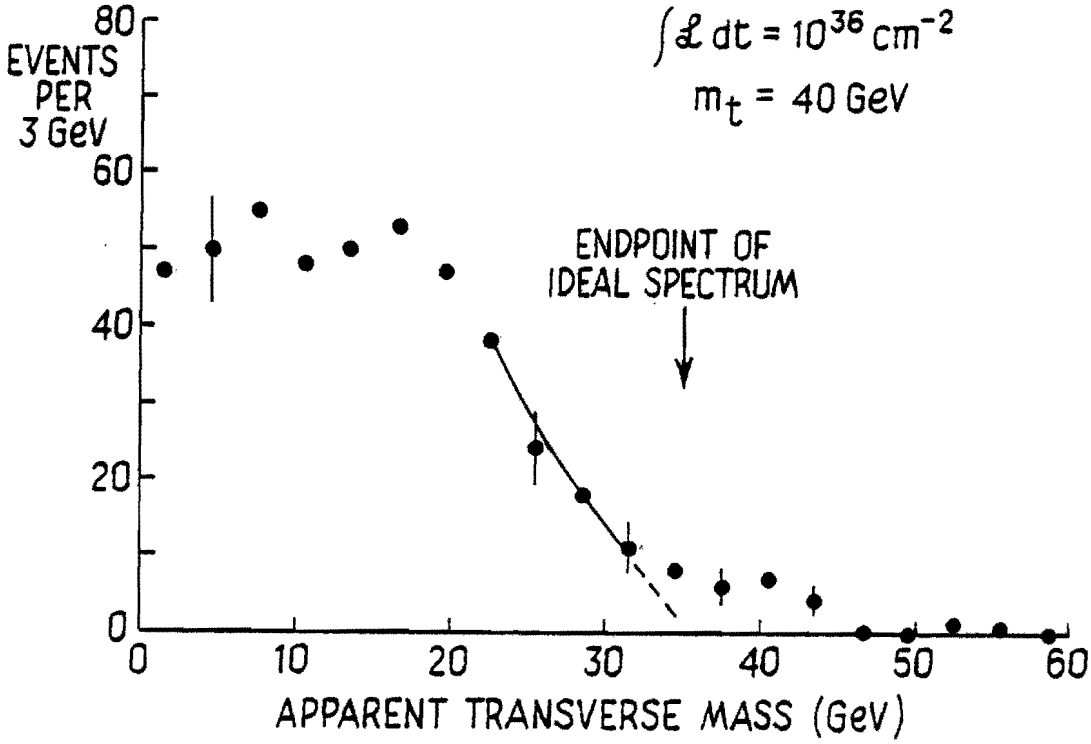


Figure II-4: Apparent transverse mass distribution for $t\bar{t}$ events which pass the cuts described in the text. The transverse mass is calculated from the $P_T$ of the electron with the largest $P_T$ and the missing $P_T$. The endpoint of the ideal spectrum calculated from the transverse momenta of the electron and neutrino from $t \to b + e + \nu$ would be $M_t - M_b$, or in this case approx. 35 GeV.

g. For $q\bar{q} \to \gamma + g$ and $gg \to \gamma g$ subprocesses, how well can your detector a) identify direct isolated photons, b) measure jet masses, c) measure associated multiplicities, and d) measure $P_T$ of the subprocess?

The most important characteristic of a detector for identifying direct photons is the ability to resolve two closely-spaced photons in the electromagnetic calorimeter. This, rather than extremely good electromagnetic energy resolution, is the crucial factor in isolating direct photon production from the $\pi^\circ$ background. Our detector, as stressed already, has much finer segmentation than any existing or proposed detector. [See Table I in Part I.] We also have much more detailed information as a function of depth than most other detectors. The LAPDOG collaboration claims that with a rather coarse lead glass array they are able to distinguish a single $\gamma$ from a pair of coincident $\gamma$'s, the energy of each of which is approx. half that of the single $\gamma$. This is done on the basis of the energy deposition profile. If this technique works for their lead-glass array, it should work for our detector which has an energy measurement every 2.5 rad. length (with the PWC's) and finer transverse segmentation If this technique works in a realistic situation it may allow single photons to be resolved from $\pi^\circ$'s even if the two $\gamma$'s from the $\pi^\circ$ cannot be resolved spatially. This in turn would allow a direct photon measurement at considerably larger $P_T$.

At the Snowmass DPF Summer Study the Hadron-Hadron Collider Group (Palmer et al.) concluded that it would only be possible to measure direct photon production out to $P_T \sim 100$ GeV/c at the Fermilab Collider, even with a detector segmented into $10^6$ towers with individual readouts. This may be unduly pessimistic because it assumes that beyond ISR energies $\gamma/\pi^\circ \sim x_T \equiv 2P_T/\sqrt{s}$. Thus in this model at $\sqrt{s} = 2000$ GeV, $\gamma/\pi^\circ$ is only $\sim 0.1$ for $P_T = 100$ GeV. However this is based on an extrapolation of relatively poor data from $\sqrt{s} \cong 60$ all the way to $\sqrt{s} = 2000$ GeV. The $\gamma/\pi^\circ$ ratio may turn out to be larger, and it will then be possible to measure direct photon production to considerably higher $P_T$.

As discussed in the previous question, it will take considerable experience with real data before the feasibility of measuring jet masses and other characteristics, such as associated multiplicity, with reasonable accuracy will be known. Our detector would be better than any of those proposed for DO for these measurements.

h. Suppose ISR charm production data are correct (e.g., $pp \to \Lambda_c + X$) and $d\sigma_Q = d\sigma_c (M_c^2/M_Q^2)$. How well does your detector measure $d\sigma_Q$ for q = b, t ($m_t > 20$ GeV)?

If we suppose the $P_T$ distribution for heavier flavors varies approx. as $e^{-2M_T}$ where $M_T^2 \equiv [M_Q^2 + P_T^2]$, which is found for charm production, the typical $P_T$ of the diffractively-produced heavy flavors will be $\sim M_Q$. If we take b quarks as an example, a $\Lambda_b$ which is diffractively produced with a momentum ~300 GeV/c will come off at an angle ~16 mrad in the lab. The $\Lambda_c$'s will come off at even smaller angles. This emphasizes the need to measure the energies of all particles from an event down to angles on the order of 5 to 30 mrad from the beams.

It may be possible to identify some of the $\Lambda_b$'s by looking for jets in this range of angles which are accompanied by one or more high energy electrons with a $P_T \sim 1.5$ GeV/c relative to the jet axis. Microvertex detectors and Cherenkov counters are not applicable in this angular region because the decay products don't leave the vacuum pipe until they are a few meters from the interaction point. Identification of jets containing K mesons or $\Lambda$'s would be a useful tool. This will be possible in some cases for $K_s^\circ$ and $\Lambda^\circ$ by observing their decays in flight.

The ISR charm production cross sections are ~1 mb. If the cross sections scale as $(M_c/M_Q)^2$, on the order of 1 in $10^3$ interactions at the Collider will contain diffractively-produced $\Lambda_b$'s, and ~1 in $10^4$ will contain $\Lambda_t$'s if $M_t \cong 20$ GeV/$c^2$. In a $10^{36}$ cm$^{-2}$ run this gives ~$10^8$ $\Lambda_b$ and ~$10^7$ $\Lambda_t$. In our response to Question f above, we described a method which would yield a very clean sample of approx. 450 identified $t\bar{t}$ events starting from a total sample of $1.8 \times 10^4$ $t\bar{t}$ events. We have verified by a Monte Carlo study of diffractive $t\bar{t}$ production that this method works for $t\bar{t}$ pairs produced at angles < 100 mrad. We have also verified that the background from diffractively-produced $b\bar{b}$ pairs which are an order of magnitude more numerous will produce very little background. A $10^{36}$ cm$^{-2}$ run would thus yield a clean sample of ~$10^5$ identified $t\bar{t}$ events!

As we explained above in Question f with the cuts described, the $t\bar{t}$ signal has no significant background. It should be possible to estimate the efficiency of events surviving the cuts. The accuracy for measuring $d\sigma_{tt}$ would then be determined only by the accuracy with which the efficiency can be estimated.

724

ADDENDUM II TO P-724

June 9, 1983

In this Addendum we answer the questions posed by the PAC following its subcommittee meeting of June 2-3. These questions concern the effect of the beam hole size on the missing $P_T$, the $P_T$ distribution assumed for Z°, and the effects of combining degraded detector characteristics on the $Z \rightarrow 2\nu$ background.

A. Missing $P_T$ distributions for jet events for various beam hole sizes

In response to the PAC's question about the missing $P_T$ distributions expected for our detector for various sizes of the beam hole, we show in Figure II-1 the missing $P_T$ spectra for jet events. These spectra were calculated with the latest version of ISAJET. The calculation includes TWOJET events with $P_T > 20$ GeV/c and u, d, s, c, b quarks; top quarks were not included. To prepare these spectra, 8000 two-jet events were generated and scaled to an integrated luminosity of $10^{36}$ cm$^{-2}$ for which $1.6 \times 10^8$ such twojet events would be expected. The detector Monte Carlo includes the following sources of missing $P_T$:

(a) the assumed detector energy resolution — $0.65/\sqrt{E}$ for hadrons and $0.20/\sqrt{E}$ for electrons and $\gamma$'s
(b) the detector angular resolution
(c) the beam holes with size as indicated
(d) neutrinos and muons
(e) hadron punch through

No cracks or dead spaces were included since our detector design has no significant cracks.

Figure II-1 shows the missing $P_T$ spectrum expected for no beam hole, a 1° beam hole, and a 5° beam hole. A 0.2° beam hole was also run, but it is not shown since it is virtually indistinguishable from no beam hole. We see from Figure II-1 that between about 5 and 15 GeV/c the background to a new physics signal would increase by a factor of 1.5 to 2.0 if the beam hole size increases from ≈0° to 1°. Beyond 15 GeV/c the statistics are too poor to be sure how much effect there is. If the beam hole is increased to 5°, the background above about 12 GeV/c goes up about an order of magnitude.

Table II-1 shows the rms missing $P_T$ for these distributions. We note that the $\sigma$ of the distribution only increases by 1.4 GeV/c if the beam hole is

increased from 0° to 5°. However, the distribution is very non-Gaussian and the tail at large missing $P_T$ increases dramatically.

We have also looked at the background from two-jet events to the $Z^\circ \to 2\nu$ signal after a charged lepton veto and topology cuts are applied as described in our proposal. For the 1° beam hole the background becomes very large for missing $P_T$ up to at least 10 GeV/c. For a 5° beam hole the $Z \to 2\nu$ signal would be overwhelmed for missing $P_T < 40$ GeV/c.

Table II-1: $\sigma$ of missing $P_T$ distributions for various beam hole sizes (TWOJET events only, no $t\bar{t}$, including all sources, no cuts)

| Beam Hole | $\sigma$ ($P_T^{mis}$) | Events with $P_T^{mis} > 10$ |
|---|---|---|
| 0° | 2.0 | $1.2 \times 10^6$ |
| 0.2° | 2.0 | $1.4 \times 10^6$ |
| 1.0° | 2.1 | $2.0 \times 10^6$ |
| 5.0° | 3.4 | $1.3 \times 10^7$ |

However, we feel obliged to insert a word of caution about the use of ISAJET for studying the effect of the beam holes. The beam holes contribute to the missing $P_T$ because some of the jet can escape out the beam hole. For example, a quark with $P_T \sim 50$ GeV/c will go off at an angle > 3°, but when it fragments some of the particles may escape even through a 1° beam hole. Bremsstrahlung by the initial quarks and gluons is <u>not</u> included in ISAJET. It probably therefore underestimates the effect of the beam holes on the missing $P_T$. Frank Paige advises us that we should consider the beam hole effects we find with ISAJET to be a <u>lower limit</u> on this contribution to the missing $P_T$. In designing a new detector which is optimized for missing $P_T$ physics, we feel it is essential to be conservative in this regard. We find, for example, that even 5 mrad beam holes cause a drastic increase in the $Z \to 2\nu$ background below a missing $P_T$ of 10 GeV/c. We would therefore like to see our smallest angle calorimeters installed at the earliest possible date.

In Figure II-1 we also show the missing $P_T$ spectra if we assume our detector can achieve a hadron energy resolution comparable to that for the UA2 detector, $\sigma_E/E \cong 0.32\ E^{-1/4}$. (A 1.5 mrad beam hole and $\sigma_E/E = 0.2/\sqrt{E}$ for photons and electrons was used.) This gives a much narrower missing $P_T$ spectrum [$\sigma \cong 1.4$ GeV/c]. It is clear that a well-designed detector which is optimized to measure missing $P_T$ can do much better than any existing detector in measuring missing $P_T$. This also shows that if the beam holes are small enough and there are no dead spaces, the hadron resolution, not the electromagnetic energy resolution or neutrinos, is the dominant factor in determining the missing $P_T$ for the bulk of the events. This reinforces our determination to achieve a hadron energy resolution better than the $0.65/\sqrt{E}$ assumed in our proposal.

B. $P_T$ spectrum for Z's and W's assumed in Monte Carlo

In Figure II-2 we show the $P_T$ spectrum of Z°'s used in our Monte Carlo for the cases $\langle P_T \rangle = 10$ and $\langle P_T \rangle = 20$ GeV/c. In both cases the total number of Z° events is the same, approx. 3000 $Z \to 2\nu$ per $10^{36}$ $cm^{-2}$. Both distributions have a tail of approximately the same shape. To vary the average $P_T$ of the Z's and W's in our Monte Carlos we have merely changed the fraction of the events in the tail. This procedure is consistent with perturbative QCD expectations. The total yield of Z's and W's is thought to be reliably predicted by QCD, but the average $P_T$ at Fermilab Collider energies is subject to considerable uncertainty.

In Figure II-3 we give several examples of QCD predictions of the $P_T$ spectrum expected for Drell-Yan production. These are for much lower center-of-mass energies, so it is hard to make a direct comparison with the spectra in Figure II-2. However the theoretical predictions have the same general shape—a long tail at large $P_T$ which falls off almost exponentially and a flattening at small $P_T$.—These same characteristics are shown by the dimuon production data, some of which are shown in Figure II-3 along with the corresponding theoretical predictions.

C. Background to $Z \to 2\nu$ for various detector assumptions

As requested by the PAC, we show in Figure II-4 the background to the $Z \to 2\nu$ signal for various detector assumptions, which was shown in our earlier Addendum as Figure I-1. In that graph several points were offscale, and we

give numerical values for these (upper left of Figure II-4). Four of the five offscale points are due to minimum bias events which get pushed out to larger missing $P_T$ as a result of the degraded detector characteristics and manage to leak through the topology cuts. If the degraded characteristics turned out to be correct (e.g. - a 5 mrad beam hole), the background would, of course, completely swamp the $Z \to 2\nu$ events below missing $P_T \cong 10$ GeV/c.

In Figure II-5 we show the effect on the $Z \to 2\nu$ background of combining two more pessimistic assumptions concerning the detector characteristics. Our "standard" background is based on a 1.5 mrad beam hole, an energy resolution for hadrons of $0.65/\sqrt{E}$ and $0.2/\sqrt{E}$ for photons, and a veto on events with charged leptons with $P > 1.5$ GeV/c. In Figure II-4 the background is shown for two cases:

(i) 5 mrad beam hole and $1.30/\sqrt{E}$ hadron resolution.

(ii) 5 mrad beam hole and 5 GeV/c lepton veto

Within the limited statistics of the Monte Carlo, these backgrounds are hardly distinguishable from those for a 5 mrad beam hole alone (Fig. II-4).

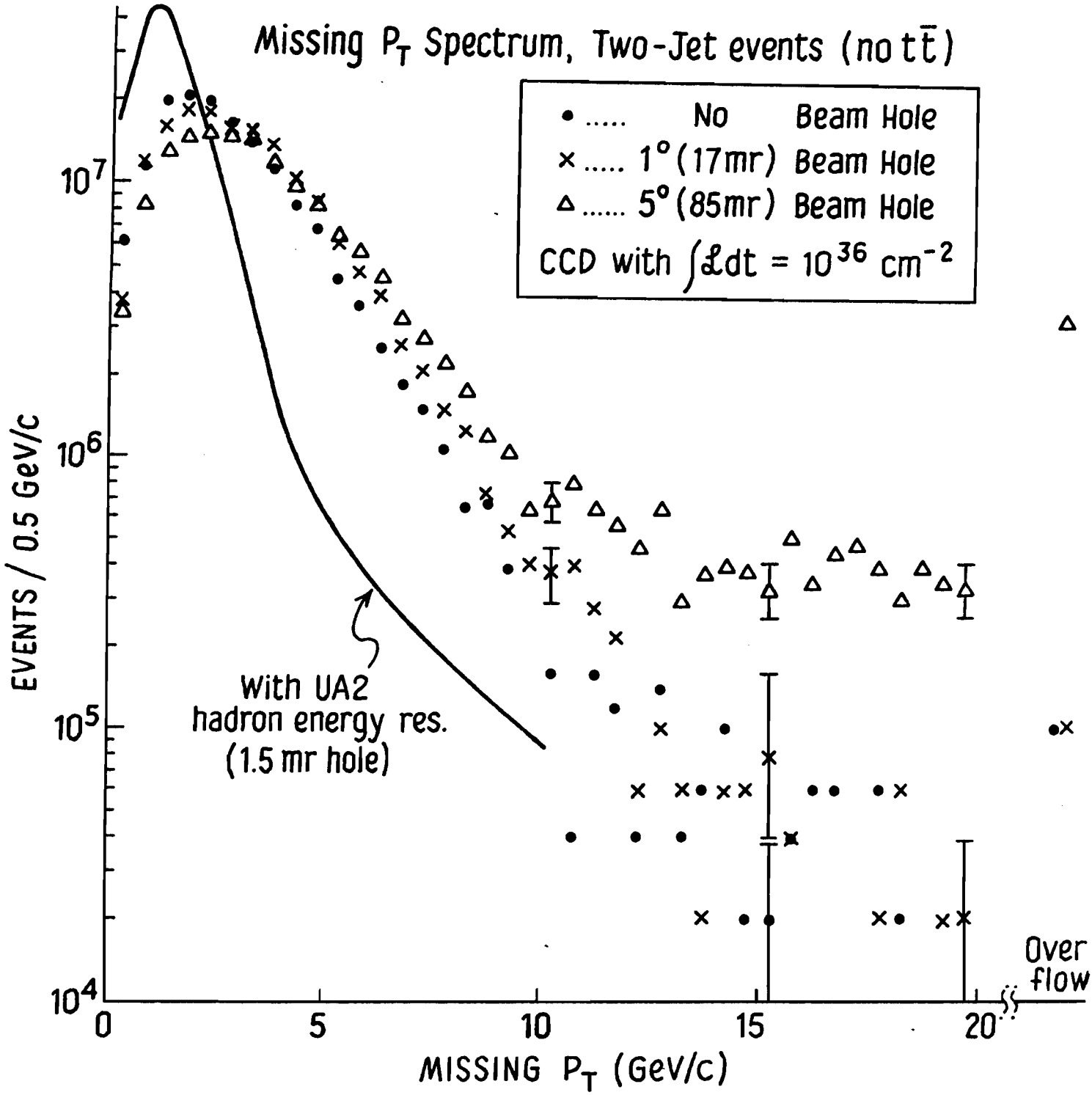


Figure II-1: Apparent missing $P_T$ spectrum from ISAJET two-jet events. The contributions of the CCD detector energy and angle resolution, the beam holes, punch through, and missing neutrinos and muons are included. The missing $P_T$ spectrum expected with the UA2 hadron energy resolution ($0.32\ E^{-0.25}$) is shown for comparison.

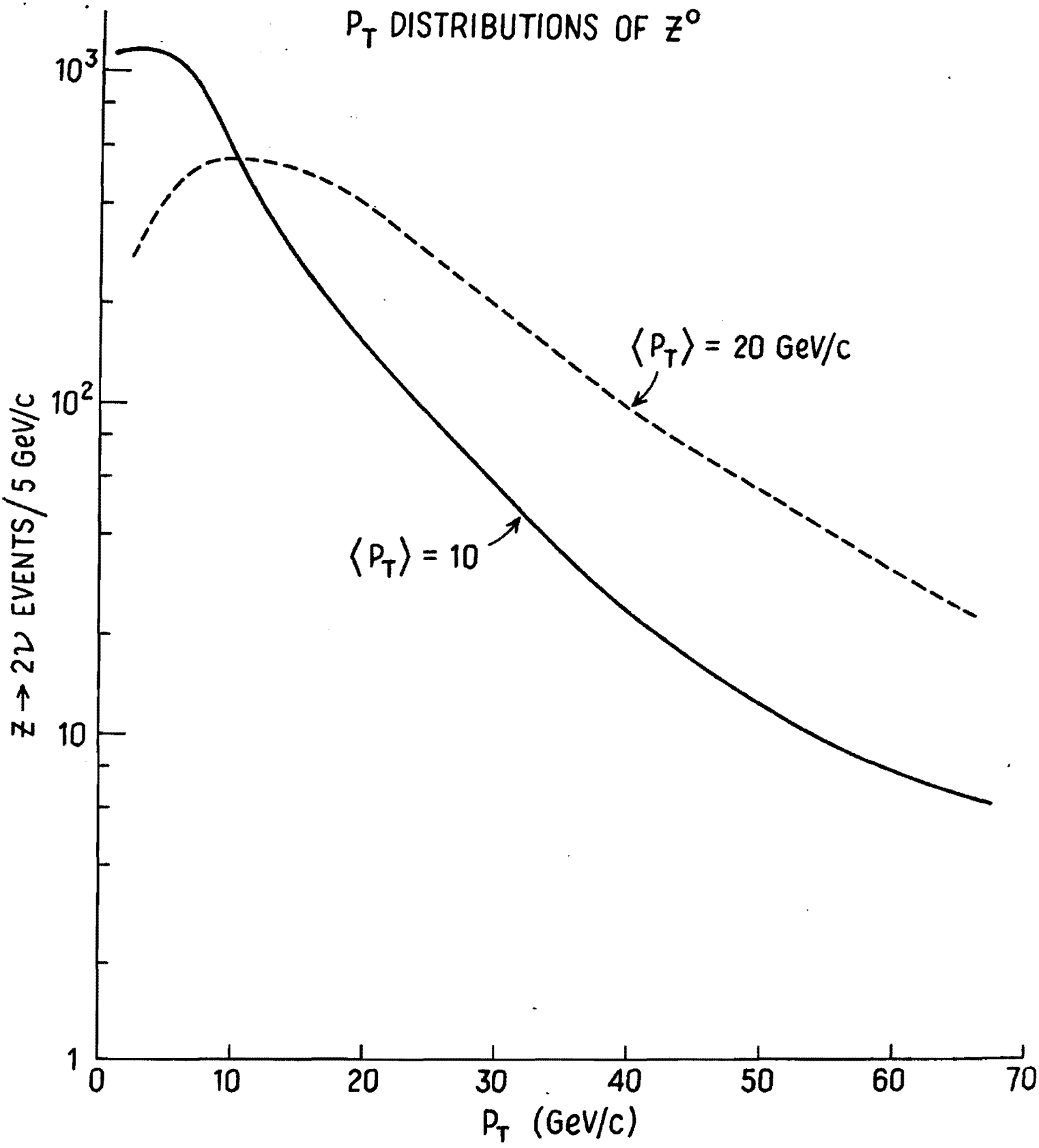


Figure II-2: The $P_T$ spectra used in our $Z \rightarrow 2\nu$ Monte Carlos discussed in our proposal and addenda. $\langle P_T \rangle$ is the mean $P_T$ for the spectrum indicated. In Fig. II-4 we show the $Z \rightarrow 2\nu$ signal and background for $\langle P_T \rangle$ = 20 GeV/c. In our proposal we show it for $\langle P_T \rangle$ = 10, 20, 35 GeV/c.

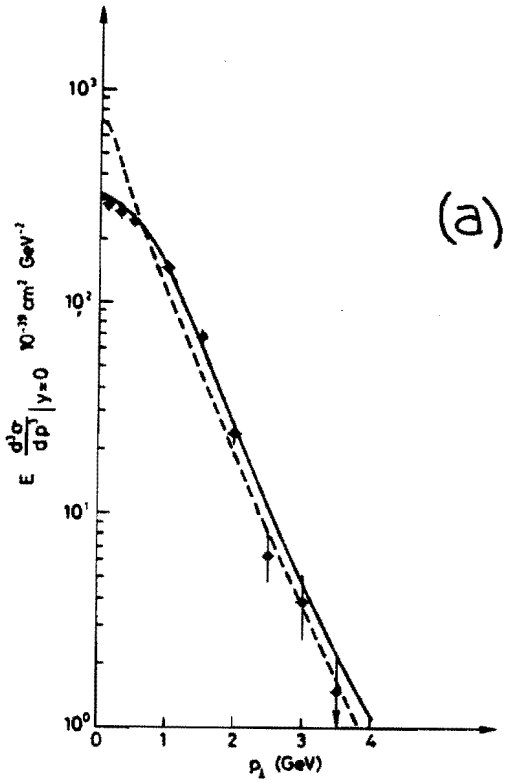


. Theoretical predictions are compared with the experimental data at $s =$ 750 GeV$^2$ and $Q^2 = 56$ GeV$^2$. We report the results obtained with two different choices of parameters $\langle p_\perp^2\rangle_{\text{intrinsic}}$ and $M$: (i) first choice: $\langle p_\perp^2\rangle_{\text{intrinsic}} = 400$ MeV$^2$, $M = 1.25$ GeV$^2$ (full line) (ii) second choice: $\langle p_\perp^2\rangle_{\text{intrinsic}} = 0$, $M = 1.75$ GeV$^2$ (dashed line).

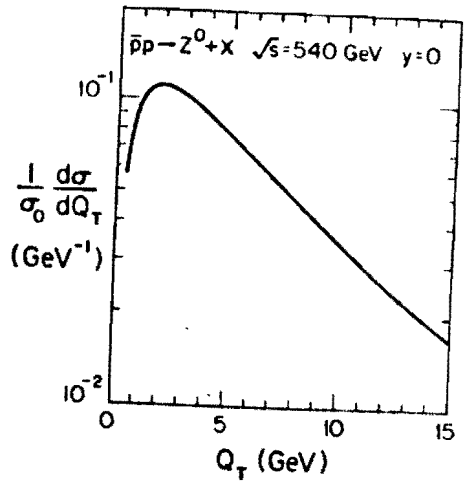


Transverse momentum distribution of a $Z^0$ produced $\bar{p}p$ collisions with $\sqrt{s} = 540$ GeV and rapidity $y = 0$. The zero at $Q_T = 0$ is kinematic; the corresponding $d\sigma/d^2Q_T$ peaks at a finite value at $Q_T = 0$

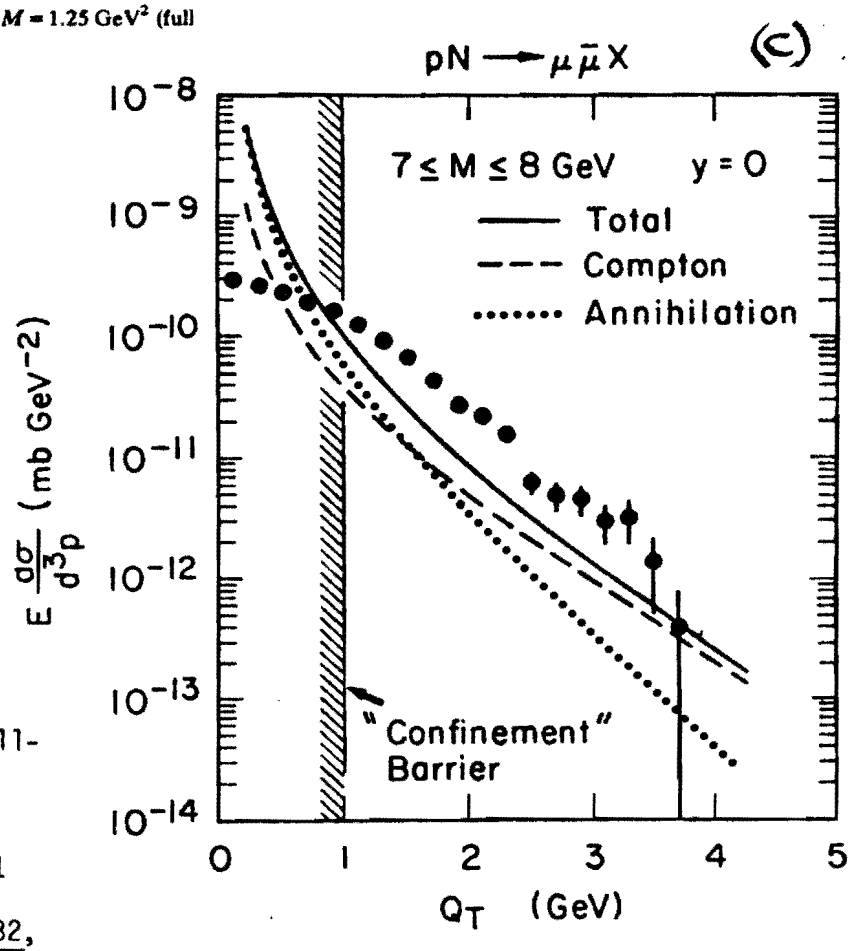


Figure II-3: Examples of theoretical predictions of $P_T$ distribution for Drell-Yan production.
(a) G. Parisi and R. Petronzio, Nucl. Phys. B154, 427 (1979).
(b) F. Halzen et al., Z. Phys. C14, 351 (1982).
(c) E. Berger, Particles and Fields-1982, p. 312. AIP Conf. Proc. No. 98, 1983.

Comparison of the QCD calculations of dimuon transverse momentum by Berger with CFS data.

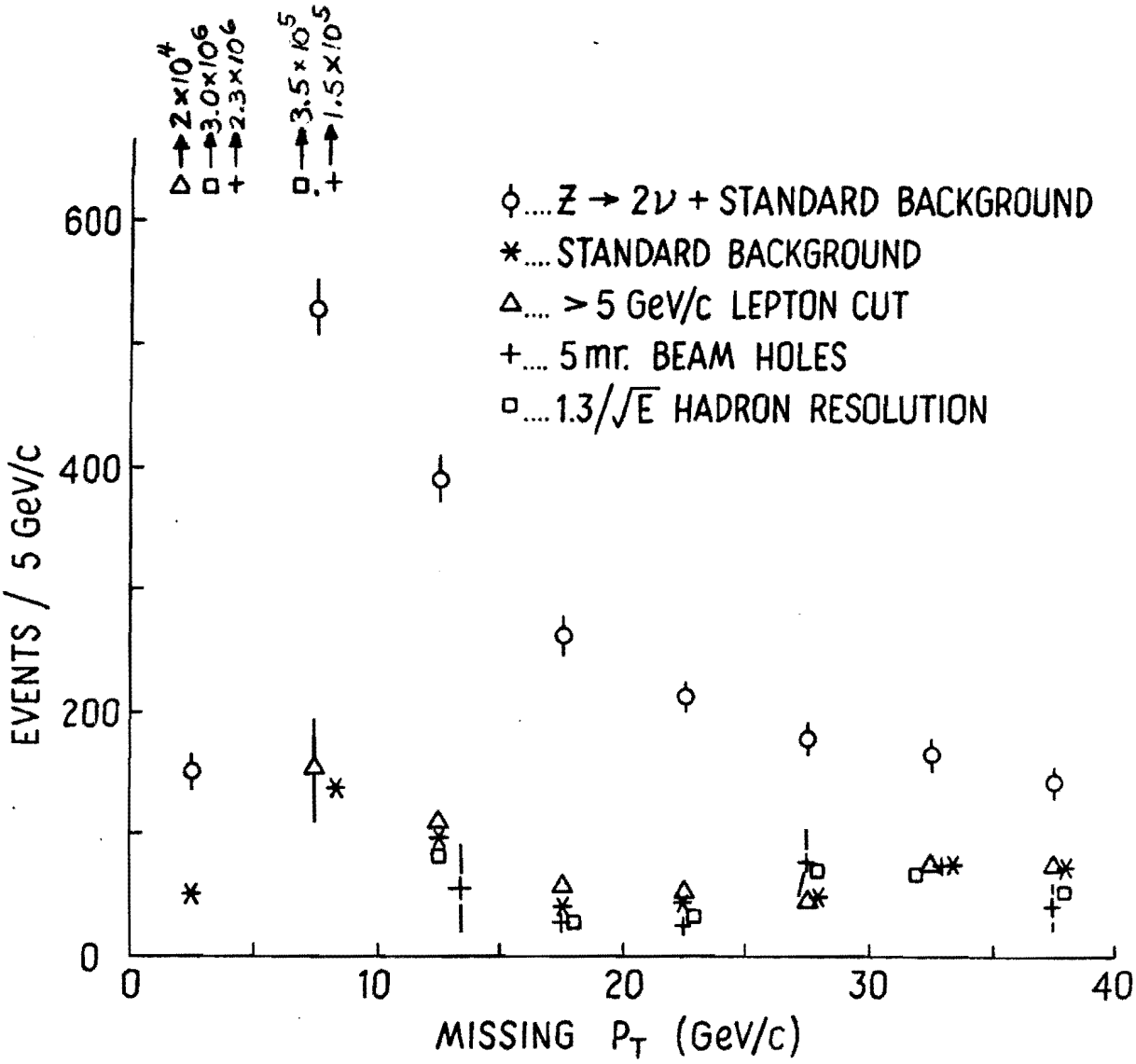


Figure II-4: Comparison of $Z^\circ \rightarrow 2\nu$ signal plus standard background with total background for different assumptions concerning the detector characteristics. The error bars shown for the (signal + background) are the estimated statistical errors for a run with integrated luminosity $10^{36}$ cm$^{-2}$. The error bars shown for the background points are the statistical errors in the Monte Carlo studies. All sources of background including jet events, heavy flavor production and decay, and W decays are included. An average $P_T$ for Z and W production of 20 GeV/c was assumed.

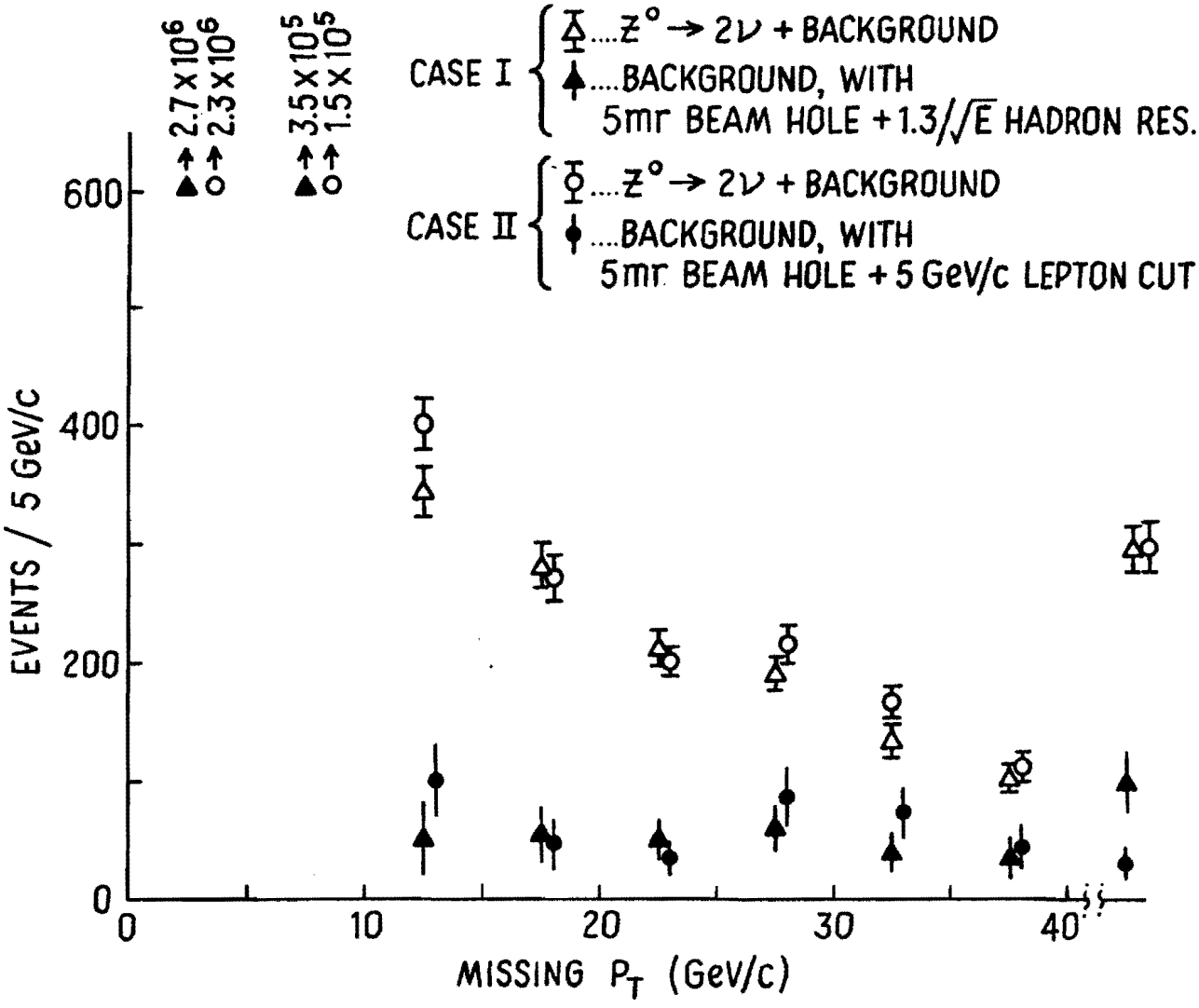


Figure II-5: Same as Fig. II-4 with the effect of combining two possible sources of poorer missing $P_T$ resolution.